VARIABLE DISTRIBUTIONS OF WATER AS A TRANSPIRATION SOURCE: CONSEQUENCES FROM THE TREE STEM TO ECOSYSTEM FUNCTIONING

by

CHELCY RAE FORD

(Under the Direction of Robert O. Teskey)

ABSTRACT

Variable distributions of water used for transpiration can have consequences on estimates of plant and ecosystem transpiration, as well as on the production potential and stability of transpiration rates for different plants within an ecosystem. Here a suite of studies, from the level of an individual tree stem to an ecosystem, illustrates this. At the tree level, the distribution of water flow within tree stems with tracheid xylem anatomy and deep sapwood was mathematically described. The distribution was Gaussian shaped, with a higher proportion of water flow in the outer sapwood compared to inner sapwood. The steepness of this distribution, β, decreased over time with increasing leaf-to-air vapor pressure deficit and decreasing soil moisture availability. At the stand level, the proportion of nighttime stored water as a source for daytime transpiration increased with seasonal declines in soil moisture availability. I modeled the difference between potential stand canopy transpiration under no soil moisture deficit compared to the actual canopy transpiration observed when soil moisture declined. Had the trees not experienced declining soil moisture, canopy transpiration would have been 12 mm higher over the 25-day drought period. This specific modeling approach illustrates how multiple

driving variables can influence transpiration on different time scales, and in linear and nonlinear ways.

Finally, at the ecosystem level, I investigated the processes by which the dominant savanna plant life forms, trees and grasses, partition and use water, and how these feedback onto carbon gain. Across a natural hydrologic gradient, we found that trees primarily used groundwater, while grasses used a higher proportion of soil water. This had ramifications for aboveground plant production and variability in transpiration rates over time, with variability in tree transpiration rates always being less than that of the grasses. For the grass plant functional type, I found that the percentage of groundwater utilized varied across the hydrologic regime. Grasses in the xeric sites used a higher percentage of groundwater than grasses in mesic sites. This pattern was correlated with aboveground productivity, with grasses in the drier sites producing more aboveground biomass compared to mesic site grass production.

INDEX WORDS: *ANPP, autocorrelation, autocorrelation function, canopy, canopy conductance, capacitance, deuterium, error analysis, fertilization, Georgia, hydraulic conductivity, longleaf pine, nitrogen, Pinus palustris, plant functional types, sap flux, sap flow, savanna, scaling, stable isotope, time series analysis, temporal variability, transpiration, tree-grass interactions, water use efficiency, wiregrass*

VARIABLE DISTRIBUTIONS OF WATER AS A TRANSPIRATION SOURCE: CONSEQUENCES FROM THE TREE STEM TO ECOSYSTEM FUNCTIONING

by

CHELCY RAE FORD

BS, Georgia Institute of Technology, 1997

MS, University of South Florida, 1999

A Dissertation Submitted to the Graduate Faculty of The University of Georgia in Partial Fulfillment of the Requirements for the Degree

DOCTOR OF PHILOSOPHY

ATHENS, GEORGIA

2004

VARIABLE DISTRIBUTIONS OF WATER AS A TRANSPIRATION SOURCE: CONSEQUENCES FROM THE TREE STEM TO ECOSYSTEM FUNCTIONING

by

CHELCY RAE FORD

Major Professor: Robert O. Teskey

Committee: Robert J. Cooper
Lisa A. Donovan
Ronald L. Hendrick
Robert J. Mitchell
Rodney E. Will

Electronic Version Approved:

Maureen Grasso
Dean of the Graduate School
The University of Georgia
December 2004

ACKNOWLEDGEMENTS

This dissertation work could not have been accomplished without the support of many people. My advisors, Bob Teskey and Bob Mitchell, provided support, encouragement, and wisdom. For me, they have been and will continue to be role models in science. I am fortunate also to have had the support and encouragement of Lindsay Boring throughout my project, and appreciate the interest he showed in my ideas. I thank my committee, Bob Cooper, Lisa Donovan, Ron Hendrick, and Rod Will, for all the feedback, equipment, and expertise they provided me. To my past and present peers in the Tree Physiology, and Forest Ecology Labs at UGA and the Forest Ecology II Lab at the Jones Center, I am deeply grateful for all the social interaction, help in the field, feedback on presentations and manuscripts, and emotional support. Rob Addington, Mary Anne McGuire, and Stephen Pecot provided help with the technical aspects of this work, and Jim Bradley and Carol Goranson provided much help in the field. The many discussions I had with Nina Wurzburger and Dali Guo about science in general were rewarding. I gratefully acknowledge Jay Brown's help and expertise in the greenhouse at UGA, and the help and expertise of Liz Cox at the Jones Center. Finally, I wish to thank my family for all their support, especially that shown by my husband.

TABLE OF CONTENTS

Page

CHAPTER

1 INTRODUCTION AND LITERATURE REVIEW 1

2 TRANSPIRATION, ABOVEGROUND PRODUCTION, AND WATER SOURCE PARTITIONING BY THE DOMINANT PLANT LIFE FORMS OF A FIRE-MAINTAINED SAVANNA 8

3 ASSESSING VARIATION IN THE RADIAL PROFILE OF SAP FLUX DENSITY IN *PINUS* SPECIES AND ITS EFFECT ON DAILY WATER USE.....50

4 DIURNAL AND SEASONAL VARIABILITY IN THE RADIAL DISTRIBUTION OF SAP FLOW: PREDICTING TOTAL STEM FLOW IN *PINUS TAEDA* TREES.....81

5 MODELING CANOPY TRANSPIRATION USING TIME SERIES ANALYSIS: A CASE STUDY ILLUSTRATING THE EFFECT OF SOIL MOISTURE DEFICIT ON *PINUS TAEDA* 114

6 CONCLUSIONS.....147

CHAPTER 1

INTRODUCTION AND LITERATURE REVIEW

Introduction and literature review

Understanding plant water use and what influences it, has perhaps been the most central issue studied in the field of plant eco-physiology. The importance of this issue is grounded in the fact that across many spatial scales, net primary production (NPP) and plant community composition are related to water availability and thus ecosystem water use (Rosenzweig 1968; Lieth 1975; Whittaker 1975; Webb et al. 1986; Huxman et al. 2004). Therefore, both accurately measuring water use, and elucidating the relationship between water use and water sources available for use are critical to understanding plant, community, and ecosystem production and function.

Because transpiration and thus primary productivity are limited by water availability, rates of these processes can potentially be sustained by a plant with access to stable water sources, compared to the plant with unstable or transient sources. This could largely be the reason that in arid environments, woody plants that persist through long droughts can have roots extending down to 50 m, reaching the water table (Canadell et al. 1996). In contrast to woody plants, grasses lack secondary thickening in roots and have shorter average root life spans (Gill and Jackson 2000) all of which can constrain root proliferation into very deep soil layers. An emerging general pattern among co-existing woody species and grasses in arid environments is that woody species, which have persistent woody roots, do exploit the stable water table as a source for transpiration, while grasses do not (Smith et al. 1997; Weltzin and McPherson 1997; Dodd et al. 1998; Ludwig 2001; Hungate et al. 2002; Moreira et al. 2003). Within an ecosystem, the extent to which this pattern manifests in relation to water use and primary production is largely unexplored.

For plants that rely primarily on soil water resources, the impact of transient reductions in soil moisture availability on plant water use is difficult to quantify. This is chiefly because

relatively quick changes in plant transpiration follow changes in the leaf-to-air vapor pressure deficit or leaf incident radiation; however, a threshold response in plant transpiration is instead observed with changes in soil moisture availability (Rutter 1968; Granier and Loustau 1994; Bauerle et al. 2002) Because of the differential response, and response time, in transpiration to these controlling variables, an accurate method allowing quantification of the impact of soil moisture availability on tree or forest water use seems lacking. Indeed, the only way to truly quantify this effect is to isolate the variable, which is impractical if not impossible to accomplish in a forest. Modeling the response, however, can provide accurate estimates of water use in which the multiple driving variables, their interactions, and their differential effect on transpiration response time are incorporated.

Other challenges in accurately measuring forest water use still remain, especially quantifying water use by large trees that have complex canopies. In these trees, much variation in leaf-to-air vapor pressure deficit and leaf incident radiation can exist. Thus, integrating the response of all the leaves in the canopy can be cumbersome. One approach to integrating this within-canopy variation is to assess tree water movement in the main stem, where considerably less variation exists. Within the stem, however, variation in water flow can exist and impact estimates of whole-tree water use. Many have noted the spatial variability in water flow the stems of trees using a variety of methods (Swanson 1967; Waring and Roberts 1979; Cohen et al. 1985; Čermák et al. 1992; Granier et al. 1996; Lüttschwager and Granier as presented in Köstner et al. 1996; Čermák and Nadezhdina 1998; Nadezhdina et al. 2002) and these qualitative or species-specific descriptions remarkably converge on a consistent pattern for trees with similar xylem anatomy, such as gymnosperms. Evaluating this seemingly consistent variation in water

flow in the stems of large trees, both in space and time, and synthesizing a quantitative description of the pattern is much needed for advances in quantifying forest water use.

Structure of dissertation

The following chapters evaluate the ecological hypotheses regarding the link between water use in a savanna, water sources exploited, and annual aboveground production by trees and grasses (Chapter 2). Additionally, improved approaches for scaling sap flux measurements spatially (Chapter 3) and temporally (Chapter 4) in trees are presented, along with a novel approach to modeling forest canopy transpiration and the impact of soil water deficit on it though time (Chapter 5). These approaches can improve the accuracy of water use estimates in trees and forests.

References

Bauerle, W.L., C.J. Post, M.F. McLeod, J.B. Dudley and J.E. Toler 2002. Measurement and modeling of the transpiration of a temperate red maple container nursery. Agric. For. Meteorol. 114:45-57.

Canadell, J., R.B. Jackson, J.R. Ehleringer, H.A. Mooney, O.E. Sala and E.-D. Schulze 1996. Maximum rooting depth of vegetation types at the global scale. Oecologia. 108:583-595.

Čermák, J., E. Cienciala, J. Kučera and J.E. Hallgren 1992. Radial velocity profiles of water flow in trunks of Norway spruce and oak and the response of spruce to severing. Tree Physiol. 10:367-380.

Čermák, J. and N. Nadezhdina 1998. Sapwood as the scaling parameter-defining according to xylem water content or radial pattern of sap flow? Ann. For Sci. 55:509-521.

Cohen, Y., F.M. Kelliher and T.A. Black 1985. Determination of sap flow in Douglas-fir trees using the heat pulse technique. Can. J. For. Res. 15:422-428.

Dodd, M.B., J.M. Lauenroth and J.M. Welker 1998. Differential water resource use by herbaceous and woody plant life-forms in a shortgrass steppe community. Oecologia. 117:504-512.

Gill, R.A. and R.B. Jackson 2000. Global patterns of root turnover for terrestrial ecosystems. New Phytol. 147:13-31.

Granier, A., P. Biron, N. Breda, J.Y. Pontailler and B. Saugier 1996. Transpiration of trees and forest stands: Short and longterm monitoring using sapflow methods. Global Change Biology. 2:265-274.

Granier, A. and D. Loustau 1994. Measuring and modelling the transpiration of a maritime pine canopy from sap-flow data. Agric. For. Meteorol. 71:61-81.

Hungate, B.A., M. Reichstein, P. Dijkstra, D. Johnson, G. Hymus, J.D. Tenhunen, C.R. Hinkle and B.G. Drake 2002. Evapotranspiration and soil water content in a scrub-oak woodland under carbon dioxide enrichment. Global Change Biology. 8:289-298.

Huxman, T.E., M.D. Smith, P.A. Fay, A.K. Knapp, M.R. Shaw, M.E. Loik, S.D. Smith, D.T. Tissue, J.C. Zak, J.F. Weltzin, W.T. Pockman, O.E. Sala, B.M. Haddad, J. Harte, G.W. Koch, S. Schwinning, E.E. Small and D.G. Williams 2004. Convergence across biomes to a common rain-use efficiency. Nature. 429:651-654.

Köstner, B., P. Biron, R. Siegwolf and A. Granier 1996. Estimates of water vapor flux and canopy conductance of Scots pine at the tree level utilizing different xylem sap flow methods. Theor. Appl. Climatol. 53:105-113.

Lieth, H. 1975. Modeling the primary productivity of the world. *In* Primary productivity of the biosphere Eds. H. Lieth and R.H. Whittaker. Springer, New York, pp. 237-283.

Ludwig, F. 2001. Tree-grass interactions on an east african savanna: The effects of competition, facilitation and hydraulic lift. Ph.D. Dissertation. Wageningen University.

Moreira, M.Z., F.G. Scholz, S.J. Bucci, L.S. Sternberg, G. Goldstein, F.C. Meinzer and A.C. Franco 2003. Hydraulic lift in a neotropical savanna. Functional Ecology. 17:573-581.

Nadezhdina, N., J. Čermák and R. Ceulemans 2002. Radial patterns of sap flow in woody stems of dominant and understory species: scaling errors associated with positioning of sensors. Tree Physiol. 22:907-918.

Rosenzweig, M.L. 1968. Net primary productivity of terrestrial communities: prediction from climatic data. Am. Nat. 102:67-74.

Rutter, A.J. 1968. Water consumption by forests. *In* Water Deficits and Plant Growth Ed. T.T. Kozolwski. Academic Press, Inc., New York, pp. 23-84.

Smith, D.M., P. Jarvis and J.C.W. Odongo 1997. Sources of water used by trees and millet in Sahelian windbreak systems. J. Hydrol. 198:140-153.

Swanson, R.H. 1967. Seasonal course of transpiration of lodgepole pine and Engelmann spruce. *In* International Symposium on Forest Hydrology Eds. W.E. Sopper and H.W. Lull, Pennsylvania State University, pp. 419-434.

Waring, R.H. and J.M. Roberts 1979. Estimating water flux through stems of Scots pine with tritiated water and phosphorous-32. J. Exp. Bot. 30:459-467.

Webb, W.L., W.K. Lauenroth, S.R. Szarek and R.S. Kinerson 1986. Primary production and abiotic controls in forests, grasslands, and desert ecosystems of the United States. Ecology. 64:134–151.

Weltzin, J.F. and G.R. McPherson 1997. Spatial and temporal soil moisture resource partitioning by trees and grasses in a temperate savanna, Arizona, USA. Oecologia. 112:156-164.

Whittaker, R.H. 1975. Communities and ecosystems. MacMillan, New York. 385 p.

CHAPTER 2

TRANSPIRATION, ABOVEGROUND PRODUCTION, AND WATER SOURCE PARTITIONING BY THE DOMINANT PLANT LIFE FORMS OF A FIRE-MAINTAINED SAVANNA[1]

[1]Ford, C. R., C. E. Goranson, M. A. McGuire, S. Pecot, R. J. Mitchell, and R. O. Teskey. To be submitted to *Oecologia*.

Abstract

Savanna systems are prevalent throughout the world and occur in both temperate and tropical biomes. The structure and diversity of these systems are well studied; however few studies have investigated the processes by which the dominant plant life forms, trees and grasses, partition and use water, carbon and nitrogen. We estimated annual water use, aboveground production, and water source utilization by overstory trees (pines and oaks) and the dominant understory grass (wiregrass, *Aristida stricta* Michx.) in a fire-maintained longleaf pine-wiregrass savanna in the coastal plain of SW Georgia. Experimental plots existed along a natural hydrologic gradient and a manipulated nitrogen gradient. We hypothesized that the different water sources used by trees and grasses were linked to their productivity, and that the proportion of groundwater used varied across the hydrologic regime. We predicted that trees would have access to deep water sources and have less variability in transpiration rates over time; while grasses would rely more on shallow water sources and have more variability in transpiration rates over time.

Total annual aboveground net primary productivity (ANPP) and transpiration were higher in the wet-mesic site type compared to the dry-xeric sites. Mesic sites averaged 2.27 Mg biomass ha^{-1} and 380.05 mm, while xeric sites averaged 1.13 Mg biomass ha^{-1} and 107.97 mm. As a result, water use efficiency was higher in the xeric sites. Nitrogen fertilization significantly increased ANPP in all plant functional types, but did not affect transpiration or water use efficiency. Trees and grasses had different temporal peaks in transpiration rates. Trees peaked in late summer, while grasses peaked in late spring. In both mesic and xeric site types, trees were almost exclusively using groundwater (94% groundwater), while grasses used a higher proportion of soil water than the trees. Furthermore, the variability in rates of transpiration was always lower for pines (average coefficient of variation, CV, 51%) compared to grasses (average

CV 62%). For grasses, the percentage of groundwater utilized varied with site type. Grasses in the xeric site used a higher percentage of groundwater than in the mesic site. This variation could be linked to annual ANPP, with grass ANPP in the xeric sites exceeding grass ANPP in the mesic sites. On a percentage basis, annual contribution of grass production to total ANPP in the mesic sites was 13.4%, compared to 34.8% in the xeric sites. Combined ANPP, transpiration and water source utilization data are consistent with the Walter's two-layer model of tree-grass functioning in savanna systems, and with previously described rooting distributions for trees and grasses in longleaf pine savannas.

Key words: ANPP, deuterium, fertilization, longleaf pine, nitrogen, plant functional types, sap flux, sap flow, savanna, stable isotope, transpiration, tree-grass interactions, water use efficiency, wiregrass,

Introduction

Savanna ecosystems are prevalent throughout the world and encompass 15% of the earth's total land surface area (Kimmins 1987). While the structure (Menaut and Cesar 1979; Higgins et al. 2000) and diversity (Walker and Peet 1983; Leach and Givnish 1999; Foster and Tilman 2003; Kirkman et al. 2004) of savanna systems are well studied, few studies have investigated the processes by which the dominant plant life forms, trees and grasses, partition and use water, carbon and nitrogen. Important questions concerning the coupling of productivity and transpiration, and the effect of increasing nitrogen availability on these relationships remain unanswered. Additionally, any relationship between the seasonal dynamics of transpiration among the dominant savanna plant life forms and primary productivity of the system is also unknown.

Some generalities relative to water, carbon and nitrogen cycling in savannas have been suggested (Scholes and Archer 1997). For example, savannas are nutrient poor, have low leaf area, and low rates of N mineralization (Reich et al. 2001). Some studies have documented annual aboveground net primary productivity (ANPP) trends over gradients of N mineralization in savanna systems. Relationships between ANPP and N mineralization are difficult to discern, because studies have reported opposite trends of annual ANPP across gradients of nitrogen mineralization (cf. Reich et al. 2001, and Mitchell et al. 1999). At the ecosystem scale, transpiration rates in savannas are also low compared to other systems that have a tree structural layer; but reported rates vary greatly. This variation is not surprising given that savannas encompass both tropical and temperate biomes and can exist in each biome with either marked seasonality in precipitation or relatively even distributions of precipitation (Johnson and Tothill 1984). Few studies have quantified transpiration of savanna systems or transpiration by the dominant plant life forms over time (e.g. Scanlon and Albertson 2004, but see Hutley et al. 2000). More importantly, productivity measurements have not been conducted concurrently with measurements of water use or water source partitioning; and conversely, water source partitioning measurements have not been conducted concurrently with productivity and water use measurements.

The prevailing conceptual model that couples the structure and function of savanna systems involves the spatial separation of functional rooting zones, and is referred to as Walter's two-layer model (Walter 1971; Walter 1973). This model (reviewed by Scholes and Archer 1997), dictates that much like the structure of the aboveground components of savannas, i.e., tall trees and short grasses, 1) the root systems are arranged in two layers and exploit resources from those soil layers, and 2) by functioning in two layers, productivity is maximized. With

functional niche-separation, competition for limited resources may be minimized or even avoided if different species, life-forms or functional groups utilize different pools of the resource (e.g. water or nitrogen). The first part of the model—spatial partitioning of functional rooting zones—has been demonstrated in seasonally dry forests and savannas (Smith et al. 1997; Weltzin and McPherson 1997; Dodd et al. 1998; Ludwig 2001; Hungate et al. 2002; Moreira et al. 2003). Other studies have used the two-layer model to hypothesize about trends in productivity, yet results have not fit model predictions. For example, Mitchell et al. (1999) hypothesized that with decreasing depth to the water table in longleaf pine-wiregrass savanna sites (i.e. water hypothetically becoming more and more available to grasses), that wiregrass would comprise a greater proportion of the total aboveground biomass than longleaf pine. Their results did not fit this model, however. Although guided by the same model, no studies have measured both the spatial partitioning of water resources and net primary productivity.

The objectives of this study are to link water sources to ecosystem water use, and ecosystem water use to the primary productivity of the ecosystem, in the framework of a spatial root separation model. We hypothesize that the different water sources used by trees and grasses are linked to their productivity. We predict that dominant overstory trees and understory grasses of the longleaf-wiregrass savanna display different patterns in water-source partitioning, and that this may vary across a savanna hydrologic regime. Specifically, we predict that trees will have access to deep water sources, and thus display less variability in transpiration rates over time; while grasses will rely more on shallow water sources and thus display more variability in transpiration rates over time. We examine these in both unaltered and nitrogen-fertilized mesic and xeric longleaf pine-wiregrass savanna sites (i.e. mesic and xeric are two extremes of this

savanna type), which predominantly support an overstory of longleaf pine (*Pinus palustris* Mill.) and various oak tree species, and an understory of wiregrass (*Aristida stricta* Michx.).

Materials and methods

Research system, site description & experimental design

This experiment was conducted at the Joseph W. Jones Ecological Research Center in SW Georgia (N31°13'16.88" W84°28'37.81"), which contains 6,000 ha of naturally regenerated second-growth longleaf pine-wiregrass savanna managed with prescribed burns every 2-5 years. Within the longleaf pine forest type (Goebel et al. 1997), a range of hydrologic regimes exists depending on soil characteristics and topography. The two extremes are wet-mesic sites and xeric sites. The former are poorly drained and have clay-textured soils, while the latter have excessively well-drained, deep, sand-textured soils. The longleaf pine forest type is comprised of an overstory of *Pinus palustris* Mill.; a co-dominant and shrub layer of *Quercus geminata* Small*, Q. laevis* Walt.*, Q. stellata* Wangenh., and *Q. virginiana* Mill.; and a herbaceous-grass layer dominated by *Aristida stricta* Michx., a C_4 bunchgrass. Using a land classification system developed on this preserve (Goebel et al. 1997), we selected four replicate tracts of mesic and xeric sites (whole plots). A range of time since last burn existed between the sites, with two plots of each site type being burned in Jan 2002 (0 years of duff), one plot in each site type having 1 year of duff, and the remaining plot in each site type having 2 years of duff. Two replicate whole plots in each site type were also part of an existing long-term ecological research study, in which above- and below-ground productivity data had been collected since the year 2000. For the present study, all data were collected during January 2002-May 2003.

We established two 1-ha split plots within each whole plot. To one randomly chosen split plot within each whole plot, a broadcast fertilization treatment consisting of 100 kg N ha^{-1} yr^{-1} of dry ammonium nitrate was applied. The other split plot served as an unfertilized control. Fertilizer was applied three times during the study year in May 2002, August 2002 and January 2003 at 60%, 20% and 20%, respectively, of the annual total treatment based on annual variation in net N mineralization (Wilson et al. 2002).

Productivity measurements

We determined annual aboveground net primary productivity (ANPP) for the oaks, pines and wiregrass in all plots. These three functional plant types represented more than 95% of the total standing biomass in these plots (Figure 2.1). All trees larger than 5 cm in diameter at 1.3 m above the ground surface were tagged and their diameters recorded in February 2002 before the study began, and again in February 2003. Using site and species specific allometric equations (Mitchell et al. 1999) we calculated annual ANPP for 2003 by difference. Five and seven 0.25 m^2 litter traps were randomly located in each of the xeric and mesic split plots, respectively. Litter traps were emptied every two weeks in the fall, and monthly during the rest of the study. All litter was sorted, dried and weighed to 0.01 g accuracy. Species specific leaf mass-area relationships (S. Pecot, unpublished data) were used to calculate leaf area index (LAI, wet leaf projected leaf area (cm^2) = 24.851*dry foliage mass (g); R^2=0.93 $P<0.001$).

Wiregrass annual ANPP was determined by destructively subsampling in a 1 m diameter circle in November 2002 before the first killing frost. Five and seven subplots were harvested in each of the xeric and mesic split plots, respectively. Biomass was pooled across the subplots for each split plot. Wiregrass biomass was sorted into live and dead tissue categories, dried and weighed.

To determine total wiregrass leaf area in the plot, one wiregrass specific leaf area (cm^2 area g^{-1} mass) relationship was determined for each site type and treatment by subsampling 25 blades, and developing specific total leaf area relationships. Regression parameters for each site type and treatment were not significantly different from one another, so all measurements were pooled across treatments, and one regression equation predicting leaf area from mass was developed ($F=90.57$, adjusted $R^2=0.95$, $P<0.001$, PBA=24.18231-0.00455BSM). Total live blade biomass was scaled to the entire plot, and then used in the regression equation to predict live blade projected leaf area in the plot.

Sap flux density measurements

To estimate plant water use, different approaches were used based on life form. For trees, we estimated whole plant water use by installing thermal dissipation probes (Granier 1985) to calculate sap flux density of the outer 2 cm of the functional xylem. In each split plot, we measured sap flux density in a subsample of five trees. For logistical reasons, trees were not randomly chosen; however, a random location within the split plot was chosen and the five nearest trees were monitored for sap flux density. In xeric sites, sap flux density measurements were made on both *P. palustris* and *Quercus sp.* trees. In mesic sites, sap flux density measurements were only made on *P. palustris* trees. *Quercus sp.* were not monitored in mesic sites because of their absence or low frequency of occurrence (Table 2.1). For each tree monitored, we installed two sets of sap flux density probes circumferentially, occurring at least 90° apart. We constructed 2-cm long Granier-style sap flux density sensors (Granier 1985), which consisted of one upper heated probe and one lower reference probe. Each probe contained 1 thermocouple junction (TC) suspended in the shaft at 1 cm. In each sample tree, approximately 1.3 m above the ground, we drilled two holes separated vertically by 5 cm, but not

separated horizontally. We used a guide template to ensure that the holes were parallel. We removed enough bark and cambium around the holes to insert the sensors entirely into the xylem with the heating probe placed directly above the reference probe. The probes were coated with thermally-conductive silicone grease before placement in the trees. The areas around the probe insertion points were protected with Styrofoam blocks, and the stem of the tree was wrapped 360° with reflective insulation (Reflectix; Reflectix Inc., Markleville, IN, USA) to shield probes from solar radiation, thermal gradients, and rainfall. All lead wires were soldered to copper, double shielded cable wires (Model 9927; Belden Inc., Richmond, IN, USA). Thermocouple wires were differentially connected to a data logger (Models 10, 10X, and 23X Campbell Scientific, Logan, UT, USA; Model EasyLogger 900, Wescor Inc. Logan UT, USA) with a multiplexer peripheral (Models AM16/32, AM416, and AM32 Campbell Scientific, Logan, UT, USA; Model EA-110, Wescor Inc. Logan UT, USA). Sensors were queried every 10 min and these readings were compiled into 1 hr averages. The temperature difference (ΔT) between the upper and lower probes was converted to sap flux density using the equation of Granier (Granier 1985). For all trees, readings for the two replicate sets of sensors were averaged. Sensors were routinely replaced throughout the monitoring period if null, out of range, or negative readings were recorded, or if probes were physically damaged. Each tree was monitored for 365 days during the period May 2002-May2003.

At the end of the monitoring period, sapwood measurements were made. For *Quercus sp.*, dye was injected into the xylem at the height the sensors were located. After 30-60 min, trees were cored above and below the injection point and the sapwood radius was measured as the length of dyed xylem. If the sapwood radius was shorter than 2 cm, a corrected temperature difference was calculated according to Clearwater et al. (1999). If the sapwood radius was

longer than 2 cm, an even distribution of sap flux density was assumed and sap flux density (v, g H_2O m^{-2} sapwood s^{-1}) was converted to sap flow (F, g H_2O s^{-1}) by multiplying by the sapwood area of the tree, assuming that the sapwood area could be estimated by the area of a circle. For *P. palustris,* one increment core was taken near the location of the probes. Heartwood can be visually identified in *P. palustris* as dark red, resinous xylem. The sapwood radius was measured with a ruler to the nearest 0.1 cm on both cores. For all *P. palustris* trees measured, sapwood radius exceeded 2 cm. To scale sap flux density (v, g H_2O m^{-2} sapwood s^{-1}) to sap flow (F, g H_2O s^{-1}), we characterized the radial distribution of sap flux density on similar trees and used a mid-day slope (β=5) to integrate from the cambium to the heartwood or the center of the tree (for details see Ford et al. 2004).

After integrating sap flux density measurements across the sapwood, we scaled the resulting tree sap flow measurements to the whole plot level. We first computed the average sap flow of the trees measured in (kg H_2O h^{-1}), and computed monthly totals (kg H_2O $month^{-1}$). We then multiplied by the number of trees per ha in the plot and converted kg H_2O to mm of H_2O. These values were then corrected for the size of the trees measured relative to the size of the trees in the entire plot. To do this, we computed a ratio of the average basal area of all the trees in the plot to the average basal area of the trees measured. We then multiplied the plot monthly water use totals (mm H_2O $month^{-1}$) by this ratio. For the xeric sites that had oaks and pines, this scaling exercise was done separately for each genus (e.g. *Quercus sp.* and *Pinus palustris*).

Transpiration modeling

A transpiration model was used to estimate plant water use for wiregrass. Six wiregrass plants were excavated adjacent to the xeric and mesic sites, but occupying the same soil types found in

this study. The model had three major components—understory climate, leaf-level responses, and ecosystem scale estimates.

For the understory climate, we used measurements or estimates of photosynthetically active radiation (PAR), soil moisture content, and vapor pressure deficit. To estimate understory PAR throughout the study, 15-min average solar radiation was measured and recorded in at an open field weather station (LI200SA, Li-Cor Inc., Lincoln NE; CR10X, Campbell Scientific, Inc., Logan, UT, USA), and 15-min average PAR values at one spatial point in each mesic whole plot were measured for validation (LI190SB; Campbell Scientific, Inc., Logan, UT, USA). In the spring, we estimated the fraction of light reaching the understory in each split-plot by measuring PAR in 11-24 transects throughout the split plot on cloudless days (LI190SA, Li-Cor Inc., Lincoln NE). To calculate PAR (μmol quanta m^{-2} s^{-1}) in the understory, we converted the open field average total solar radiation measurements (R, Wm^{-2}) to PAR. We first assumed that 50% of R was in the 400-700nm wavelength, then used the conversion factor of 4.608μmol quanta J^{-1}, and lastly used the fraction of PAR reaching the understory as a scalar. This resulted in a time series of 15-min average PAR in the understory for each split-plot.

To estimate understory soil moisture content throughout the study, we made monthly measurements of soil moisture content in the 0-30 cm soil layer in each site type and treatment combination using time domain reflectometry ($\theta_{0\text{-}30,}$ TDR, model 1502-B, Tektronix, Inc., Beaverton, OR). We modeled daily soil water content using an exponential decay function in the form of

$$\boldsymbol{\theta_{0-30} = \theta_{max} \cdot e^{-k \cdot DSR} + \varepsilon} \qquad \text{(Equation 2.1)}$$

where θ_{max} is the maximum soil moisture content, $-k$ is a coefficient representing water lost from the 0-30 cm soil layer due to the processes of evaporation, transpiration, and water percolation

into deeper soil layers, and DSR is days since last rainfall event. A relationship between DSR and measured $\theta_{0\text{-}30}$ was developed for each site type and treatment combination using PROC GLM in SAS software (v8.02, SAS Inc., Carey, NC) on log and constant transformed data. Because relationships were different between site types ($P<0.001$), but not treatments ($P=0.986$), we pooled the data across treatments and developed one equation between DSR and measured $\theta_{0\text{-}30}$ for each site type using PROC NLIN in SAS software (v8.02, SAS Inc., Carey, NC), which estimated the two parameters above using the iterative Gauss-Newton method. During the wiregrass growing season, DSR ranged from 0 to 15 days, the median number of DSR was 1, and the average DSR was 2.3. Only two drying periods existed where DSR exceeded 10 days (both were 15 days). All of the TDR measurements were made between 0 and 6 DSR.

For understory vapor pressure deficit throughout the study, we assumed that open-field vapor pressure deficit (*D*) would approximate understory *D*. The open-field weather station measured ambient air temperature, relative humidity, and precipitation (Models HMP35C and TE525; Campbell Scientific, Inc., Logan, UT, USA), and recorded 15 min values (CR10X, Campbell Scientific, Inc., Logan, UT, USA). We used 15 minute averaged air temperature to calculate saturation vapor pressure (e_{sat}) using the Tetens formula (v. Murray 1967). Relative humidity and e_{sat} were used to compute *D*.

Wiregrass leaf level responses to understory climate were modeled using a normalized multiplicative reduction function on maximum transpiration rate (*E*, mmol H_2O m^{-2} s^{-1}; Jarvis 1976; Reed et al. 1976). Briefly, using the six wiregrass plants that were excavated adjacent to the xeric and mesic sites and planted in pots, we developed relationships between PAR, *D*, and $\theta_{0\text{-}30}$ and wiregrass *E* in the greenhouse. Under well-watered soil conditions and humid leaf chamber conditions ($D \leq 1$ kPa), *E* was measured under varying levels of PAR with an infrared

gas analyzer (Li-Cor 6400, Li-Cor Inc., Lincoln NE). Under saturating light (PAR=2000 μmol m^{-2} s^{-1}) and well-watered soil conditions, we measured *E* under varying levels of leaf *D*. Finally, under saturating light (PAR=2000 μmol m^{-2} s^{-1}) and humid leaf chamber conditions ($D \leq 1$ kPa), we measured *E* under varying levels of $\theta_{0\text{-}30}$. One function was fit to each data set, and then these predictive relationships were combined into the following reduction form:

$$E = E_{\max} \cdot \left(fE_{\max}\left(\frac{PAR}{PAR + k_p} \right) \right) \cdot \left(fE_{\max}\left(\frac{\theta_{0-30}}{\theta_{0-30} + k_d} \right) + \theta_{0-30} \cdot k_s \right) \cdot \left(fE_{\max} \cdot D \right) \qquad \text{(Equation 2.2)}$$

where *E* is the estimated transpiration rate of wiregrass (mmol H_2O m^{-2} s^{-1}); E_{max} is the maximum measured transpiration rate (12.4 mmol H_2O m^{-2} s^{-1}); and k_p, k_d, and k_s are constants (185.1, 0.56, and 0.004, respectively). Lastly, the parameter fE_{max} is the fraction of the maximum transpiration rate that is fitted for each environmental variable (for the PAR function, fE_{max} =0.706; for $\theta_{0\text{-}30}$, fE_{max} =0.755; for *D*, fE_{max} =0.232). Functions for PAR and $\theta_{0\text{-}30}$ were fit using non-linear iterative estimation, and the function for *D* was fit using least-squares linear regression using SigmaPlot software (SigmaPlot v8.02, SPSS Inc., Chicago IL). All functions and estimated parameters were significant at the α=0.05 level. Estimated rates of wiregrass *E* were evaluated against actual rates of *E* measured on wiregrass plants in the field during May (modeled peak of wiregrass transpiration). Using a linear model with no intercept, we regressed estimated rates against actual rates and the slope was not significantly different than 1 (F=2.86, P=0.15, slope=0.85, R^2=0.95).

Leaf level responses were scaled to the ecosystem level on an hourly time step. We first calculated the fraction of annual leaf area present in each plot over time. We estimated wiregrass leaf-elongation through time using data collected over three years from Parrott (1967). Transpiration rates were multiplied by the fraction of leaf area in the plot, and then scaled to the

hectare level and converted to mm H_20. Transpiration estimates are presented for January 2002-December 2002.

Experimental design and statistics

We used a paired t-test to test for pre-treatment differences between split plots (fertilized and control). We calculated aboveground standing tree biomass for each split plot before the fertilization treatment was applied. The difference in biomass between fertilized and control split plots was compared against zero.

For ANPP, transpiration (*E*) and water use efficiency (WUE, ANPP/transpiration), data were analyzed as a split-split-plot design with three fixed factors: site-type (mesic, xeric), treatment (fertilized, control), and plant functional type (oak, pine, grass). For *E* and WUE, the design was not balanced at the level of plant function type (i.e. oaks were not monitored for *E* in mesic sites). In this case, data were analyzed two separate ways. One analysis used each site type in a split-plot design with treatment and plant functional type as fixed factors. The second analysis used plot totals (the plant functional type factor was collapsed by summing) in a split-plot design with site type and treatment as fixed factors.

We used PROC GLM in SAS software (SAS v8, SAS Inc., Carey NC), and specified the following F tests: to test for the whole-plot effect, we used the whole-plot mean square error; to test for the effect of the split-plot and the whole-plot by split-plot interaction, we used the split plot mean square error; all other tests of effects used the full model mean square error term. When appropriate, a post-hoc means separation was performed on plant functional type using Tukey's HSD.

Source water determination

In each whole plot, we installed piezometer wells in 2001. During the monitoring period, ground water table depths and fluctuations were measured weekly with a water level indicator (Slope Indicator, Mukilteo, WA, USA). Groundwater was also sampled periodically by priming the well, and then collecting ground water into a sterile vial. Precipitation samples were collected from each event during the monitoring period. A clean, dry collection bottle was placed in an open field during precipitation events. Immediately after precipitation events, a subsample of the precipitation water was placed in a sterile vial. All precipitation and groundwater sample vials were immediately capped, wrapped with Parafilm, and stored at 4°C until analysis.

To estimate the water sources used by the trees and grass, we sampled xylem tissue for xylem water extraction in August 2003. For the oaks (n=3), small branches were clipped and placed in sterile vials. For the pines (n=3), 3 cm increment cores were sampled from the stems and placed in sterile vials. For the grasses (n=3), the non-photosynthetic root collars were sampled from individual plants that were in open areas (i.e. outside of the canopy areas). Bulk soil samples (n=3) from 0-15 cm were also sampled and placed in sterile vials. All vials were capped, caps were wrapped in Parafilm, and samples were stored at 4°C until extraction. All plant tissue and soil samples were cryogenically extracted under vacuum (Ehleringer et al. 2000). Extracted tissue and soil water, precipitation and groundwater samples were analyzed for stable hydrogen isotope ratio (δD), and precipitation samples were also analyzed for stable oxygen isotope ratio ($\delta^{18}O$) at University of California, Berkeley Center for Stable Isotope Biogeochemistry. A two-end member mixing model was used to estimate the fraction of groundwater (f_{GW}) utilized by the plant functional groups sampled (Phillips and Gregg 2001). The two-end member mixing model had the general form:

$$f_{GW} = \frac{\delta_X - \delta_{SW}}{\delta_{GW} - \delta_{SW}} \quad \text{(Equation 2.3)}$$

where δ is the stable isotope ratio, and the subscripts GW, SW, and X refer to groundwater, soil water and extracted xylem water, respectively. The two end members were groundwater from the water table lying on top of the limestone layer bounding the Upper Floridan Aquifer, and soil water in the 0-15 cm profile (bulked sample). For the groundwater signal, we used the temporally averaged groundwater signal. For the soil water signal, we used a point-in-time signal that was the average of three spatial points. For the plant signal, we averaged the xylem isotopic signals of three individuals sampled at one time in each whole plot.

Results

Climate and ANPP patterns

During the study period, 24 h average temperatures ranged 30.2 to -3.6 degrees C and total precipitation was 1980.9 mm (Figure 2.2). Precipitation is generally evenly distributed throughout the year; however, in year 2002, 62% of the annual total precipitation fell in the 5-month period between June and November, with April and May having the lowest precipitation. Water table depths fluctuated throughout the period (Figure 2.2), but in general, water tables among the sites were approximately 6 m deep, with the deepest being 10 m at one site and the shallowest being 2 m. Seasonal fluctuations in the water table were correlated with leaf area, such that when understory leaf area and demand for water was low, precipitation recharged the groundwater table.

Stand structure, standing biomass and tree density were markedly different between mesic and xeric sites (Table 2.1). In general, mesic sites had more trees per hectare, more

standing aboveground tree biomass, and fewer oak stems compared to xeric sites. Although the xeric sites had an equal number of pine and oak stems per ha, oaks constituted only 18% of the total tree standing biomass. Before treatment application, total tree standing biomass did not differ between control and fertilized split-plots ($t=1.32$ $P=0.23$).

Annual ANPP estimates were greater in mesic compared to xeric sites ($F=6.35$, $P=0.08$; Figure 2.3). In the mesic sites annual ANPP ranged from 1.34 to 3.26 Mg ha^{-1}, and averaged 2.27 Mg ha^{-1}. The xeric stands tended to be less productive on an annual basis. Annual ANPP ranged from 0.94 to 1.61 Mg ha^{-1}, and averaged 1.13 Mg yr^{-1}. When fertilized, both site types became significantly more productive ($F=29.34$ $P<0.01$; Figure 2.3). Annual ANPP for the fertilized mesic sites ranged from 2.54 to 3.66 Mg ha^{-1}, and averaged 3.09 Mg yr^{-1}. Annual ANPP for the fertilized xeric sites ranged from 1.48 to 2.51 Mg ha^{-1}, and averaged 1.95 Mg yr^{-1}. Fertilization did not differentially affect mesic and xeric sites (i.e. no significant site type by treatment interaction).

Annual ANPP by the three plant functional types differed (Figure 2.4), but differences were not consistent between mesic and xeric sites (i.e. significant interaction between plant functional type and site type, $F=20.80$ $P<0.001$). In the mesic sites, pine production dominated grass and oak production (Figure 2.4), and averaged 1.86 Mg ha^{-1}. Grass and oak ANPP did not differ and averaged 0.34 and 0.06 Mg ha^{-1}, respectively. When fertilized, ANPP was significantly greater by all plant functional types in the mesic sites. On average, increasing N increased pine production by 0.49 Mg ha^{-1} and grass production by 0.33 Mg ha^{-1}. Grass and oak ANPP were not different from one another and averaged 0.67 and 0.06 Mg ha^{-1}, respectively. On a percentage basis, annual contribution to ANPP in the control sites was 3.8% oak, 82.8%

pine and 13.4% grass. When fertilized, annual contribution to ANPP on a percentage basis was 1.7% oak, 76.7% pine and 21.6% grass (Figure 2.5).

In the xeric sites, pine and grass production exceeded the oak production. Pine ANPP (Figure 2.4) averaged 0.59 Mg ha^{-1}. Grass ANPP averaged 0.39 Mg ha^{-1}. Pine and grass annual ANPP were not different from one another, but significantly different from oak ANPP. Oak ANPP (Figure 2.4) averaged 0.15 Mg ha^{-1}. When fertilized, ANPP was significantly higher by all plant functional types in the xeric sites. On average, increasing N increased pine production by 0.19 Mg ha^{-1}, grass production by 0.53 Mg ha^{-1}, and oak production by 0.09 Mg ha^{-1}. On a percentage basis, annual ANPP in the control sites was 13.8% oak, 51.4% pine and 34.8% grass. When fertilized, annual ANPP on a percentage basis was 13.9% oak, 38.9% pine and 47.2% grass (Figure 2.5).

Annual and seasonal water use: patterns between sites and plant functional types

Annual transpiration was significantly higher in the mesic site type compared to xeric ($F=136.65$ $P<0.01$; Figure 2.3). In the mesic sites annual transpiration ranged 277.17 to 500.52 mm H_2O, and averaged 380.05 mm. The drier stands transpired less water on an annual basis. Annual transpiration ranged 59.47 to 136.47 mm H_2O, and averaged 107.97 mm. Fertilization did not significantly affect either site type (Figure 2.3). Annual transpiration for the fertilized mesic sites ranged 258.35 to 528.93 mm H_2O, and averaged 370.31 mm. Annual transpiration for the fertilized xeric sites ranged 101.41 to 190.99 mm H_2O, and averaged 146.14 mm.

Annual transpiration by the three plant functional types differed (Figure 2.4). Fertilization had no effect on transpiration by the plant functional types in the xeric and mesic sites (no fertilization by plant functional type interaction); however, wiregrass tended to have higher transpiration rates when fertilized (Figure 2.6). In the mesic sites, pine transpiration,

averaging 350.65 mm, was more than an order of magnitude greater then grass transpiration, which averaged 24.53 mm (note: averages reported here are pooled across treatments) (Figure 2.4). On a percentage basis, 91 to 96% of total annual transpiration in the mesic sites was due to only pine, while 9 to 4% was attributed to wiregrass (Figure 2.5). In the xeric sites, transpiration was significantly different among pine and oak plant functional types. Pine transpiration, averaging 73.64 mm, was higher than grass and oak transpiration, averaging 31.20 and 22.21 mm respectively (Figure 2.4). On a percentage basis, annual transpiration in the xeric sites was comprised of 54 to 56% pine, 17 to 30% grass, and 16 to 27% oak (Figure 2.5).

The highest rates of transpiration occurred during May-September (Figure 2.6) when both the overstory and understory supported leaf area. A strong seasonal pattern was evident in the grass plant functional type in both the mesic and xeric site types, and in the pine functional type in the mesic sites. In general, the period of peak transpiration by the different structural layers (trees and grass) was out of synchrony in both mesic and xeric sites; thus a bimodal distribution of transpiration was evident, with the grass functional type peaking in late spring to early summer, and the trees peaking in late summer (Figure 2.6). Because of this temporal difference in the plant functional types, the xeric sites had an earlier peak in transpiration than the mesic sites. At the leaf level, we found that for any *D*, pine transpiration in the mesic sites was much greater compared to the xeric sites (Figure 2.7). Compared to pines, the grass functional type had a much higher transpiration per LAI, and could maintain a higher rate of transpiration at high vapor pressure deficits (Figure 2.7).

Water use efficiency

WUE was greater in xeric site plants compared to mesic site plants (Figure 2.3; $F=13.76$, $P=0.03$). WUE for xeric site plant communities averaged 18.82 and 20.71 kg mm^{-1} in the

fertilized and control plots, while community-based WUE for mesic sites averaged 14.28 to 13.25 kg mm^{-1} in the fertilized and control plots (Figure 2.3). Fertilization did not influence WUE regardless of site type or plant functional type. Within the xeric site type, the plant functional types were similar in their annual water use efficiencies (Figure 2.4); however, within the mesic site type, wiregrass showed greater water use efficiency than that observed for pines ($F=183$, $P<0.001$; Figure 2.4).

Stable isotope patterns (δD)

Precipitation (*P*) δD signals analyzed throughout the study varied depending on the temperature, with winter *P* showing greater depletion in the heavier isotope (mean -36‰, Figure 2.8), while *P* during other periods was more enriched (mean -10‰). The average groundwater (GW) signal was -34.9 ‰ (SMOW) and did not differ between mesic and xeric sites. In August the mesic and xeric sites in which we sampled trees and grasses for xylem water had a groundwater table depth of 326 cm and 780 cm, respectively. Given the variability in GW and soil signatures, coupled with the GW table rising in the winter (winter recharge) and falling during the growing season (Figure 2.2), we assumed that these two end members reflected the temporal pattern in precipitation signals. In August, at the peak of tree transpiration, the average soil water signal in the xeric site was -8.4‰ and -3.3‰ in the mesic site. From these two end members, during this time the percent groundwater signal found in the pines was 94%, 77-85% in the oaks, and 32% in the mesic grasses, and 62% in the xeric grasses (Figure 2.9).

Discussion

Savanna productivity is generally constrained due to low LAI, which in turn is limited by climate, fertility and/or disturbance. In the present study system, the stand structure is

maintained, and production and LAI are limited by a frequent fire disturbance regime (1-3 year return interval), low soil nutrient status, and low water holding capacity by soils. Net N mineralization in the top 10 cm of soil on typical xeric and mesic sites in our system averages 12.3 and 3.7 kg N ha^{-1} yr^{-1} (Wilson et al. 2002), and measured annual ANPP demand for N exceeds supply of N on both site types (Wilson et al. 2002). Our estimates of projected LAI were similar to those made by Addington (2001) in this same system. For example, our average mesic and xeric site pine LAI was 1.76 and 1.07, respectively, compared to an average pine LAI in mesic and xeric sites of 1.1 and 0.4, respectively, measured by Addington (2001) during a four-year drought period. In general, the range of LAI in this system is low compared to other mesic southeastern forests, mean projected LAI 5.8 (Bolstad et al. 2001), and southeastern pine plantations, mean projected LAI 3.5 (Jokela et al. 2004). Our estimates of LAI for this system, however, are comparable to LAI reported for seasonally dry Australian savannas (Hutley et al. 2000; O'Grady et al. 2000), California blue oak savannas (Baldocchi et al. 2004), and northern bur oak savannas (Reich et al. 2001). The range of mean total annual ANPP that we measured in this study was 1.13 (xeric control site) to 3.09 (mesic fertilized site) Mg biomass ha^{-1} yr^{-1}, which adjusting for tree density is similar to the rates of ANPP measured by (Mitchell et al. 1999). Our estimates of total annual ANPP were also similar to those of seasonally dry Australian savannas, measured at 3.0 Mg C ha^{-1} yr^{-1} (Chen et al. 2003) with an overstory LAI of 0.95 (Hutley et al. 2000), and similar to the annual ANPP of low nutrient savannas in Minnesota (Reich et al. 2001). In general, the range of annual ANPP in this system is low compared to other southeastern forests, average 9 Mg biomass ha^{-1} yr^{-1} (Bolstad et al. 2001) and intensively managed southeastern pine plantations, average 10 Mg biomass ha^{-1} yr^{-1} (McNulty et al. 1996). With an increased supply of N, annual ANPP increased across all site types and plant functional

types. These results are consistent with the pattern of increasing ANPP across a range of sites with increasing N mineralization in bur oak savannas (Reich et al. 2001). However, our results are contrary to the results of Mitchell et al. (1999) who found that ANPP increased across a natural gradient of decreasing N mineralization. This may be due to the relatively large amounts of N applied in the present study compared to the in-situ rates of N mineralization measured across these site types (Wilson et al. 2002).

The grass structural layer in savannas, in general, constitutes a large fraction of annual ANPP. In the present study, we found that in the mesic site type production by the overstory exceeded production by the understory by a ratio of four to one. However, production in the two structural layers was about equal in the xeric site type. These differences are within the range reported for seasonally dry savannas. For example, in dry African savanna woodlands, understory production constitutes 70% of the total annual ANPP (Menaut and Cesar 1979). In seasonally dry Australian savannas, tree ANPP is 2.5 Mg biomass ha^{-1} yr^{-1} and understory ANPP is 0.5 Mg biomass ha^{-1} yr^{-1} (Chen et al. 2003), i.e. understory production was 17% of total annual ANPP.

Transpiration is also low in savanna systems due to limited leaf area. We found relatively low annual rates of transpiration (108 to 380 mm ha^{-1} yr^{-1}) in this system. Transpiration on the xeric sites was much lower (108-146 mm ha^{-1} yr^{-1}) than the mesic sites (370-380 mm ha^{-1} yr^{-1}), due to lower leaf area and lower soil moisture. In addition to lower leaf area, for any given *D*, rates of transpiration per LAI were greater for mesic site trees compared to xeric site trees. These results are similar to those of Addington (2001) who also found that xeric site trees have a significantly greater stomatal sensitivity to increasing vapor pressure deficit compared to mesic site trees. Integrating across our sites, our rates of annual transpiration are

somewhat lower than those measured for Piedmont oak pine hickory forests, 278 mm yr^{-1} (Oren and Pataki 2001), Piedmont loblolly pine hardwood forests, 355 mm yr^{-1} (Phillips and Oren 2001), and an Appalachian mature upland oak forest, 313 mm yr^{-1} (Wullschleger et al. 2001). In the present study, the average (n=4 plots) maximum daily rate of transpiration reached 1.21 and 0.91 mm day^{-1} in the xeric fertilized and control plots, respectively, and 2.83 and 2.61 mm day^{-1} in the mesic fertilized and control plots, respectively (data not shown). These rates were typically achieved during clear, sunny days with a relatively large VPD following rain events. These rates are similar to those obtained for widely-spaced old-growth Ponderosa pine ecosystems. Summer rates of mean evapotranspiration in old-growth Ponderosa pine have been reported as 1.6-1.7 mm day^{-1} and maximum rates have been reported to be approximately 4 mm day^{-1} (Anthoni et al. 1999). Although we did not quantify evaporation from the soil or interception in this study, if we assume soil evaporation is 15-25% of daily transpiration, as has been reported for grasslands and savannas (Ferretti et al. 2003; Yepez et al. 2003), then our rates of average maximum daily evapotranspiration would be in the range of 1.5-3.5 mm day^{-1}.

During times when grass and pine functional types were transpiring concurrently (see Figure 2.6), daily grass transpiration exceeded daily pine transpiration an average (n=4 plots) of 20% and 9% of the time in the xeric control and fertilized sites, respectively, and this primarily occurred during May when *D* was relatively large. In contrast, grass transpiration never exceeded pine transpiration in the mesic sites. In a mesquite and C_4 bunchgrass semi-arid savanna, total evapotranspiration after a wet period was 3.5 mm day^{-1}, of which 85% was transpiration. This was further partitioned into savanna structural layers (trees and grass), 70% of total evapotranspiration was transpired from the tree-layer and 15% was transpired from the

grass-layer (Yepez et al. 2003). This is similar to the percentages of annual water use transpired by grasses in our system.

We found that xeric sites were more water use efficient compared to the mesic sites. Similarly, Addington (2001) found that the $\delta^{13}C$ of xeric long leaf pine leaf tissue was more enriched in the heavier isotope compared to trees on the mesic sites (xeric -26.7‰ vs. mesic -28.3‰), indicating a greater integrated water use efficiency. Interestingly, in the xeric sites, no differences existed in water use efficiency among plant functional types, regardless of leaf habit (evergreen vs. deciduous) or carbon metabolism (C_3 vs. C_4). McNulty et al. (1996) modeled evapotranspiration and total NPP of a fully stocked (~1500 trees ha^{-1}), unfertilized loblolly pine plantation in southwest Georgia. The model predicted an average annual evapotranspiration rate of 791 mm yr^{-1} and NPP of 9.4 Mg biomass ha^{-1} yr^{-1}, which is a WUE of 1.18 kg mm^{-1}. This estimate is less than what we report for the least water use efficient component in our system; longleaf pine in mesic sites averaged 5 kg aboveground biomass mm^{-1} water.

Consistent with Walter's two-layer model, we found that across site types trees were using groundwater almost exclusively, while grasses used a higher proportion of soil water. This finding is consistent with reported rooting distributions of trees and grasses across diverse biomes (Jackson et al. 1996). Our results are also consistent with descriptions of longleaf pine rooting systems. For example, Heyward (1933) excavated the root system of a mature longleaf pine growing on deep sandy soils and found that the long tap root ended at 431.8 cm, but that thick cordlike roots extended vertically beyond that depth. Although Heyward (1933) concluded that these deep roots were not important in water or nutrient uptake but seemed more important as an anchoring system for the tree, our results suggest that these deep roots are functional, at least in water conduction. Other studies have found that trees and grasses in savannas utilize

different water sources. For example, Weltzin and McPherson (1997) showed that mature *Quercus emoryi* trees used primarily deep-water sources while coexisting bunchgrasses used shallow water sources. Similarly, Ludwig (2001) demonstrated that *Acacia tortilis* trees use deep groundwater sources compared to shallow soil water sources used by grasses in an African savanna. In Australian savannas, Eamus et al. (2001) have shown that tree water use is not seasonally variable, but that understory grass water use peaks in the wet season, suggesting that the trees have a deeper and more stable water source than the grasses. In the present study we found that the variability in transpiration rates was affected by the source water utilized. In savannas dominated by *Quercus* and *Juniperus spp.*, Jackson et al. (1999) found that roots down to 22 and 65 m were functional in water uptake. In the present study, because trees were able to rely on groundwater for transpiration, presumably a more stable water source than shallow soil water, the variability in rates of transpiration was always lower for pines (average coefficient of variation, CV, 51%) compared to grasses (average CV 62%) regardless of site type. Within the grass plant functional type, we found that percentage of groundwater utilized varied with site type. Grasses in the xeric site used a higher percentage of groundwater than grasses in the mesic site. Moreover, we found that this variation could be linked to annual ANPP. Because the xeric sites have lower soil moisture content in the upper 15 cm of the soil, we might have expected productivity of grasses to be constrained. However, grasses were significantly more productive in the xeric sites compared to mesic (plant functional type and site type interaction, $F=20.80$ $P<0.001$). These data are consistent with our observation that xeric grasses used more groundwater, which is a more stable water source, compared to mesic grasses. This finding suggests that grasses on the xeric site type may have a dimorphic rooting pattern, while grasses on the mesic site type may have a shallower rooting system.

Implications for land-use change and future studies

Longleaf pine wiregrass savanna covered 24 million ha of the Southeastern Coastal Plain prior to European settlement. In the current landscape, longleaf pine wiregrass savannas have been reduced to 2% of their pre-settlement extent and are listed as an endangered ecosystem (Noss et al. 1995). The reduction in area of this ecosystem is due to a combination of human-mediated factors—logging of the overstory pines for timber, land conversion to center-pivot irrigated crop land and pine plantations, decreased seedling survivorship due to introduced feral pigs, and succession to hardwoods following fire-suppression practices (see Outcalt 2000). Although the vegetation types replacing the longleaf pine wiregrass savanna are more productive, they are less species diverse (Kirkman et al. 2001) and less water-use efficient. Although this study quantified annual plant water use, long-term comparative studies of ecosystem water use between pine plantations, center-pivot irrigated crop lands, and native forests are much needed in this region, because land-use conversions, such as those described above, are likely affecting the long term dynamics of the local hydrologic cycle.

Acknowledgements

This study was supported by the University of Georgia Daniel B. Warnell School Of Forest Resources, the Robert W. Woodruff Foundation and the Joseph W. Jones Ecological Research Center. This publication was also developed under EPA STAR Fellowship Agreement No. 91617001-0 awarded by the U.S. Environmental Protection Agency. It has not been formally reviewed by EPA. The views expressed in this document are solely those of the authors and EPA does not endorse any products or commercial services mentioned in this publication. We thank the FEII Lab, Jay Brown, Bob Cooper, Lisa Donovan, Ron Hendrick, Jon Miniat, Jason Nedlo, and Rod Will for their logistical help, help with field work, and overall support.

References

Addington, R. 2001. Water use patterns and stomatal responses to environment in longleaf pine on contrasting sites. MS thesis. University of Georgia, Athens, GA. p. 68.

Anthoni, P.M., B.E. Law and M.H. Unsworth 1999. Carbon and water vapor exchange of an open-canopied ponderosa pine ecosystem. Agric. For. Meteorol. 95:151-168.

Baldocchi, D., L. Xu and N. Kiang 2004. How plant functional-type, weather, seasonal drought, and soil physical properties alter water and energy fluxes of an oak-grass savanna and an annual grassland. Agric. For. Meteorol. 123:13-39.

Bolstad, P.V., J.M. Vose and S. McNulty 2001. Forest productivity, leaf area, and terrain in southern Appalachian deciduous forests. For. Sci. 47:419-427.

Chen, X., L.B. Hutley and D. Eamus 2003. Carbon balance of a tropical savanna of northern Australia. Oecologia. 137:405-416.

Clearwater, M.J., F.C. Meinzer, J.L. Andrade, G. Goldstein and N.M. Holbrook 1999. Potential errors in measurement of nonuniform sap flow using heat dissipation probes. Tree Physiol. 19:681-687.

Dodd, M.B., J.M. Lauenroth and J.M. Welker 1998. Differential water resource use by herbaceous and woody plant life-forms in a shortgrass steppe community. Oecologia. 117:504-512.

Eamus, D., L.B. Hutley and A.P. O'Grady 2001. Daily and seasonal patterns of carbon and water fluxes above a north Australian savanna. Tree Physiol. 2:977–988.

Ehleringer, J.R., J.S. Roden and T.E. Dawson 2000. Assessing ecosystem-level water relations through stable isotope ratio analysis. *In* Methods in Ecosystem Science Eds. O.E. Sala,

R.B. Jackson, H.A. Mooney and R.W. Howarth. Springer-Verlag, New York, pp. 181-198.

Ferretti, D.F., E. Pendall, J.A. Morgan, J.A. Nelson, D. LeCain and A.R. Mosier 2003. Partitioning evapotranspiration fluxes from a Colorado grassland using stable isotopes: Seasonal variations and ecosystem implications of elevated atmospheric CO_2. Plant and Soil. 254:291-303.

Ford, C.R., M.A. McGuire, R.J. Mitchell and R.O. Teskey 2004. Assessing variation in the radial profile of sap flux density in *Pinus* species and its effect on daily water use. Tree Physiol. 24:241–249.

Foster, B.L. and D. Tilman 2003. Seed limitation and the regulation of community structure in oak savanna grassland. J. Ecol. 91:999-1007.

Goebel, P.C., B.J. Palik, L.K. Kirkman and L. West. 1997. Field Guide: Landscape ecosystem types of Ichauway. Joseph W. Jones Ecological Research Center, Newton, GA.

Granier, A. 1985. Une nouvelle méthode pour la mesure du flux de sève brute dans le tronc des arbres. Annales des Sciences Forestieres. 42:193-200.

Heyward, F. 1933. The root system of longleaf pine on the deep sands of western Florida. Ecology. 14:136-148.

Higgins, S.I., W.J. Bond and W.S.W. Trollope 2000. Fire, resprouting and variability: A recipe for grass-tree coexistence in savanna. J. Ecol. 88:213-229.

Hungate, B.A., M. Reichstein, P. Dijkstra, D. Johnson, G. Hymus, J.D. Tenhunen, C.R. Hinkle and B.G. Drake 2002. Evapotranspiration and soil water content in a scrub-oak woodland under carbon dioxide enrichment. Global Change Biology. 8:289-298.

Hutley, L.B., A.P. O'Grady and D. Eamus 2000. Evapotranspiration from Eucalypt open-forest savanna of Northern Australia. Functional Ecology. 14:183-194.

Jackson, R.B., J. Canadell, J.R. Ehleringer, H.A. Mooney, O.E. Sala and E.D. Schulze 1996. A global analysis of root distributions for terrestrial biomes. Oecologia. 108:389-411.

Jackson, R.B., L.A. Moore, W.A. Hoffmann, W.T. Pockman and C.R. Linder 1999. Ecosystem rooting depth determined with caves and DNA. Proceedings of the National Academy of Sciences of the United States of America. 96:11387-11392.

Jarvis, P.G. 1976. The interpretation of the variations in leaf water potential and stomatal conductance found in canopies in the field. Philosophical Transactions of the Royal Society of London, B. 273:593-610.

Johnson, R.W. and J.C. Tothill 1984. Definition and broad geographic outline of savanna lands. *In* International Savanna Symposium 1984 Eds. J.C. Tothill and J.C. Mott. Australian Academy of Science, Canberra, pp. 1-13.

Jokela, E.J., P.M. Dougherty and T.A. Martin 2004. Production dynamics of intensively managed loblolly pine stands in the southern United States: a synthesis of seven long-term experiments. For. Ecol. Manage. 192:117-130.

Kimmins, J.P. 1987. Forest Ecology. Macmillan, New York. 531 p.

Kirkman, L.K., K.L. Coffey, R.J. Mitchell and E.B. Moser 2004. Ground cover recovery patterns and life-history traits: implications for restoration obstacles and opportunities in a species-rich savanna. J. Ecol. 92:409-421.

Kirkman, L.K., R.J. Mitchell, R.C. Helton and M.B. Drew 2001. Productivity and species richness across an environmental gradient in a fire-dependent ecosystem. Amer. J. Bot. 88:2119-2128.

Leach, M.K. and T.J. Givnish 1999. Gradients in the composition, structure, and diversity of remnant oak savannas in southern Wisconsin. Ecol. Monogr. 69:353-374.

Ludwig, F. 2001. Tree-grass interactions on an east African savanna: The effects of competition, facilitation and hydraulic lift. Ph.D. Dissertation. Wageningen University. p. 139.

McNulty, S., J.M. Vose and W.T. Swank 1996. Loblolly pine hydrology and productivity across the southern United States. For. Ecol. Manage. 86:241-251.

Menaut, J.C. and J. Cesar 1979. Structure and Primary Productivity of Lamto Savannas, Ivory Coast. Ecology. 60:1197-1210.

Mitchell, R.J., L.K. Kirkman, S.D. Pecot, C.A. Wilson, B.J. Palik and L.R. Boring 1999. Patterns and controls of ecosystem function in longleaf pine-wiregrass savannas. I. Aboveground net primary productivity. Can. J. For. Res. 29:743-751.

Moreira, M.Z., F.G. Scholz, S.J. Bucci, L.S. Sternberg, G. Goldstein, F.C. Meinzer and A.C. Franco 2003. Hydraulic lift in a neotropical savanna. Functional Ecology. 17:573-581.

Murray, F.W. 1967. On the computation of saturation vapor pressure. J. Appl. Meteorol. 6:203-204.

Noss, R.F., E.T. LaRoe and J.M. Scott. 1995. Endangered ecosystems of the United States: A preliminary assessment of loss and degradation. Natl. Biol. Serv., Dept. Interior, Washington, DC, p. 58.

O'Grady, A.P., X. Chen, D. Eamus and L.B. Hutley 2000. Composition, leaf area index and standing biomass of eucalypt open forests near Darwin in the Northern Territory, Australia. Australian Journal of Botany. 48:629-638.

Oren, R. and D.E. Pataki 2001. Transpiration in response to variation in microclimate and soil moisture in southeastern deciduous forests. Oecologia. 127:549-559.

Outcalt, K.W. 2000. The longleaf pine ecosystem of the south. Native Plants Journal. 1:42-51.

Parrott, R.T. 1967. A study of wiregrass (*Aristida stricta* Michx.) with particular reference to fire. *In* Botany. Duke University, Durham, p. 137.

Phillips, D.L. and J.W. Gregg 2001. Uncertainty in source partitioning using stable isotopes. Oecologia. 127:171-179.

Phillips, N. and R. Oren 2001. Intra- and inter-annual variation in transpiration of a pine forest. Ecol. Appl. 11:385–396.

Reed, K.L., E.R. Hamerly, B.E. Dinger and P.G. Jarvis 1976. Analytical model for field measurements of photosynthesis. Journal of Applied Ecology. 13:925-942.

Reich, P.B., D.W. Peterson, D.A. Wedin and K. Wrage 2001. Fire and vegetation effects on productivity and nitrogen cycling across a forest-grassland continuum. Ecology. 82:1703-1719.

Scanlon, T.M. and J.D. Albertson 2004. Canopy scale measurements of CO_2 and water vapor exchange along a precipitation gradient in southern Africa. Global Change Biology. 10:329-341.

Scholes, R.J. and S.R. Archer 1997. Tree-grass interactions in savannas. Annu. Rev. Ecol. Systemat. 28:517-544.

Smith, D.M., P. Jarvis and J.C.W. Odongo 1997. Sources of water used by trees and millet in Sahelian windbreak systems. J. Hydrol. 198:140-153.

Walker, J. and R.K. Peet 1983. Composition and species diversity of pine-wiregrass savannas of the Green Swamp, North Carolina. Vegetatio. 55:163-179.

Walter, H. 1971. Ecology of tropical and subtropical vegetation. Oliver and Boyd, Edinburgh. 539 p.

Walter, H. 1973. Vegetation of the earth in relation to climate and the ecophysological conditions. Springer-Verlag, New York. 237 p.

Weltzin, J.F. and G.R. McPherson 1997. Spatial and temporal soil moisture resource partitioning by trees and grasses in a temperate savanna, Arizona, USA. Oecologia. 112:156-164.

Wilson, C.A., R.J. Mitchell, L.R. Boring and J.J. Hendricks 2002. Soil nitrogen dynamics in a fire maintained forest ecosystem: results over a 3-year burn interval. Soil Biology and Biochemistry. 34:679-689.

Wullschleger, S.D., P.J. Hanson and D.E. Todd 2001. Transpiration from a multi-species deciduous forest as estimated by xylem sap flow techniques. For. Ecol. Manage. 143:205-213.

Yepez, E.A., D.G. Williams, R.L. Scott and G.H. Lin 2003. Partitioning overstory and understory evapotranspiration in a semiarid savanna woodland from the isotopic composition of water vapor. Agric. For. Meteorol. 119:53-68.

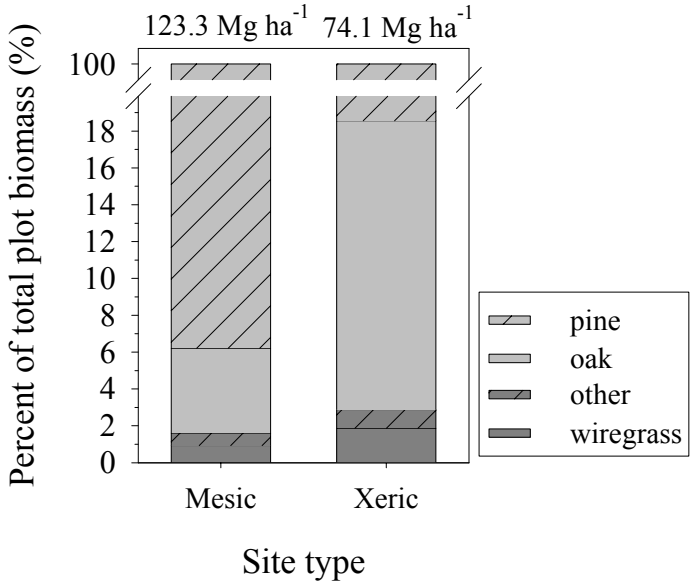

Figure 2.1 Average percent of total standing plot biomass comprised by each plant functional group. Total standing biomass is given above the bars, and represents the average of 8 replicate plots. Understory is represented by the wiregrass and other groups, and was determined by clipping all shrubs, forbs, and grasses in a circular plot (see methods for details). Overstory is represented by the pine and oak group. Within the oak group, roughly 1-2% of non-pine and non-oak trees were included and were represented by species such as *Diospyros virginiana*.

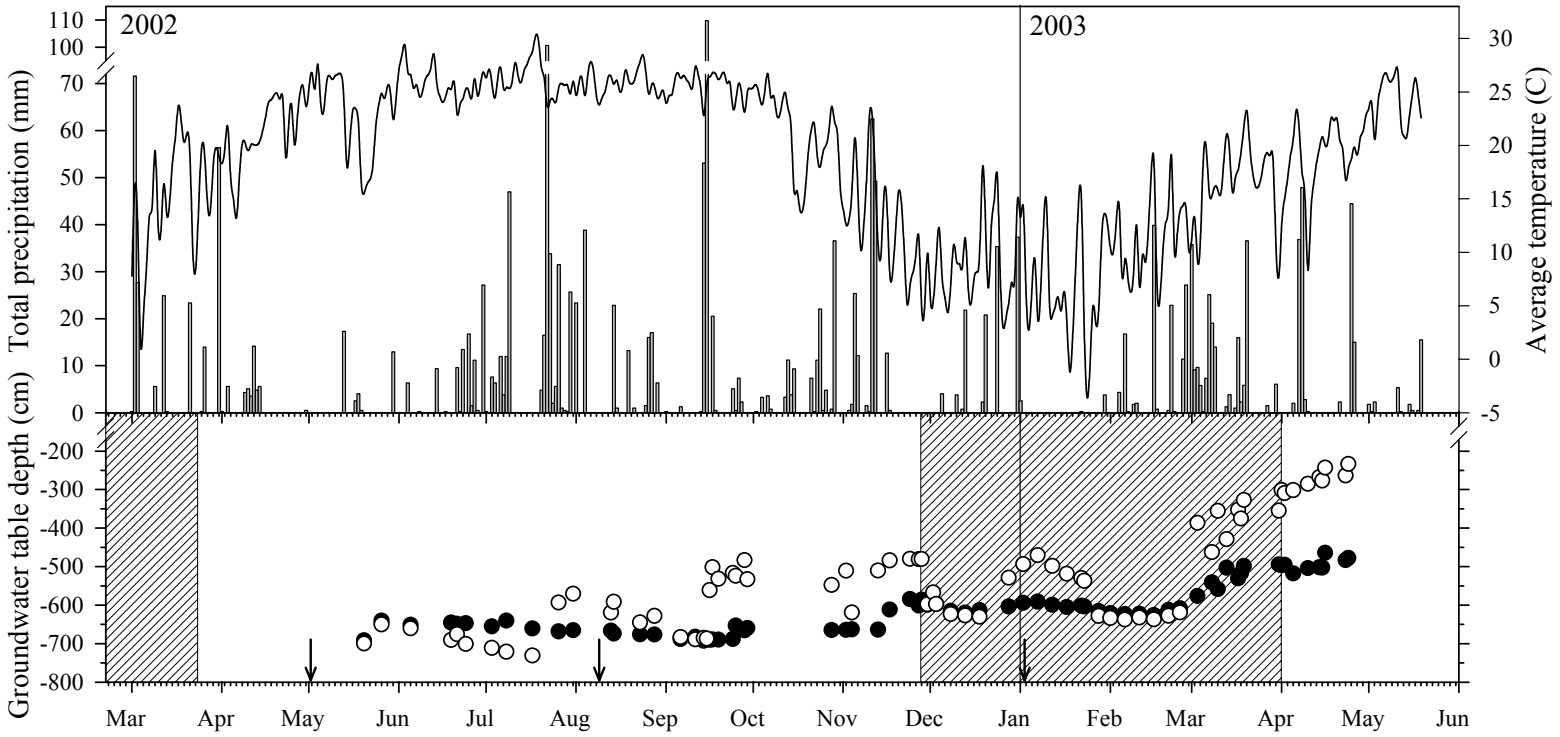

Figure 2.2 Total daily precipitation and average daily temperature during study period. Groundwater table position time series represents the average water table position of two mesic (open symbols) and two xeric (closed symbols) sites. Due to data collection schedule, positions of all four sites did not occur on the same day. Arrows represent timing of broadcast fertilization. Hatched areas represent periods with frost events.

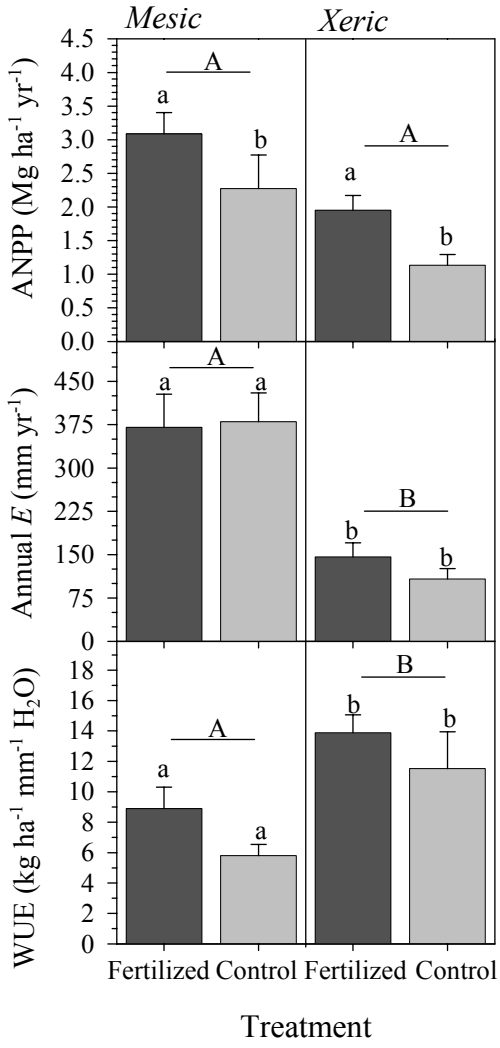

Figure 2.3 Total ANPP, *E*, and WUE for fertilized and control, mesic and xeric site types, (total was calculated as the sum of oak, pine and grass ANPP, *E*, and WUE). Mean and standard error bar shown. Different capital letters denote significant differences among whole-plots (mesic and xeric). Different lowercase letters denote significant differences among split-plots within whole-plots (fertilized and control).

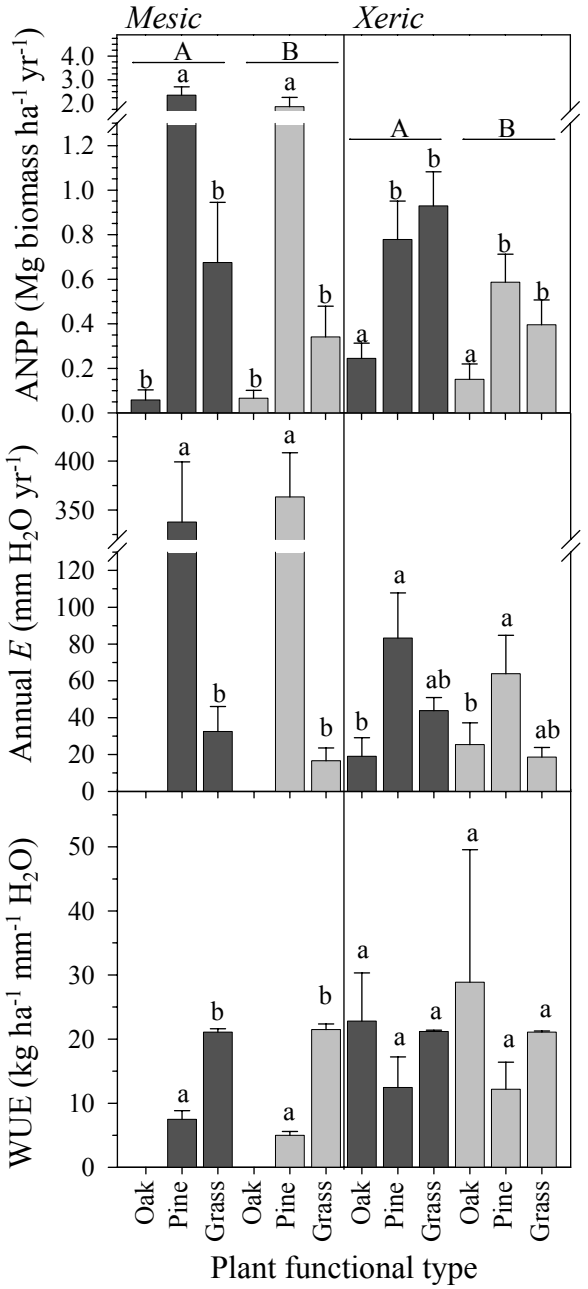

Figure 2.4 Annual ANPP, *E*, and WUE by the three plant functional types measured for fertilized (dark bars) and control (light bars), mesic and xeric site types. Mean and standard error bars shown. Different capital letters denote significant differences among split-plots (treatments). Different lowercase letters denote significant differences among split-split-plots (plant functional types). Note that for *E* and WUE, treatment was not a significant effect and differences among plant functional types were tested on data pooled across treatments.

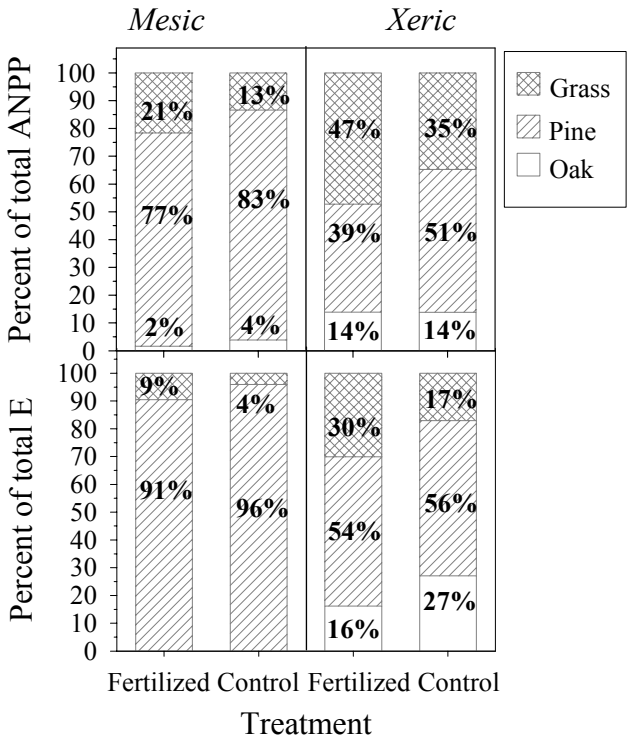

Figure 2.5 Percent contribution of total annual ANPP and *E* (total was calculated as the sum of oak, pine and grass ANPP and *E*) by the three plant functional types. Stacks shown are the average percentages (shown in bars) for each site type and treatment. Average percent of total ANPP by oak in mesic fertilized and control plots is 2% and 4%, respectively.

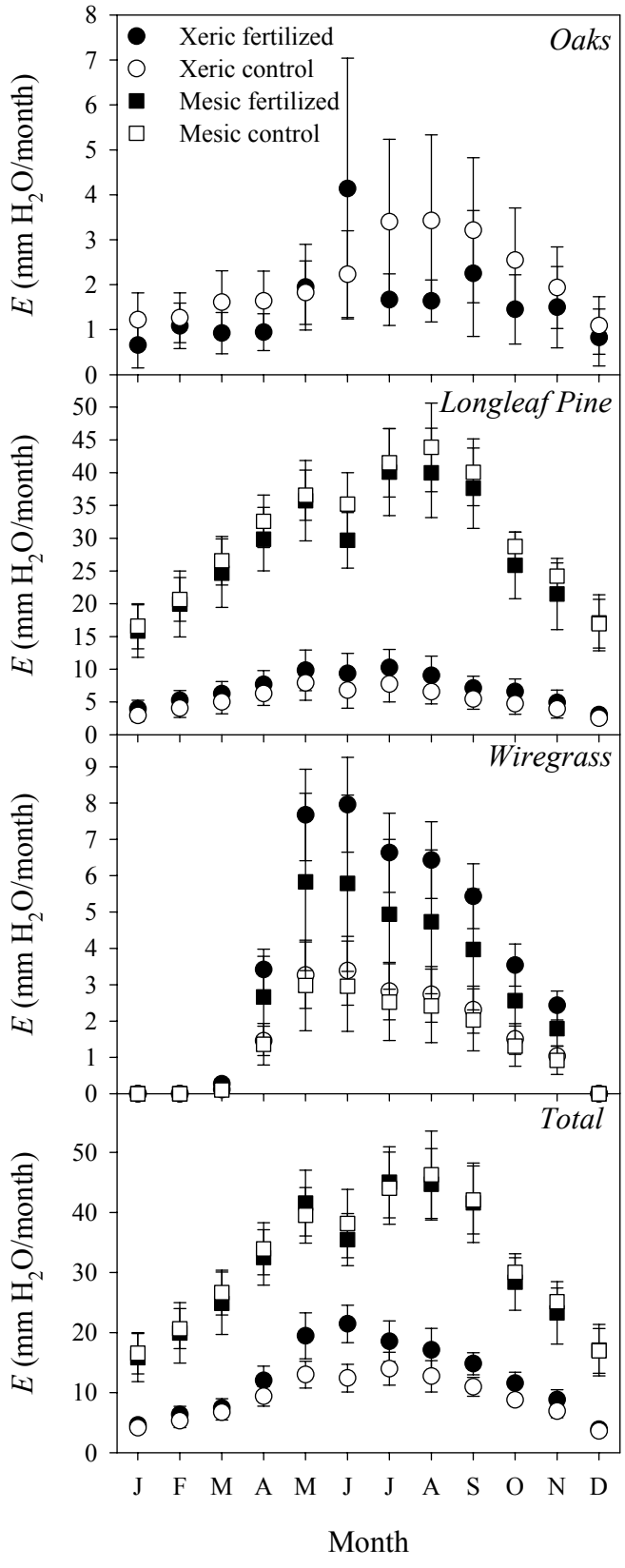

Figure 2.6 Total monthly transpiration, *E*, for oaks, pine and grass in fertilized and control mesic and xeric sites (total was calculated as the sum of oak, pine and grass *E*). Points represent the average of four sites, bars are one standard error.

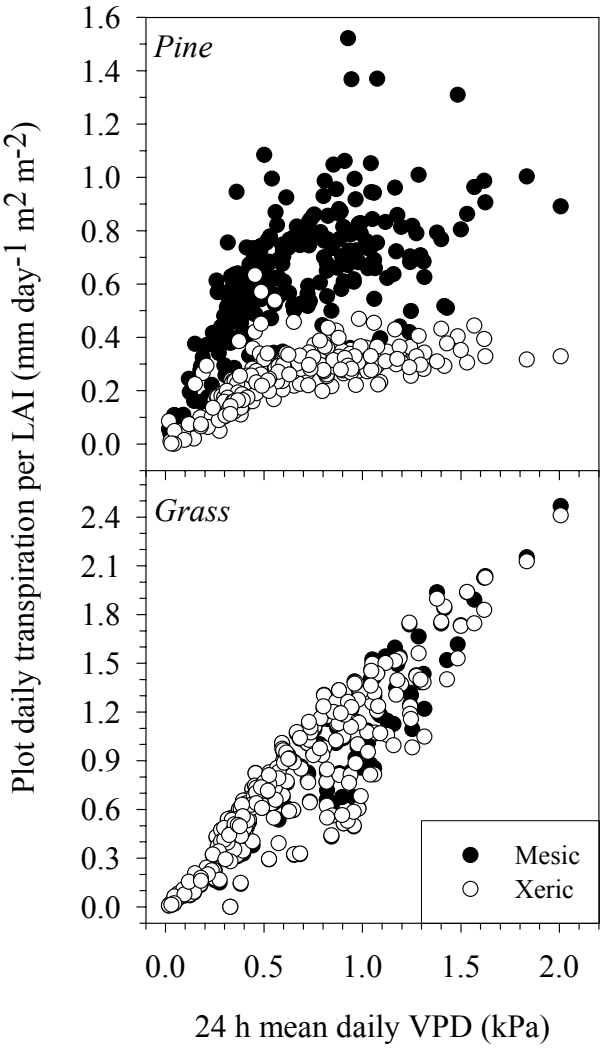

Figure 2.7 Average daily transpiration per LAI for fertilized mesic and xeric site pine (upper panel) and grass (lower panel) plant functional types during times of concurrent transpiration for study period. Each point represents the mean of four replicate plots for one 24 h period.

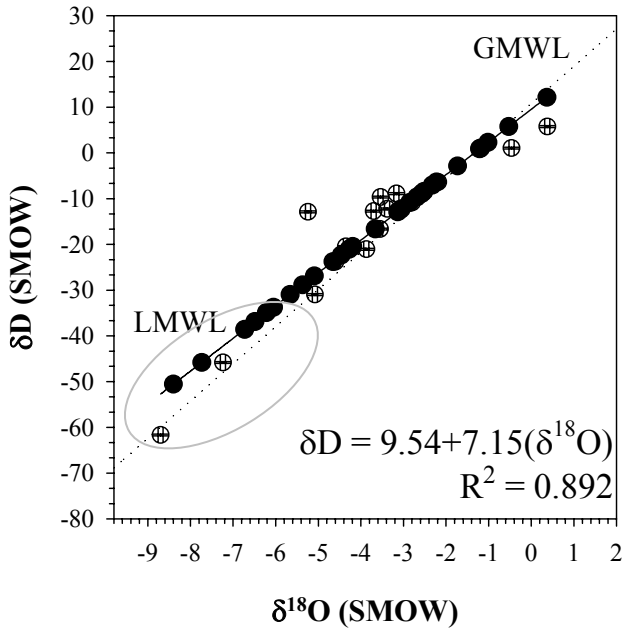

Figure 2.8 Local meteoric water line (LMWL, solid line) developed from precipitation (*P*) samples (open symbols are *P* samples analyzed for δD and δ18O; closed symbols are *P* samples analyzed for δD only, and plotted using LMWL regression). Global meteoric water line (GMWL, dotted line) shown for reference. Winter precipitation is noted in the grey circle.

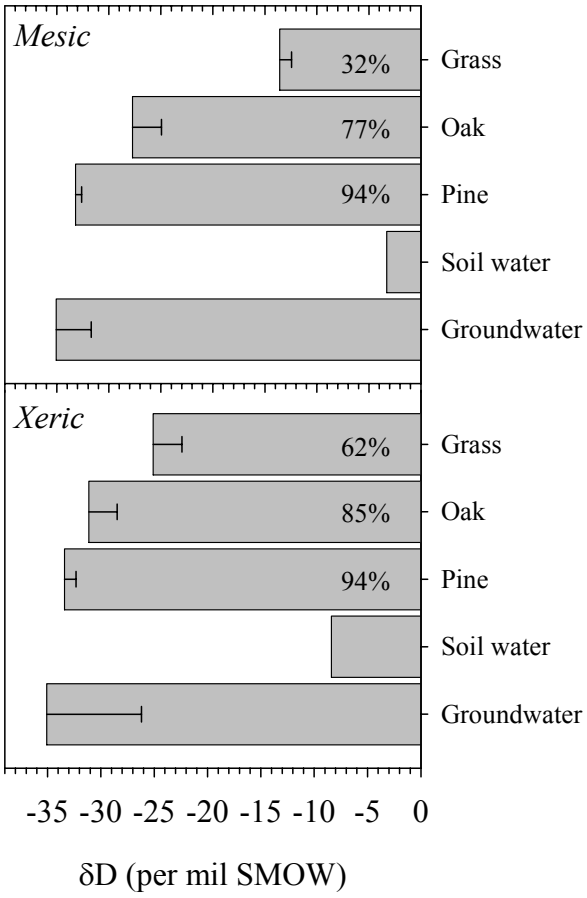

Figure 2.9 Average (SE bars) δD signatures for groundwater (GW), soil water, and stem xylem water for plant functional types in mesic and xeric control sites in Aug 2003. Percentages given in the bars correspond to the average percent GW signature found in the xylem water sample.

Table 2.1 Stand characteristics of replicate plots in 2001 before treatments were applied. Means and parenthetical standard errors given, for all cases n=8, except LAI where n=4 (control plots only). Pine LAI estimates are based on litter fall collected for one year and multiplied by two given the 2-year retention time of longleaf pine needles.

Site type	Plant functional group	Tree density (trees ha^{-1})	Aboveground tree biomass (Mg ha^{-1})	Tree basal area (m^2 ha^{-1})	Projected LAI (m^2 m^{-2})
Mesic	Oak	6 (1)	3.29 (0.47)	0.57 (0.08)	
	Pine	205 (16)	115.28 (3.50)	14.59 (0.48)	1.76 (0.09)
	Grass				0.08 (0.03)
	Total	209 (16)	118.54 (3.29)	15.15 (0.45)	
Xeric	Oak	59 (7)	7.27 (0.66)	1.25 (0.11)	
	Pine	54 (3)	32.10 (2.02)	4.05 (0.23)	1.07 (0.09)
	Grass				0.10 (0.03)
	Total	113 (8)	39.37 (1.43)	5.30 (0.13)	

CHAPTER 3

ASSESSING VARIATION IN THE RADIAL PROFILE OF SAP FLUX DENSITY IN *PINUS* SPECIES AND ITS EFFECT ON DAILY WATER USE[1]

---

[1] Ford, C. R., M. A. McGuire, R. J. Mitchell, and R. O. Teskey. 2004. *Tree Physiology* 24:241–249.
Reprinted here with permission of publisher.

Abstract

We monitored sap flux density (v) diurnally in nine mature southeastern pine (*Pinus spp.)* trees with a thermal dissipation probe that spanned the sapwood radius. Our data show the expected pattern of high v near the cambium, and decreasing v with depth toward the center of the trees. However, the pattern was not constant within a day or between trees. We found that the radial profiles of trees were steeper earlier in the day, and became less steep with time. As a result, time-dependent changes in the shape of the radial profile of v were sometimes correlated with daily changes in evaporative demand. As the radial profile became less steep, the inner xylem contributed relatively more to total tree sap flow than it did earlier in the day. We present a 3-parameter Gaussian function that can be used to describe the radial distribution of v in trees. Parameters in the function represent depth in the xylem from the cambium, maximum v, depth in the xylem where the maximum v occurs, and the rate of radial change in v with radial depth (β). β varied significantly among trees and with time, and was sometimes correlated with air vapor pressure deficit (D). We hypothesize that this may have occurred when, during periods of high transpiration, the water potential gradient became great enough to move water in the inner sapwood despite its probable high hydraulic resistance. In addition, we examined discrepancies in estimates of daily water use based on single-point, two-point and multi-point (i.e., every 20 mm in the sapwood) measurements. When radial distribution of v was not considered, a single-point measurement caused errors as large as 154% in the estimate of daily water use, relative to the estimate obtained from the multi-point measurement. Measuring v using two close sample points (10 & 30 mm) did not improve the estimate; however, estimates derived from v measured at two distant sample points (10 & 70 mm) significantly improved the estimated daily water use

substantially, although errors were as great as 32% in individual trees. The variability in *v* with depth in the xylem, over time, and between trees indicates that measurements of the radial distribution of *v* are necessary to accurately estimate water flow in trees with large sapwood areas.

Key-words: error analysis, Georgia, hydraulic conductivity, longleaf pine, scaling

Introduction

Sap flow and sap flux density are robust measurements that can be used to estimate a range of plant ecophysiological attributes including: whole plant water-use (Myers et al. 1998; James et al. 2002), whole-plant hydraulic conductance (K_h) (Pataki et al. 1998; Ryan et al. 2000), whole-plant or canopy transpiration (E_c) (Granier et al. 1996b; Teskey and Sheriff 1996; Hunt and Beadle 1998; Meiresonne et al. 1999; Oren et al. 1999; Schaeffer et al. 2000; Wilson et al. 2001; Wullschleger and Norby 2001; Bernier et al. 2002; Köstner et al. 2002), canopy conductance (g_c) (Granier et al. 1996b; Pataki et al. 1998; Ewers et al. 1999; Oren et al. 1999; Catovsky et al. 2002), and leaf stomatal conductance (g_s) (Köstner et al. 1992; Granier and Loustau 1994; Martin et al. 1997; Oren et al. 1998; Pataki et al. 1998; Ryan et al. 2000; Catovsky et al. 2002). Particularly in trees, transpiration and conductance are often estimated from sap flux density measurements because the height and complexity of canopies makes leaf-level measurements cumbersome to scale. To estimate any of these leaf-level processes from stem sap flux density (v, g H_2O m^{-2} sapwood s^{-1}), one must first estimate mass flow of sap in the stem (F) as the product of v and the conducting area (A) of the stem cross section ($F = v \cdot A$). Thus, if v varies radially one must know its radial distribution of v to accurately estimate F in the stem.

A large body of work has been conducted on *v* of coniferous species with tracheid xylem anatomy. Some of these studies have experimentally described the radial distribution of *v*

(henceforth radial profile) in mature pines. Mark and Crews (1973) showed that the radial profile of two *Picea engelmannii* Parry and two *Pinus contorta* Dougl. trees peaked at 24 mm into the xylem and declined toward the heartwood. This basic pattern has been confirmed for other coniferous species including *Picea abies* (L.) Karst., *Picea engelmannii* Parry, *Pinus contorta* Dougl., *Pinus pinea* L., *Pinus sylvestris* L., *Pseudotsuga menziesii* (Mirb.) Franco, using sap flow methods as well as radioactive isotope and dye staining methods (Swanson 1974; Waring and Roberts 1979; Cohen et al. 1985; Čermák et al. 1992; Granier et al. 1996a; Lüttschwager and Granier as presented in Köstner et al. 1996; Čermák and Nadezhdina 1998; Nadezhdina et al. 2002).

While the general radial profile seems remarkably consistent among tree species with tracheid xylem anatomy, several studies have reported that the radial profile in trees can vary with time (Swanson 1967; Mark and Crews 1973; Lassoie et al. 1977). Becker (1996) noted that the radial profiles were not constant between wet and dry periods in three tree species in the family *Dipterocarpaceae*. Diurnal changes in the radial profile in conifer stems have been related to air vapor pressure deficit, *D* (Nadezhdina et al. 2002) and soil drying (Phillips et al. 1996; Čermák and Nadezhdina 1998). These studies suggest temporal variation in the radial profile that may be due to dynamic changes in environmental conditions.

Although there have been many estimates of water use based on sap flux density measurements, unfortunately, very few studies have actually characterized a radial profile in at least one tree. Some studies assume that the radial profile of sap flux density in trees with deep sapwood is uniform across the entire sapwood; others assume that the distribution is step-wise (usually calculating and combining two discrete fluxes corresponding to two discrete areas of sapwood). Our objectives in this study were 1) to measure the radial profile of sap flux density

in trees with tracheid xylem anatomy in order to assess its consistency; 2) to calculate the error in using single-point and two-point sap flux measurements to estimate whole-plant daily water use; and 3) to present a function that can be used to describe and analyze the radial profile in trees with large sapwood areas. Our approach was to monitor diurnal sap flux density in mature trees of four southeastern pine species (*Pinus spp.)* with a unique probe that spanned the sapwood radius. We hypothesized that 1) the radial profile would change with changing evaporative demand, and 2) using one or two sample points and assuming a more simple radial sap flux density profile would result in significant errors in estimating whole-tree daily water use.

Materials and methods

Site description and environment

This experiment was conducted at Joseph W. Jones Ecological Research Center in SW Georgia (N31°13'16.88" W84°28'37.81"), which is comprised of over 11,700 ha of natural second-growth longleaf pine savanna, mixed hardwood riparian forest, and oak hardwood hammocks. Within the longleaf pine savanna type (Goebel et al. 1997), four species are present: *Pinus palustris* Mill., *P. echinata* Mill., *P. elliottii* Engelm., and *P. taeda* L. We measured sap flux density in these species on a site where all four species were growing on the same soil type. We measured sap flux density on six *P. palustris* trees (the focus of our research efforts) and one tree each of the other three species, for a total of nine trees. The diameters of the trees ranged from 32 to 60 cm (Table 3.1). An open-field weather station was located less than 700 m away, which measured ambient air temperature and relative humidity (Model HMP35C; Campbell Scientific, Inc., Logan, UT, USA). We used 15 minute averaged air temperature to calculate saturation

vapor pressure (e_{sat}) using the Tetens formula (v. Murray 1967). Relative humidity and e_{sat} were used to compute vapor pressure deficit (*D*).

Probe Design and Sap Flux Density Measurements

We constructed one set of Granier-style thermal dissipation probes (Granier 1985) using thin-walled brass tubing. It consisted of one upper heated probe (4.78 mm outside tube diameter, 26 cm in length, containing 312 cm of constantan wire with a resistance of 0.4 Ω cm^{-1} that was coiled around a 26 cm long inner solid brass wire) and one lower reference probe of the same outside tube diameter and length. Each probe contained 13 independent thermocouples (TC) suspended in its shaft every 2 cm starting at 1 cm. The heated probe TC junctions were suspended between the shaft and the coiled resistance wire. The probes were placed in each sample tree approximately 1.3 m above the ground by drilling two holes separated vertically by 5 cm, but not separated horizontally (i.e. heating probe was directly above the reference probe). We used a guide template and a level to ensure that the holes were parallel. The probes were coated with thermally-conductive silicone grease before placement in the trees, and were shielded from solar radiation, thermal gradients, and rainfall using reflective insulation (Reflectix; Reflectix Inc., Markleville, IN, USA). Each tree (n=9) was monitored for one 24 h period during the period between April 16 and May 26 (days of year 106-146), 2002.

The function relating sap flux density to thermal dissipation was originally developed (Granier 1985) and revalidated (Clearwater et al. 1999) using probes that dissipated 0.2 W for a probe 2 cm in length. We used the same relationship, calculating that our 26 cm heated probe would need to dissipate 2.6 W, or have a current of 144.3 mA applied to the heating wires. All lead wires were soldered to copper, double shielded cable wires (Model 9927; Belden Inc., Richmond, IN, USA). Thermocouple wires were differentially connected to a data logger

(Model 23X; Campbell Scientific, Logan, UT, USA) measured every 5 s and compiled into 5 min averages. The temperature difference (ΔT) between the probes was converted to sap flux density using the equation of Granier (1985).

Probe Validation

To validate the new probe design, we compared calculated and gravimetrically determined flow rates through an excised 43.5 cm-long, 26.1 cm-diameter *P. palustris* stem. We applied a constant pressure head of 8 cm across the stem by sealing a reservoir containing deionized water to the top of the stem. A total of 10 gravimetric measurements were recorded every 10 min. The average gravimetric flow rate was 78.86 ± 3.63 g H_2O m^{-2} sapwood s^{-1}. Thermocouples in the probe were measured every 5 s and averaged into 10 min values. Sap flux density was calculated according to Granier (1985). Flow was calculated using Equation 3.1 described below. The average calculated flow rate using the probe was 73.75 ± 2.05 g H_2O m^{-2} sapwood s^{-1}.

Scaling Sap Flux Density to Daily Whole Tree Water Use

All sample trees were cored at the end of the measurement period just below the area where the probe was installed. On each core, the length of the heartwood (if present) radius was determined visually and measured. This visual measurement was validated with the probe output (i.e. TC depth in xylem where continuous day and night ΔT probe output or calculated sap flux density measurements were zero). We also measured the radius to the cambium. We converted sap flux density (v) to sap flow (F, g H_2O s^{-1}) using four different spatial scaling methods: one-point, two-point close, two-point distant, and multi-point (using 10-13 thermocouple measuring points depending on sapwood radius). Sap flux density (v) was converted to sap flow (F, g H_2O s^{-1}) by

weighting each sap flux density (v_k) measurement by the sapwood area each TC junction was assumed to measure (Hatton et al. 1990):

$$F = \sum_{k=1}^{n} \pi \left(r_k^2 - r_{k-1}^2 \right) \cdot v_k \qquad \text{(Equation 3.1)}$$

We assumed that a) adjacent TC junction measurement zones did not overlap, b) TCs were centered on the sapwood area defined by an inner radius (r_k) and an outer radius (r_{k-1}), and c) that the sapwood area could be estimated by the area of a circle. For the one-point scaling, we calculated *F* from *v* measured by the TC junction at 10 mm depth multiplied by the entire sapwood area. For two-point close scaling, we calculated *F* using data from the TCs located at 10 mm and 30 mm and summed them to obtain total flow (*F)* using Equation 3.1. Similarly, for two-point distant scaling, we calculated *F* using data from the TCs located at 10 mm and 70 mm and summed them to obtain total flow (*F)* using Equation 3.1. These depths were selected because they are typical probe depths reported in studies using dual TC probes. Flow was calculated by multiplying *v* measured at the 10 mm junction by the sapwood area in the 0-20 mm depth, combined with *v* measured at the other junction that represented the remaining area of the sapwood.

To scale temporally and calculate daily whole tree water use, we converted the 5 min *F* values to 1 s *F* values by multiplying by 300 (*i.e.* interpolating), and summed these values for a 24 h period. This was done for each scaling method described above.

We tested for significant differences in whole-tree daily water use scaled with the four methods using the GLM procedure and a post-hoc LSD test on the treatment means with SAS software (SAS v9; SAS Institute Inc., Cary, NC, USA). The model used tree as a blocking factor, scaling method as a treatment factor, and whole-tree daily water use as the dependent

variable. The tree blocking factor was a random effect, and scaling method was a fixed effect in the model. For both analyses, α=0.05.

Developing a General Radial Profile Function

To create a general radial profile function, we used estimates of *v* from the multi-point TC measurements. First *v* was normalized for each 5 min time step by creating an index equal to v_k/v_{10mm}, where v_k is sap flux density calculated at each TC junction (k = 1,…13) and v_{10mm} is sap flux density calculated at the outermost TC junction, located at a depth of 10 mm in the sapwood, and assumed to measure *v* in the 0-20 mm area of sapwood. For each tree and for each time, this index was plotted with depth from the cambium. We then fit the following 3-parameter Gaussian function to these data:

$$f(x) = \alpha \cdot e^{-0.5 \cdot \left(\frac{x - x_0}{\beta} \right)^2} \qquad \text{(Equation 3.2)}$$

where x is the depth in the xylem from the cambium, α is the maximum sap flux density, x_0 is the depth in the xylem where the maximum sap flux density occurs, and β is inversely related to the rate of decrease in sap flux density with radial depth (Figure 3.1). The *v* of the 0 -20 mm band of sapwood position must equal unity, or 1, which was considered a reasonable assumption based on numerous reports in the literature of maximum *v* in this region of the xylem (e.g. Mark and Crews 1973; Cohen et al. 1985). We fitted the rate of decrease, or β, for every tree and time (i.e. we allowed for the possibility that the rate of radial decrease in *v* varied from tree to tree and with time). Curve fitting was performed using SigmaPlot software (SigmaPlot v7.101; SPSS Inc., Chicago, IL, USA).

We used the fitted β values for each tree and up to 17 systematically sampled time steps (occurring during time of active sap flux) to test for significant differences in β with time (n=17) and with tree (n=9) using the GLM procedure with SAS software (SAS v9; SAS Institute Inc., Cary, NC, USA). The model used tree as a blocking factor, time as a treatment factor, and β as the dependent or response variable. The tree and time factors were random effects. We also computed Pearson's correlation coefficients between β and D (kPa) to determine if the shape of the radial profile was correlated with evaporative demand.

Results

Radial Profiles

The trees sampled ranged from 32 to 60 cm in diameter and from 277 to 1320 cm^2 in sapwood area (Table 3.1). Peak diurnal v in the outer 20 mm of sapwood ranged from 37.3 to 97.4 g m^{-2} s^{-1} (Figure 3.2). The diurnal course of v for all trees measured, regardless of species, was generally bell-shaped (Figure 3.2). At this height in the stem (1.3 m), v was typically initiated between 0600 and 0730 h, and was greatest during 1000 to 1900 h. Some trees experienced a brief transient afternoon depression in v (Figure 3.2), but in general, changes in v corresponded to changes in air vapor pressure deficit (D). Sap flux density decreased towards the heartwood and was almost always highest in the outer 20 mm of sapwood (Figure 3.2). However, the specific pattern of the radial profile changed from tree to tree and with time. When v values were normalized, the radial profile of v appeared to conform with a Gaussian function (Figure 3.3). The rate of decline in radial v with depth, β, was significantly different among the trees we measured ($F=119.64$, $P<0.001$). Similarly, within each tree, β was significantly different over time ($F=2.96$, $P<0.001$). In four of the nine trees the rate of decline in radial sap flux density,

β, was positively correlated to D (P=0.05) (Table 3.2, Figure 3.4). In those trees the radial profile of v generally became less steep (more positive β, Figure 3.1) in the afternoon, and the contribution of the inner xylem to total tree sap flow became greater (Figure 3.4 a, b, c, h). This effect was correlated with evaporative demand, although a number of other factors such as changes in sapwood water content or xylem water potential may contribute to, or cause the change in β over time. In other trees β remained nearly constant (Figure 3.4 d, g) or was variable within the day (Figure 3.4 e, f).

Errors in Assuming More Simplistic Radial Profiles

Calculating daily water use for the same trees using v measured by the 10 mm and 70 mm thermocouple junctions (two-point distant scaling), the average daily water use was determined to be 116.6 kg day^{-1}, which is within 5% of the average for the multi-point estimates. However, the differences in two-point distant and multi-point estimates for individual trees were as high as 32% (Table 3.1). When daily water use was calculated for the same trees using v measured by two closer point measurements, the 10 mm and 30 mm thermocouple junctions (two-point close scaling), the daily average was 179.6 kg day^{-1}, with systematic overestimates in each tree. The average overestimate was 42%.

The four scaling methods yielded significantly different estimates of whole-tree daily water use (Table 3.3). Using two distant radial points to scale (two-point distant) whole-tree water use resulted in a drastic improvement in the estimate compared to using either a single point estimate or a two-point estimate derived from thermocouples close together (two-point close), both of which produced substantially higher values than the multi-point estimate. The average daily water use calculated using two close points was not significantly different from the one-point scaling estimate. Likewise, the multi-point and the two-point distant scaling methods

did not produce significantly different estimates, but the tree-to-tree variation in the two estimates was quite large in some cases.

The scaling error associated with one-point measurements was greater for trees that had a more rapid decrease in v with distance from the cambium (*i.e.* smaller β), than in trees that had more even radial distributions of v (*i.e.* greater β) (Figure 3.5). There was a systematic overestimate in whole tree daily water use when scaling with two close points. With both two-point scaling method estimates, there was no relationship between β and the amount of discrepancy between daily water use estimates.

Discussion

The radial profile of v was skewed, with higher rates toward the cambium in these trees, and with v decreasing with depth into the xylem from the cambium. In this study and others, this pattern has been reported for mature trees with tracheid xylem anatomy. Consistent with this type of radial profile of v, other studies have shown that in mature trees as the heartwood is approached, hydraulic conductivity of the sapwood declines (Spicer and Gartner 2001). Age-related changes may thus cause the inner xylem to be nonfunctional or have a higher hydraulic resistance than it once did. Tracheids and bordered pit membranes closer to the heartwood may gradually experience chemical or biological changes that add resistance to flow. Mark and Crews (1973) showed that the bordered pit membranes in *P. engelmannii* and *P. contorta* trees were most open at the 24 mm xylem depth and became progressively blocked and encrusted as distance to the heartwood decreased. Older tracheids may also be damaged and nonfunctioning due to repeated, unrepaired cavitation events that reduce sapwood water content. Older xylem elements have been shown to be more vulnerable to embolism via increased pit membrane permeability to air

(Sperry et al. 1991). It has also been suggested that because the inner xylem originally supplied water to branches and leaves that are now shaded or dead, the inner xylem is not as well-connected or functional as the outer sapwood (v. Dye et al. 1991; Jiménez et al. 2002).

The rate of decline of v towards the heartwood differed among the trees we measured. This could be a result of different radial profiles of sapwood hydraulic conductivity among the trees. We also found that the rate of decline in v with increasing distance from the cambium (β) differed with time. Thus, in studies that assess a radial profile on one tree at one time, it cannot be assumed that the radial profile measured is representative of the radial profile of all trees and at all times. We found that the radial profiles of trees were steeper earlier in the day, and became less steep later in the day. As a result, time-dependent changes in the shape of the radial profile of v were sometimes correlated with daily changes in evaporative demand. As the radial profile became less steep, the inner xylem contributed relatively more to total tree sap flow than it did earlier in the day. We speculate that as the root-to-leaf water potential gradient becomes greater under higher evaporative demand, and the driving force to move water in the stem increases, flow in the inner sapwood increases. At this point, the inner xylem with its presumably higher hydraulic resistance begins to contribute to sap flow. This pattern could also be explained by stem water availability, or capacitance. Earlier in the day when stem water is readily available, the outer xylem supplies more water than the inner xylem. Later in the day, when stem water becomes depleted, water in the inner sapwood is mobilized. The results from this study differ from those of two other studies in conifers in which it was reported that the outer xylem conducted disproportionately more water than the inner xylem under conditions associated with higher v compared to conditions associated with lower v (Nadezhdina et al. 2002; Phillips et al. 1996). The reason for the difference between those studies and the present study is not readily

apparent, but could be related to tree size, as the trees measured in this study were larger than those in the other two studies. Our results are consistent with those of Medhurst et al. (2002), who found that a greater proportion of sapwood area contributed to sap flow in *Euaclyptus nitens* trees following thinning treatments that caused transpiration to increase. Temporal variability of the radial profile shape may also be affected by other factors, such as cavitation, and water withdrawal from ray cells, or changes in the distribution of incident radiation across the canopy.

We found that single-point scaling of *v* overestimated whole-tree daily water use by an average of 67% in the nine trees studied. In individual trees, the error using single-point scaling was as much as 154%. Errors of similar magnitude have been noted in other studies in which single- and multi-point scaling methods were compared. Nadezhdina et al. (2002) reported errors up to 300% when total sap flow in *P. sylvestris* was calculated from *v* measured at the outermost TC junction (14 mm) and assuming a uniform radial profile across the entire sapwood radius (125 mm), compared to sap flow calculated from *v* measured at 5 depths every 10 mm into the xylem. Similarly, Čermák and Nadezhdina (1998) reported overestimating total sap flow in conifers by 169% when scaling was based on *v* measured in the outermost xylem layers and assuming a uniform radial profile, compared to sap flow calculated from *v* measured at 6 depths every 15 mm into the xylem. In four species of large-diameter tropical trees with deep sapwood, James et al. (2002) found that assuming uniform radial *v* profiles and scaling whole-tree water use based on the outermost (0-20 mm) sensors resulted in an overestimation of more than 100%, compared to estimates of flow calculated from *v* measured at five successive depths in the xylem. Nadezhdina et al. (2002) found that errors in estimating whole-tree sap flow from single-point measurements were less for smaller trees. This may have been due to a more homogeneous distribution of *v* in the sapwood than in larger trees. In the present study, when evaporative

demand and total tree sap flow were high, the radial profile of *v* became more even. When total tree sap flow is greatest, the scaling error is the smallest. This finding is similar to that of Oren et al. (1998), who calculated canopy transpiration (E_c) based on *v* measured at a single point and two-points for 13-year old *P. taeda* trees and found that the estimates were more similar when E_c was high, and that as the soil dried and transpiration decreased, the difference in E_c estimates became larger. Interestingly, scaling using *v* measured at two close points did not improve estimates of in daily water use. However, scaling using *v* measured at two distant points substantially improved the estimate of whole-tree water use over using either a single point or two close points. Two-point distant scaling both underestimated and overestimated daily water use by as much as –22% and +32%. These errors were compensating, and when combined, the over- and underestimates resulted in an average difference of only 6% from that scaled from the multi-point estimate.

In conclusion, our results may have important implications for future sap flow studies. First, we have presented a general function that describes the radial distribution of *v* in xylem with tracheid anatomy. The versatility of this general function allows both the temporal variation of the radial profile to be assessed and the calculation of total flow using only one thermocouple junction via integration of a definite integral rather than two-point scaling, which requires two thermocouple junctions. Hatton et al. (1990) discussed how integration of a fitted second-order polynomial could be used to estimate total sap flow in diffuse porous trees with deep sapwood. They discussed the common radial profile in conifers, but presented no function to integrate that would allow flow to be estimated with one thermocouple. The Gaussian function we present above can be generalized further. For example, the *x* variable can be normalized to percent of hydroactive xylem radius rather than absolute depth into xylem from

the cambium. Normalization of the *x* variable in this way could be useful in studies that include trees of differing DBH, age, and sapwood area. Although the development of this function was based on reports in the literature as well as the data presented in this paper, we do not recommend using it to scale *v* to sap flow without first determining the radial profile on at least one tree. Second, our data show that the radial distribution of *v* is not constant with time, from tree to tree, or under different evaporative demands. As in previous reports, the radial profile of *v* was skewed toward the cambium, but the inner xylem contributed more to total tree sap flow later in the day compared to earlier in the day. We hypothesize that this may have occurred when, during periods of high transpiration, the water potential gradient became great enough to move water in the inner sapwood despite its probable high hydraulic resistance. In some cases, such as in plantations of trees that are genetically and ontogenetically similar, the radial profile could be constant from tree to tree (Zang et al. 1996). Finally, our analysis of scaling *v* to whole plant water use demonstrates the egregious errors that result when a more simplistic radial profile is assumed. When scaling two-point measurements of *v* to total sap flow, care must be taken to position the sensors at depths in the sapwood that will capture the spatial variation in the flow area. The trees in this study had deep sapwood and much better estimates of daily water use were obtained from sensors placed at 10 and 70 mm depths compared to sensors placed at 10 and 30 mm depths in the sapwood. Our results show that errors can be further minimized if many points along a sapwood radius are measured. Limitations of our measurement protocol include the inability to assess circumferential variability, and possible interference between adjacent thermocouple junctions. An alternative approach is to use probes of varying lengths inserted in a spiral pattern around the stem (see Wullschleger and King 2000) to spatially separate TC junctions and eliminate interference. Limitations of this technique include the inability to

distinguish between radial and circumferential variability, and drilling many holes into the stem. Using a probe or probes that measure multiple points in the sapwood, such as the probe described in this paper, is advantageous in species with deep sapwood. Standardization and accuracy in scaling sap flux density measurements are necessary as measurements of sap flow continue to be used to validate and compare whole-ecosystem estimates of water use and storage in vegetation dominated by woody species (Wilson et al. 2001).

Acknowledgements

This study was supported by the University of Georgia Daniel B. Warnell School Of Forest Resources, the Robert W. Woodruff Foundation and the Joseph W. Jones Ecological Research Center. This publication was also developed under EPA STAR Fellowship Agreement No. 91617001-0 awarded by the U.S. Environmental Protection Agency. It has not been formally reviewed by EPA. The views expressed in this document are solely those of the authors and EPA does not endorse any products or commercial services mentioned in this publication. We thank Dali Guo for comments on an earlier version of this manuscript. We thank Rob Addington, Bob Cooper, Lisa Donovan, Carol Goranson, Ron Hendrick, Tim Martin, Jon Miniat, Barry Moser, and Rod Will for their logistical help, help with field work, and overall support.

References

Becker, P. 1996. Sap flow in Bornean heath and dipterocarp forest trees during wet and dry periods. Tree Physiol. 16:295-299.

Bernier, P.Y., N. Bréda, A. Granier, F. Raulier and F. Mathieu 2002. Validation of a canopy gas exchange model and derivation of a soil water modifier for transpiration for sugar maple (*Acer saccharum* Marsh.) using sap flow density measurements. For. Ecol. Manage. 163:185-196.

Catovsky, S., N.M. Holbrook and F.A. Bazzaz 2002. Coupling whole-tree transpiration and canopy photosynthesis in coniferous and broad-leaved tree species. Can. J. For. Res. 32:295-309.

Čermák, J., E. Cienciala, J. Kučera and J.E. Hallgren 1992. Radial velocity profiles of water flow in trunks of Norway spruce and oak and the response of spruce to severing. Tree Physiol. 10:367-380.

Čermák, J. and N. Nadezhdina 1998. Sapwood as the scaling parameter-defining according to xylem water content or radial pattern of sap flow? Ann. For Sci. 55:509-521.

Clearwater, M.J., F.C. Meinzer, J.L. Andrade, G. Goldstein and N.M. Holbrook 1999. Potential errors in measurement of nonuniform sap flow using heat dissipation probes. Tree Physiol. 19:681-687.

Cohen, Y., F.M. Kelliher and T.A. Black 1985. Determination of sap flow in Douglas-fir trees using the heat pulse technique. Can. J. For. Res. 15:422-428.

Dye, P.J., B.W. Olbrich and A.G. Poulter 1991. The influence of growth rings in *Pinus patula* on heat pulse velocity and sap flow measurement. J. Exp. Bot. 42:867-870.

Ewers, B.E., R. Oren, T.J. Albaugh and P.M. Dougherty 1999. Carry-over effects of water and nutrient supply on water use of *Pinus taeda*. Ecol. Appl. 9:513-525.

Goebel, P.C., B.J. Palik, L.K. Kirkman and L. West 1997. Field Guide: Landscape ecosystem types of Ichauway. Joseph W. Jones Ecological Research Center, Newton, GA.

Granier, A. 1985. Une nouvelle méthode pour la mesure du flux de sève brute dans le tronc des arbres. Ann. Sci. For. 42:193-200.

Granier, A., P. Biron, N. Breda, J.Y. Pontailler and B. Saugier 1996a. Transpiration of trees and forest stands: Short and longterm monitoring using sapflow methods. Glob. Chang. Biol. 2:265-274.

Granier, A., R. Huc and S.T. Barigah 1996b. Transpiration of natural rain forest and its dependence on climatic factors. Agric. For. Meteorol. 78:19-29.

Granier, A. and D. Loustau 1994. Measuring and modeling the transpiration of a maritime pine canopy from sap-flow data. Agric. For. Meteorol. 71:61-81.

Hatton, T.J., E.A. Catchpole and R.A. Vertessy 1990. Integration of sapflow velocity to estimate plant water-use. Tree Physiol. 6:201-209.

Hunt, M.A. and C.L. Beadle 1998. Whole-tree transpiration and water-use partitioning between *Eucalyptus nitens* and *Acacia dealbata* weeds in a short-rotation plantation in northeastern Tasmania. Tree Physiol. 18:557-563.

James, S.A., M.J. Clearwater, F.C. Meinzer and G. Goldstein 2002. Heat dissipation sensors of variable length for the measurement of sap flow in trees with deep sapwood. Tree Physiol. 22:277-283.

Jiménez, M.S., N. Nadezhdina, J. Čermák and D. Morales 2000. Radial variation in sap flow in five laurel forest tree species in Tenerife, Canary Islands. Tree Physiol. 20:1149-1156.

Köstner, B., P. Biron, R. Siegwolf and A. Granier 1996. Estimates of water vapor flux and canopy conductance of Scots pine at the tree level utilizing different xylem sap flow methods. Theor. Appl. Climatol. 53:105-113.

Köstner, B., E. Falge and J.D. Tenhunen 2002. Age-related effects on leaf area/sapwood area relationships, canopy transpiration and carbon gain of Norway spruce stands (*Picea abies*) in Fichtelgebirge, Germany. Tree Physiol. 22:567-574.

Köstner, B., E.-D. Schulze, F.M. Kelliher, D.Y. Hollinger, J.N. Byers, J.E. Hunt, T.M. McSeveny, R. Meserth and P.L. Weir 1992. Transpiration and canopy conductance in a pristine broad-leaved forest of *Nothofagus*: an analysis of xylem sap flow and eddy correlation measurements. Oecologia. 91:350-359.

Lassoie, J.P., D.R.M. Scott and L.J. Fritschen 1977. Transpiration studies in Douglas -fir (*Pseudotsuga menziesii*) using the heat pulse technique. For. Sci. 23:377-390.

Mark, W.R. and D.L. Crews 1973. Heat-pulse velocity and boardered pit condition in living Engelmann spruce and Lodgepole pine trees (*Picea engelmannii, Pinus contorta*). For. Sci. 19:291-296.

Martin, T.A., K.J. Brown, J. Čermák, R. Ceulemans, J. Kučera, F.C. Meinzer, J.S. Rombold, D.G. Sprugel and T.M. Hinckley 1997. Crown conductance and tree and stand transpiration in a second- growth *Abies amabilis* forest. Can. J. For. Res. 27:797-808.

Medhurst, J.L., M. Battaglia and C.L. Beadle. 2002. Measured and predicted changes in tree and stand water use following high-intensity thinning of an 8-year-old *Eucalyptus nitens* plantation. Tree Physiol. 22:775-784.

Meiresonne, L., N. Nadezhdina, J. Čermák, J. van Slycken and R. Ceulemans 1999. Measured sap flow and simulated transpiration from a poplar stand in Flanders (Belgium). Agric. For. Meteorol. 96:165-179.

Murray, F.W. 1967. On the computation of saturation vapor pressure. Journal of Applied Meteorology. 6:203-204.

Myers, B.A., R.J. Williams, I. Fordyce, G.A. Duff and D. Eamus 1998. Does irrigation affect leaf phenology in deciduous and evergreen trees of the savannas of northern Australia? Aust. J. Ecol. 23:329-339.

Nadezhdina, N., J. Čermák and R. Ceulemans 2002. Radial patterns of sap flow in woody stems of dominant and understory species: scaling errors associated with positioning of sensors. Tree Physiol. 22:907-918.

Oren, R., N. Phillips, B.E. Ewers, D.E. Pataki and J.P. Megonigal 1999. Sap-flux-scaled transpiration responses to light, vapor pressure deficit, and leaf area reduction in a flooded *Taxodium distichum* forest. Tree Physiol. 19:337-347.

Oren, R., N. Phillips, G. Katul, B.E. Ewers and D.E. Pataki 1998. Scaling xylem sap flux and soil water balance and calculating variance: a method for partitioning water flux in forests. Ann. For Sci. 55:191-216.

Pataki, D.E., R. Oren and N. Phillips 1998. Responses of sap flux and stomatal conductance of *Pinus taeda* L. trees to stepwise reductions in leaf area. J. Exp. Bot. 49:871-878.

Phillips, N., R. Oren and R. Zimmermann 1996. Radial patterns of xylem sap flow in non-, diffuse- and ring- porous tree species. Plant Cell Environ. 19:983-990.

Ryan, M.G., B.J. Bond, B.E. Law, D. Woodruff, E. Cienciala and J. Kučera 2000. Transpiration and whole-tree conductance in ponderosa pine trees of different heights. Oecologia. 124:553-560.

Schaeffer, S.M., D.G. Williams and D.C. Goodrich 2000. Transpiration of cottonwood/willow forest estimated from sap flux. Agric. For. Meteorol. 105:257-270.

Sperry, J.S., A.H. Perry and J.E.M. Sullivan 1991. Pit membrane degredation and air-embolism formation in ageing xylem vessels of *Populus tremuloides* Michx. J. Exp. Bot. 42:1399-1406.

Spicer, R. and B.L. Gartner 2001. The effects of cambial age and position within the stem on specific conductivity in Douglas-fit (*Pseudotsuga menziesii*) sapwood. Trees. 15:222-229.

Swanson, R.H. 1967. Seasonal course of transpiration of lodgepole pine and Engelmann spruce. *In* International Symposium on Forest Hydrology. Eds. W.E. Sopper and H.W. Lull. Pennsylvania State University, pp. 419-434.

Swanson, R.H. 1974. Velocity distribution patterns in ascending xylem sap during transpiration. *In* Flow: Its Measurement and Control in Science and Industry. Ed. R.B. Dowell. Instrument Society of America, Pittsburgh, PA, pp. 1425-1430.

Teskey, R.O. and D.W. Sheriff 1996. Water use by *Pinus radiata* trees in a plantation. Tree Physiol. 16:273-279.

Waring, R.H. and J.M. Roberts 1979. Estimating water flux through stems of Scots pine with tritiated water and phosphorous-32. J. Exp. Bot. 30:459-467.

Wilson, K.B., P.J. Hanson, P.J. Mulholland, D.D. Baldocchi and S.D. Wullschleger 2001. A comparison of methods for determining forest evapotranspiration and its components:

sap-flow, soil water budget, eddy covariance and catchment water balance. Agric. For. Meteorol. 106:153-168.

Wullschleger, S.D. and A.W. King 2000. Radial variation in sap velocity as a function of stem diameter and sapwood thickness in yellow-poplar trees. Tree Physiol. 20:511-518.

Wullschleger, S.D. and R.J. Norby 2001. Sap velocity and canopy transpiration in a sweetgum stand exposed to free-air CO_2 enrichment (FACE). New Phytol. 150:489-498.

Zang, D., C.L. Beadle and D.A. White. 1996. Variation in sapflow velocity in *Eucalyptus globulus* with position in sapwood and use of a correction coefficient. Tree Physiol. 16:697-703.

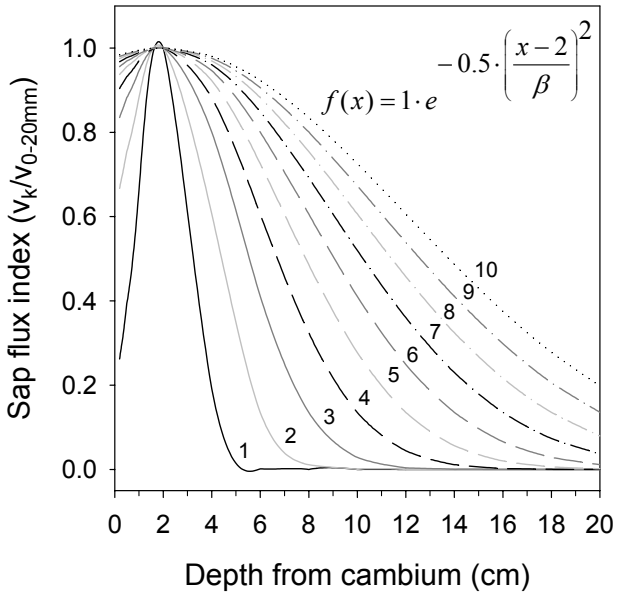

Figure 3.1 Shape of expected normalized radial profiles for *Pinus spp.* follows a 3-parameter Gaussian function with peak sap flux density (index = 1) occurring in the 0-2 cm depth from the cambium. Graph shows the effect of varying β. Numbers next to curves correspond to the value of β for that curve (range shown corresponds to the range fitted to our data).

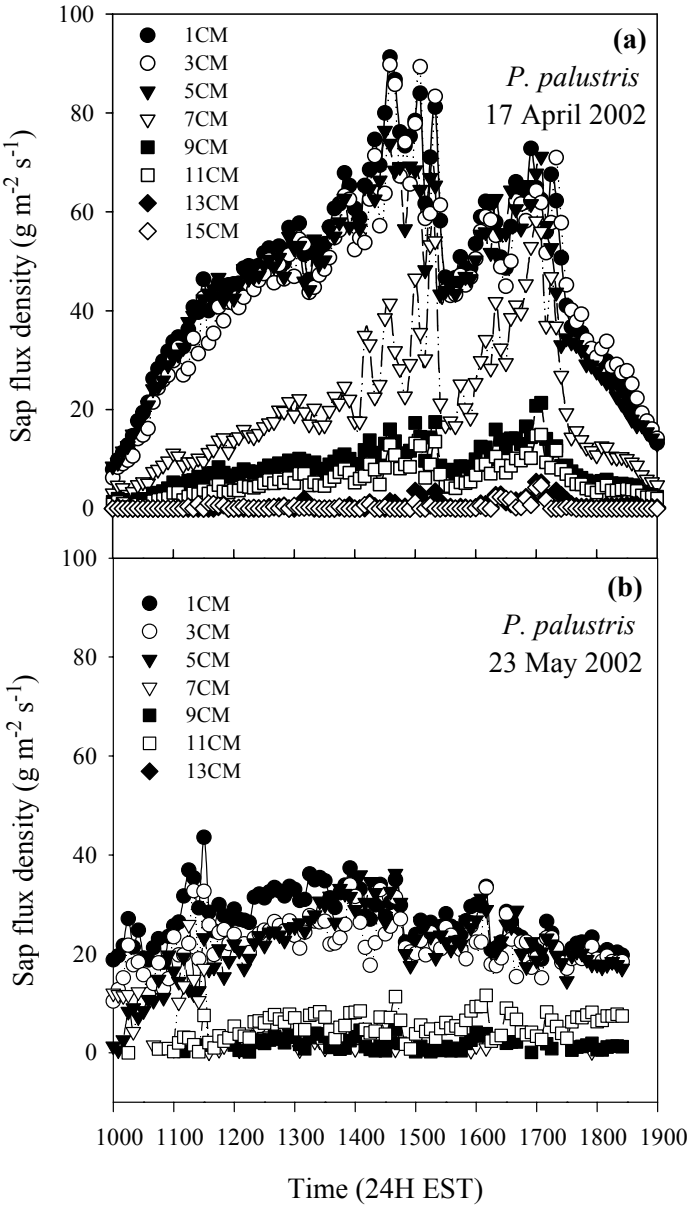

Figure 3.2 Diurnal sap flux density for two *Pinus palustris* trees, panels (a) and (b) show the range and typical shape of the radial pattern of sap flux measured and correspond to trees (a) and (c), respectively (see Table 3.2). Symbols represent the radial position of the thermocouple in the xylem from the cambium, where the cambium is set to 0 cm.

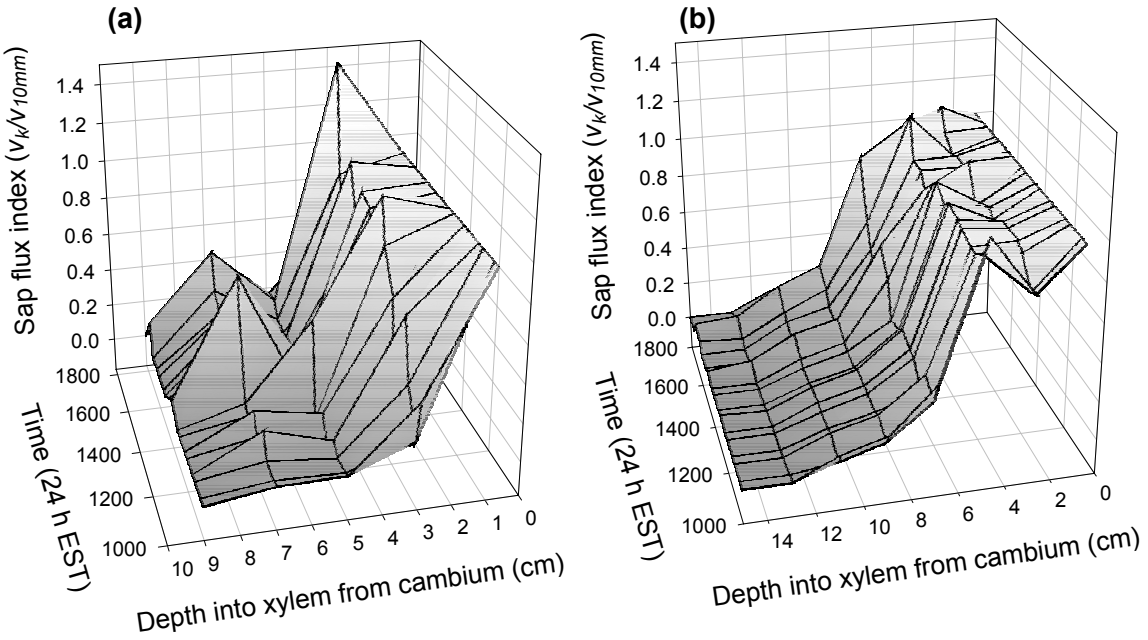

Figure 3.3 Normalized radial profile of sap flux over time for two *Pinus palustris* trees illustrate the range of shape in the profiles with time. Panels (a) and (b) correspond to April 16 and May 25 (days of year 106 and 145), respectively; and trees (a) and (e), respectively (see Table 3.2).

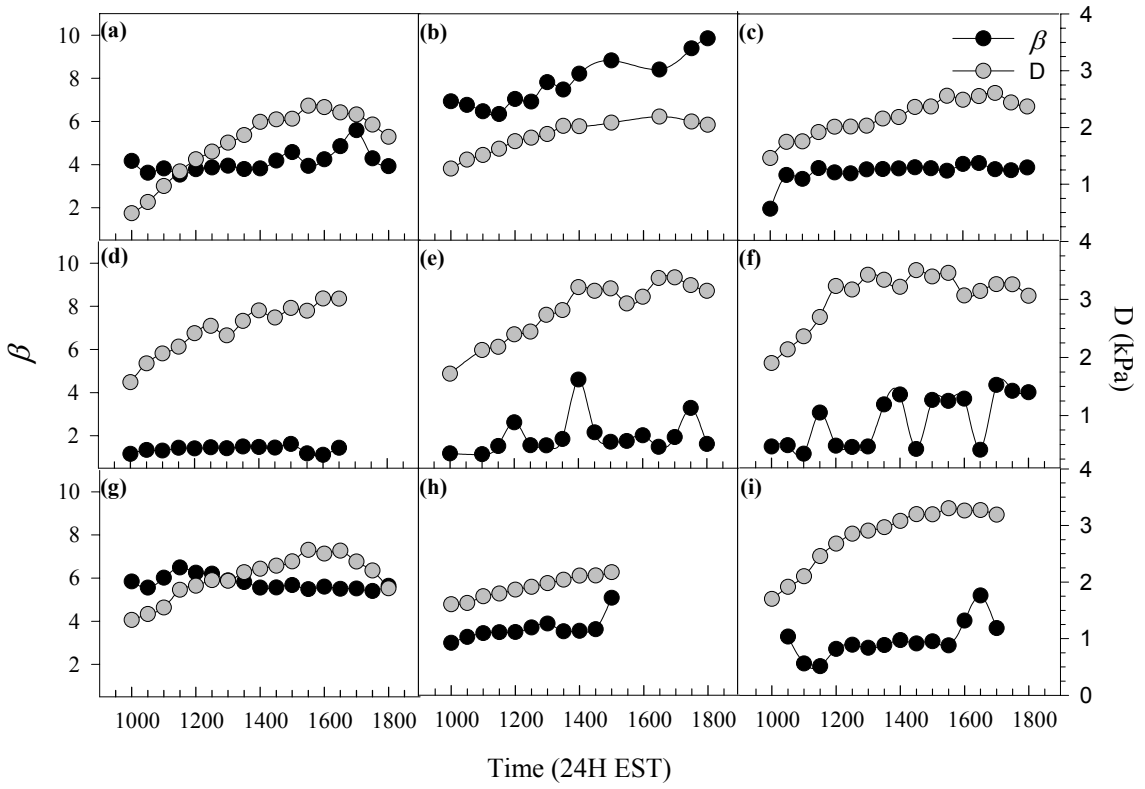

Figure 3.4 Fitted Gaussian β parameter for the radial profile of each tree sampled over time (black symbols). Grey symbols are vapor pressure deficit, *D*. Panel letters correspond to the following tree species sampled: (a)-(f), *P. palustris*; (g), *P. echinata*; (h), *P. elliottii*; (i), *P. taeda*.

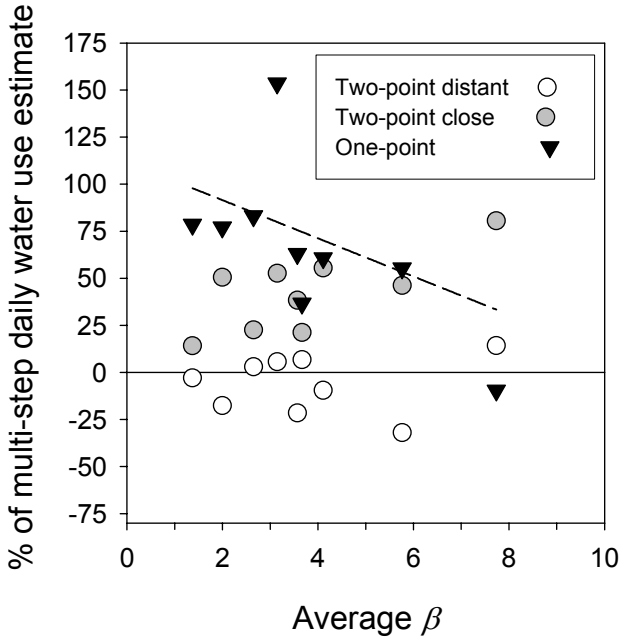

Figure 3.5 The magnitude of discrepancy between multi-point scaling the other scaling method estimates of daily water use in relation to β. See Table 3.1 for description of scaling methods. Dashed line is trend line between one-point scaled overestimate and β (R=0.656, P=0.003). Average β refers to the average of the 17 systematically sampled time periods.

Table 3.1 Stem characteristics of *Pinus spp.* trees and whole tree daily water use calculated using sap flux density (*v*) measured at TCs spaced 20 mm apart starting at 10 mm from the cambium to the heartwood (multi-point); using *v* measured at two distant points (10 & 70 mm) (two-point distant), and two close points (10 & 30 mm) (two-point close); and using *v* measured by only a single TC at 10 mm (one-point). Percent over- or under-estimate of the three latter methods from multi-point is also shown (see methods for more details).

					Daily water use (kg day^{-1}) and percent overestimate or underestimate (%) from multi-point scaled estimate						
		DBH (cm)†	SW‡ radius (cm)	SW area (cm^2)	Multi-point	Two-point distant (10 & 70 mm)	Per-cent (%)	Two-point close (10 & 30 mm)	Per-cent (%)	One-point	Per-cent (%)
P. palustris	a	53.7	18.8	1110.4	111.7	101.0	-10	173.6	55	179.6	61
	b	59.8	16.9	897.3	218.3	249.5	14	394.2	81	197.4	-10
	c	41.7	17.3	940.2	98.9	105.6	7	119.9	21	133.6	37
	d	36.4	9.4	277.6	60.3	58.5	-3	68.8	14	107.7	79
	e	33.4	12.5	490.9	36.8	30.3	-18	55.4	51	65.2	77
	f	46.3	12.0	452.4	148.6	153.0	3	182.1	23	272.1	83
P. echinata	g	44.3	20.5	1320.3	187.6	127.6	-32	274.4	46	291.5	55
P. elliottii	h	51.4	11.1	387.1	99.3	77.9	-22	137.4	38	161.9	63
P. taeda	i	31.6	13.5	572.6	138.1	145.9	6	210.9	53	350.3	154
Average		44.3	14.6	716.5	122.2	116.6	-6	179.6	42	195.7	67

†DBH is over-bark diameter at breast height.
‡Sapwood.

Table 3.2 Individual tree correlation coefficients between β and D (kPa). Letters for trees correspond to the panels in Figure 3.4.

		D	
		R	P
Pinus palustris	a	0.484	0.049
	b	0.773	0.002
	c	0.735	0.001
	d	0.266	0.357
	e	0.425	0.101
	f	0.383	0.129
P. echinata	g	-0.438	0.079
P. elliottii	h	0.686	0.020
P. taeda	i	0.513	0.061

Table 3.3 Results of GLM procedure testing for significant differences in estimated daily whole-tree water use (kg day^{-1}, response variable) with scaling method (n=4, treatment factor, fixed effect) and with tree (n=9, blocking factor, random effect). Post-hoc LSD at α =0.05 is 44.159 (see means in Table 3.1).

Source	DF	MS	F	P
Model	11	19193.89	9.32	<0.001
Tree	8	21004.42	10.20	<0.001
Scaling Method	3	14365.78	6.97	0.0016
Error	24	2060.05		
Corrected Total	35			

CHAPTER 4

DIURNAL AND SEASONAL VARIABILITY IN THE RADIAL DISTRIBUTION OF SAP FLOW: PREDICTING TOTAL STEM FLOW IN *PINUS TAEDA* TREES [1]

---

[1] Ford, C. R., C. E. Goranson, R. J. Mitchell, R. E. Will, and R. O. Teskey. 2004. *Tree Physiology* 24:951-960.
Reprinted here with permission of publisher.

Abstract

We monitored the radial distribution of sap flux density (v, g H_2O m^{-2} s^{-1}) in the sapwood of six *Pinus taeda* trees growing in a plantation during wet and dry soil moisture periods. Mean basal diameter of the 32-year old trees was 33.3 cm. For all trees, the radial distribution of sap flow in the base of the stem (i.e. radial profile) was Gaussian shaped, with maximum sap flow occurring in the outer 4 cm of sapwood and decreasing towards the heartwood. Sap flow in the outer 4 cm of sapwood typically comprised 50-60% of total stem flow (F), while sap flow occurring in the innermost 4 cm of sapwood (11-15 cm) typically comprised less than 10% of F. The percent of flow occurring in the outer 4 cm of sapwood was stable with time (average CV < 10%); however, the percentage of flow occurring in the remaining sapwood was more variable over time (average CV > 40%). Diurnally, we found that the radial profile changed predictably with time and with total stem flow. Seasonally, we found that the radial profile became less steep as the soil moisture content (θ) declined from 0.38 to 0.21. Throughout the season, daytime sap flow also decreased as θ decreased; however, nighttime sap flow (an estimate of stored water use) remained relatively constant. As a result, the percentage of stored water use increased as θ declined. Time series analysis of 15 min values of F, θ, photosynthetically active radiation (PAR) and vapor pressure deficit (D) showed that F lagged D by 0-15 min and lagged PAR by 15-30 min. Diurnally, the relationship between F and D was much stronger than that between F and PAR, while no relationship was found between F and θ. Using an autoregressive moving average (ARIMA) model, 97% of the variability in F could be predicted by D alone. We show that although total sap flow in all trees responds similarly to D, the radial distribution of sap flow comprising total flow can change temporally, both on daily and seasonal scales.

Keywords: Canopy conductance, capacitance, sap flow, time series analysis, transpiration, temporal variability

Introduction

Sap flow measurements are widely used to validate and compare whole-ecosystem estimates of water use and storage in vegetation dominated by woody species (Wilson et al. 2001). Woody species with deep functional sapwood, however, present a challenge in scaling point measurements of sap flux to whole stem sap flow. Moreover, woody species with a large volume of sapwood and considerable height present an additional challenge in temporally scaling whole stem basal sap flow to canopy transpiration due to time lags arising from the use of stored water in the sapwood (Whitehead and Jarvis 1981).

Challenges in scaling point sap flux measurements to whole stem sap flow include accounting for the spatial distribution of sap flux in the stem. Recently, Ford et al. (2004) presented a general mathematical function that describes the spatial distribution of sap flux in stems of tracheid xylem anatomy trees. While we reported that the radial distribution of sap flux density in stems was Gaussian shaped, the slope of the radial profile changed throughout the day, becoming less steep. Several studies have also reported that the radial profile in trees can vary with time (Swanson 1967, Mark and Crews 1973, Lassoie et al. 1977, Becker 1996). Diel changes in the radial profile of conifer stems have been correlated to air vapor pressure deficit, D (Nadezhdina et al. 2002) and soil drying (Phillips 1996, Čermák and Nadezhdina 1998). Understanding the temporal variation and the variables that regulate it presents a challenge in scaling point measurements of sap flux to the entire cross-sectional area of the conducting area. Furthermore, the degree to which the radial profile changes over long and short time scales is unknown.

Additional challenges arise in scaling temporally. Studies often use basal stem flow measurements to estimate canopy transpiration and conductance. Time lags arising from the use of stored water in the sapwood result in basal stem flow and canopy transpiration being asynchronous. Often, canopy transpiration is estimated as the manually-shifted time series of basal stem flow (Granier and Loustau 1994, Martin et al. 2001); however, some studies do not account for the temporal asynchrony.

In the present experiment, our objectives were to a) describe the daily and seasonal temporal variability in the radial distribution of sap flux, b) characterize the variability in total stem flow, and c) relate the variability in total stem flow to environmental variables such as photosynthetically active radiation (PAR), vapor pressure deficit (*D*), and soil moisture. A plantation of genetically and ontogenetically similar trees provided an ideal system on which to evaluate the above objectives. A secondary goal of this paper is to present an alternative method to those currently used to identify and determine time lags in tree stems.

Materials and methods

Site description and environmental measurements

This experiment was conducted at the University of Georgia's Whitehall Forest in northeast Georgia USA (N33°57' W83°19'). Our study site within the forest was a 32-year-old loblolly pine (*Pinus taeda* L.) plantation, with approximately 3 x 3 m tree spacing. The soil type at the site is classified as a Pacolet Series, Fine, kaolinitic, thermic Typic Kanhapludults (Soil Survey Division, Natural Resources Conservation Service 2003), and is an eroded clay soil with a sandy loam texture approximately 0.9 m deep with a poorly developed A horizon and low nutrient availability. The site index, or expected height for 25-year old dominant trees, is 16.6 m, which

indicates low to moderate height growth potential for this region. Within the site, we measured and recorded sap flux density (v) on six trees. The diameters of the trees ranged 29.1 to 38.6 cm and averaged 33.3 cm, sapwood area averaged 754.9 cm^2, and sapwood radius averaged 15.5 cm. We also measured soil water content in the 0-30 cm depth using time domain reflectometry (CS616; Campbell Scientific, Inc., Logan, UT, USA) every 5 min and recorded 15 min averages with a datalogger (CR23X; Campbell Scientific, Inc., Logan, UT, USA).

A weather station was located in an adjacent open field less than 20 m away, which measured the following parameters every 5 min and logged 15 min averages (CR10X, Campbell Scientific, Inc., Logan, UT, USA): ambient air temperature and relative humidity (CS500; Campbell Scientific, Inc., Logan, UT, USA); PAR (LI190SB; Campbell Scientific, Inc., Logan, UT, USA); and rainfall (TE525; Campbell Scientific, Inc., Logan, UT, USA). Ambient vapor pressure (e, kPa) and saturation vapor pressure (e_{sat}, kPa) were used to compute vapor pressure deficit ($D = e_{sat} - e$).

Probe Design and Sap Velocity Measurements

We constructed six Granier-style thermal dissipation probes using thin-walled brass tubing that spanned the sapwood in the sample trees. Probes consisted of one upper heated probe (4 mm outside diameter, 16 cm in length, containing constantan wire with a resistance of 0.4 Ω cm^{-1}) and one lower reference probe of the same diameter and length. Each probe contained 8 independent thermocouples (TC) mounted in the shaft of the probe every 2 cm starting at 1 cm. As a validation of the 16 cm long probes, we also constructed and installed one 2 cm long Granier-type probe in each tree, which had a TC junction at 1 cm (2.32 mm outside diameter of aluminum tubing, 2 cm in length, containing constantan wire with a resistance of 0.4 Ω cm^{-1}). These served as an independent check on the first junction of the 16 cm long probes. When sap

flux values measured in the outer 2 cm of xylem by the 2 cm probe were plotted against sap flux values measured in the outer 2 cm of xylem by the 16 cm probe, a linear and 1:1 relationship existed. We have also previously shown good agreement between stem sap flux estimated with long probes and actual stem flux measured gravimetrically (Ford et al. 2004).

The 16 cm long probes were placed in each sample tree approximately 1.5 m above the ground, while the 2 cm probes were placed 30 cm below the corresponding heated and reference probes of the 16 cm long probe. Both sets of probes were installed on the north side of all trees. For both sets of probes, heated and reference probes were separated vertically by 5 cm. We used a guide template to drill holes for the probes to ensure the probes were parallel. All probes were coated with high-conducting silicone grease (Heat sink grease; Chemtronics, Kennesaw, GA, USA) before placement in the trees, and a 30 cm section of stem above and below the probes was wrapped in reflective insulation (Reflectix; Reflectix Inc., Markleville, IN, USA) to shield the probes from solar radiation, thermal gradients, and rainfall. Each tree (n=6) was monitored during April 13- July 21 (days of year 103-202), 2003. We analyzed data from days 143-153, 160-174, and 184-202. Data could not be analyzed for the other days because of equipment failure caused by severe thunderstorms.

The function relating v to thermal dissipation was developed (Granier 1985) and revalidated (Clearwater et al. 1999) using probes that dissipated 0.2 W for a probe 2 cm in length. We used the same relationship, calculating that our 16 cm heated probe would need to dissipate 1.6 W. All lead wires were soldered to copper, double shielded cable wires (Model 9927; Belden Inc., Richmond, IN, USA). Thermocouple wires were differentially connected to a data logger (CR23X; Campbell Scientific, Logan, UT, USA) measured every 5 min and

compiled into 15 min averages. The temperature difference (ΔT) between the probes was converted to *v* using the equation of (Granier 1985).

All sample trees were cored at the end of the measurement period just above the areas where the probes were installed. The length of the sapwood radius was measured with a ruler on each core. For all trees, the radius of the increment core was found to be sapwood (i.e. no heartwood). We converted each 15 min average *v* to tree sap flow (F, g H_2O s^{-1}) by weighting each sap flux density (v_k) measurement by the sapwood area each TC junction was assumed to measure (Hatton et al. 1990):

$$F = \sum_{k=1}^{n} \pi \left(r_k^2 - r_{k-1}^2 \right) \cdot v_k \qquad \text{(Equation 4.1)}$$

We assumed that a) each TC junction measurement zone was 2 cm wide and did not overlap adjacent zones and b) TCs were centered on the sapwood area defined by an inner radius (r_k) and an outer radius (r_{k-1}).

Assessing change in the radial profiles

Using each v_k and tree stem flow (F), we calculated the percent of F through each sapwood area defined by r_k and r_{k-1}. We further calculated two values for sectional stem flow: outer flow (F_o), which was comprised of flow in the outer 4 cm of xylem; and inner flow (F_i), which was all remaining xylem flow. To assess the change in the radial profile, the difference between F_i and F_o was evaluated for a range of given F.

Modeling transpiration from stem flow

To assess daily total stem flow we integrated the 15 min F values to 24 h. For daytime water use, values were summed during times when PAR > 0 μmoles m^{-2} s^{-1}, which was during 530-

2000 h EST. For nighttime water use, we summed the values when PAR = 0 μmoles m^{-2} s^{-1}, which was during 2015-515 h.

We used a time series approach to identify and model the relationship between the environmental variables and sap flow. This approach is appropriate because of the serial dependence inherent in sap flow data collected in time (e.g. sap flow observations at time *t* are highly correlated and dependent upon observations at time *t*-1). Because of this autocorrelation, observations over time for a single individual are not independent; therefore, correlations with observations of environmental data at various times violate the underlying assumptions of the correlation analysis. Serial dependence can be a characteristic of data collected at the time scale of minutes, as well as at daily and seasonal scales. To account for this serial dependence, we used the general set of time series models termed autoregressive integrated moving average (ARIMA) models (for general reference see Box and Jenkins 1976, Rasmussen et al. 2001, Brockwell and Davis 2002). Briefly, ARIMA models can have an autoregressive term (AR) of order *p*, a differencing (integrating) term (I) of order *d*, and a moving average term (MA) of order *q*. Notation for specific models takes the following form: (*p*, *d*, *q*). Determination of the order of each term in the model is made by examining the raw data and plots of the autocorrelation function of the data. For example, if a series has significant autocorrelation coefficients between x_t and x_{t-1} and x_{t-2}, that would indicate that a second order AR (p=2) term in the model would be appropriate. As in linear regression methods, the AR and MA parameters, *p* and *q,* can have coefficients, ϕ and θ, respectively. ARIMA models fit to time series data use AR and MA terms to describe the serial dependence, and use other time series data from independent variables to describe the dependence on outside factors. The residual series remaining should have characteristics of random error (e.g. uncorrelated random variables with a

mean of 0 and variance of σ^2). An underlying assumption of ARIMA models is that the series being modeled is stationary, i.e. the series exhibits the same mean level and variance in time. Differencing the series by a period of d can yield a series that satisfies this assumption, (e.g. $x_t - x_{t-1}$ for d=1). In practice, stationarity allows statistical inference and estimation in time without genuine replication (Rasmussen et al. 2001).

We assumed that the environmental variables of PAR, D, and soil moisture determined canopy transpiration. We also assumed that the time series of basal sap flow from each tree (F_t) shifted forward in time relative to canopy transpiration due to a time lag associated with long-distance water transport in the stem and the use of stored water in the sapwood could estimate the time series of canopy transpiration (E_t):

$$\boldsymbol{E_t = f^n(F_t)} \qquad \text{(Equation 4.2)}$$

where f^n is a forward shift operator, which shifts the F_t series forward n observations in time. A forward shift operator is similar to a backward shift operator (b^n), in that a backward shift operator shifts a series backward n observations in time. We used both forward and backward shift operators in our analysis at different stages of developing candidate models. For example, although our assumption was that the dependent variable of basal sap flow (F_t) would need shifting forward in time to estimate canopy transpiration, in practice we shifted the series of independent variables— PAR (P_t), D (D_t), and fractional moisture in the upper 30 cm of soil (S_t)— backward in time to estimate basal sap flow. For this analysis we only used times of sap flow during 0800-2000 h EST. We used PROC ARIMA in SAS software (v8.02 SAS Institute Inc., Cary, NC, USA) for this analysis; however, many software packages include time series analysis procedures. A differencing period of 1 (e.g. d=1) resulted in all series being stationary. We used plots of cross correlation coefficients between the independent and dependent variables

to identify direct and inverse relationships at various lags or time shifts. For example, we computed correlation coefficients between PAR at time *t* and sap flow at time *t*, *t*+1, *t*+2..., *t*+10. If variation in the independent variable causes variation in the dependent variable, variation in the independent series should always precede variation in the independent series (i.e. significant correlations between sap flow and *D* at time *t*, and at positive time lags (or shifts) of sap flow). We then fit ARIMA models to the dependent variable using independent variables as predictor variables. We used maximum likelihood to estimate the model parameters. ARIMA models are versatile and can incorporate many series of independent variables (SAS 1991). For a general series differenced by a period of 1 (F_t) that can be predicted by one independent variable (Z_t), the (1, 1, 1) ARIMA model has the general form:

$$F_t = \mu + \omega_0\left(\frac{1-\omega_1 b^1}{1-\delta_1 b^1}\right)Z_t + \left(\frac{\left(1-\theta_1 b^1\right)}{\left(1-\phi_1 b^1\right)}\right)a_t \qquad \text{(Equation 4.3)}$$

where μ is a constant; b^1 is the backward shift operator (shifting the independent series backward 1 period in time relative to the dependent series); ϕ_1 is the coefficient for the first order autoregressive parameter; θ_1 is the coefficient for the first order moving average parameter; a_t is noise; and ω_0, ω_1 and δ_1 are coefficients for the polynomial parameters in the numerator and denominator for the transfer function relating the independent variable to the dependent variable.

We developed many models for each F_t. We used autocorrelation plots of the residuals to verify that the residual series had characteristics of random error, or white noise (i.e. all non-zero time lags have a correlation coefficient of zero). For model selection, we computed Akaike's information criterion (AIC) for each model, which is a statistic used to evaluate the goodness of fit of a candidate model, with smaller values indicating a better fitting model than

larger values. We used the differences in the AIC values among candidate models (Δ_i=AIC$_i$-AIC$_{min}$) to compute a relative weight (w_i) for each model relative to all models fit:

$$w_i = \frac{e^{-0.5\Delta_i}}{\sum_{r=1}^{R} e^{-.5\Delta_r}} \qquad \text{(Equation 4.4)}$$

with the sum of all w_i equal to 1. The final model selected was the model with the highest AIC weight (Burnham and Anderson 2002).

Results

Temporal variability in radial profile

The radial profile was Gaussian shaped, with maximum sap flow occurring in the outer 4 cm of sapwood and decreasing towards the heartwood. Relative sap flux density (v_k/v_{max}) was greatest in the outer 4 cm of sapwood and lowest in the inner 12-16 cm of sapwood (Figure 4.1a). Sap flow measured by the outer two TC junctions typically comprised 50-60% of total stem flow (F), while sap flow measured by the innermost two TC junctions (13-15 cm) typically comprised less than 10% of total stem flow (Figure 4.1b). The percent of flow occurring in the outer 4 cm of sapwood was stable with time; however, the percentage of flow occurring in the remaining sapwood was more variable over time, i.e. higher variance. The coefficient of variation of F increased with increasing depth into the xylem from the cambium, with flow measured in the inner sapwood (measured by the 11-15 cm TC junctions) being most variable (Figure 4.1c).

Diurnal variability in the shape of the radial profile was predictable, with all trees responding similarly. Outer minus inner flow (F_o-F_i) showed a trend with time and with total flow (Figure 4.2). The difference between outer and inner flow was greatest in the late morning

hours (~1100 h). Outer and inner flow were most similar early and late in the day (~0800 and 2000 h). Finally, the difference between outer and inner flow was stable during maximum flow rates (~1400 h). The value of F_o-F_i at mid-day was also normally between the morning and late day values (Figure 4.2). In other words, for any given flow rate through the stem or for different times during the day, the radial distribution of sap flow in the stem was different. At high flow rates (>1.5 g s^{-1}) achieved in the afternoon, F_o-F_i was more stable than at other times during the day. Because a trend is evident with time and with total flow, if flow is held constant, the temporal trend can be analyzed. For example, in tree 1 on day 145, a total flow rate of 0.784 g s^{-1} was measured in both the morning and afternoon; however, a steeper radial profile existed early in the day while a more even profile existed later in the day (Figure 4.3). Earlier in the day, the amount of sap flow measured in the outer 4 cm of sapwood was 11% higher compared to later in the day at the same flow rate. Similarly, flow measured in the inner sapwood (4-15 cm) later in the day was 11% higher compared to earlier in the day at the same stem flow rate. All trees showed the same general pattern for all days.

Daytime *F* for the six trees during 0530-2000 h ranged 28.46 to 125.03 L, and over the entire measurement period averaged 80.9 L (Figure 4.4b). Nighttime recharge, an estimate of capacitance, was approximately 8% of daytime *F* during the wetter soil moisture regime, and increased to approximately 12.5% during the drier soil moisture period, i.e., after Day 195 (Figure 4.4c). This pattern was due to a decline in daytime sap flow during the drier soil moisture period, with a constant nighttime sap flow (Figures 4.4a and 4.4b).

In general, the time course of *F* in all trees closely followed the time course of *D* (Figure 4.5). Changes in *D* were subsequently followed by changes in *F* measured at 1.5 m above the ground surface (Figure 4.5 outset).

In addition to diurnal variability in the radial profile, seasonal variability also occurred. As fractional soil moisture declined during the season from 0.38 to 0.21, the radial profile (F_o-F_i) for some trees became less steep (Figures 4.6b and 4.6c); however in other trees, the radial profile remained unchanged (Figure 4.6a). For four of the six trees, under drier soil moisture regimes (θ<0.25), for any given vapor pressure deficit sap flow in the inner xylem (5-15 cm) contributed relatively more to total stem flow than under wetter soil moisture regimes (θ>0.35; Figures 4.6b and 4.6c). In the remaining trees, there was no seasonal change in the shape of the radial profile (Figure 4.6a). Clearly, although total sap flow in all trees responded similarly to *D* (Figure 4.5), the radial distribution of sap flow could either be dynamic or static under different soil moisture regimes (Figure 4.6).

Modeling the variability in stem flow

Total stem flow (*F*) for all trees was positively related to *D* and PAR. The relationship of *F* with *D* was much stronger than the relationship with PAR (Figure 4.7). Cross-correlation coefficients calculated between *F* and *D* series clearly showed a strong correlation at a lag of 0, with weaker correlations at positive lags. This indicated that changes in *F* lagged changes in *D* by 0-15 min, but were also related to previous values of *D*. Cross-correlation coefficients calculated between *F* and PAR series showed a weaker correlation compared to those with *D*, with changes in PAR lagging changes in *F* by +1. This indicated that changes in *F* lagged changes in PAR by 15-30 min. No correlation was found between diurnal moisture in the top 30 cm of soil and diurnal *F*. There was little or no diurnal variation in soil moisture; therefore, it was not correlated with *F*.

Of all the models fit to each F_t series, *D* explained the most diurnal variance. Neither PAR nor moisture in the top 30 cm of soil was in any of the best models. Weighted AIC values of the final model selected relative to all models fitted were generally high for all trees,

indicating that the one model selected fit the data best (Table 4.1). In general, the F_t series for monitored trees had a second order autoregressive structure. All final models for individual trees explained more than 94% of the total variance in the F_t series, ranging 94.8 to 97.9%. When we averaged all the F_t series into an average series, the best fitting model was a (2, 1, 2) model, which explained 97% of the variance (Table 4.1).

Discussion

Temporal variability in the radial profile

Diurnally, for any given flow rate, sap flow measured in the inner xylem was higher later in the day compared to earlier in the day. This trend is in agreement with our earlier observation in four southeastern pine species, in which the radial profile became more even later in the day compared to earlier in the day (Ford et al. 2004). This diurnal pattern could be occurring for a number of reasons. First, water stored in the inner xylem could only be withdrawn late in the day (i.e. a function of capacitance and relative water content). Studies have found that relative water content of the xylem varies on daily (Teskey et al. unpublished data, Holbrook 1992, Sparks et al. 2001), seasonal and yearly time scales (Constantz and Murphy 1990, Wullschleger et al. 1996, Irvine and Grace 1997, Cinnirella et al. 2002), with typical daily fluctuations of 10% stem water content in conifers (reviewed in Whitehead and Jarvis 1981). Second, the driving force necessary to move water in the inner xylem of these trees, with its probable higher resistance (Spicer and Gartner 2001), could be met late in the day under higher vapor pressure deficits and not early in the day under lower vapor pressure deficits. Third, the inner xylem sapwood area could be compensating for the reduced flow in the outer xylem caused by cavitation events. When the outer xylem tracheids become air-filled, the water conducted by the

cavitated conduits becomes available for conduction by the functional tracheids in the inner xylem (Lo Gullo and Salleo 1992), i.e. the inner xylem is compensating for the reduced flow in the outer xylem. For this latter mechanism to contribute to the diurnal pattern, refilling of the tracheids would have to occur.

Seasonally, as soil moisture content declined from 0.38 to 0.21, we found that the shape of the radial profile in some trees became more even, while in other trees the shape of the radial profile did not change. A more even radial profile under drier soil conditions indicates that the inner xylem was contributing relatively more to total sap flow than it was contributing under wetter soil conditions. For trees displaying this seasonal pattern, the flow in the inner xylem remained relatively constant while the flow in the outer xylem decreased. This pattern is similar to that found by (Nadezhdina and Čermák 2000) for a *Pinus sylvestris* tree. They found that under conditions of drought stress, flow in the outer 3 cm of sapwood was reduced when compared to non-drought conditions, but flow in the inner 4-8 cm of sapwood remained unchanged. This seasonal pattern could be caused by a number of factors; however, in our study nighttime sap flow remained relatively constant throughout the season. If a constant amount of water stored in the inner xylem was recharged at night and withdrawn during the day, this would explain why inner xylem flow remained relatively constant.

Our results have scaling implications for sap flow studies in woody species with deep functional sapwood. Many sap flow studies in woody species with deep functional sapwood measure sap flow at one point the in xylem. To scale these measurements spatially to the whole sapwood area, a common practice is to assess a radial profile on a representative tree at a point in time and use this to calculate a correction factor or a ratio (Teskey and Sheriff 1996, Wullschleger and King 2000, Medhurst et al. 2002). Based on our results, using a radial profile

assessed during maximum flow rates to scale point measurements is a good strategy that will result in estimates of daily sap flow that approximate actual daily sap flow. Using this strategy to scale will result in underestimating within-day sap flow during the early portion of the day, and overestimating within-day sap flow during the later portion of the day. However, these errors will be compensating and the daily estimate of sap flow will approximate actual daily sap flow. Our results also suggest that over seasons the radial profile during times of maximum sap flow may not be constant; therefore, in scaling studies, radial profiles should be assessed under varying soil moisture conditions.

Models, time lags, and stem water storage

Studies that use stem sap flow measurements to model canopy transpiration have used physiologically-based process models such as the Penman-Monteith equation. A simplified version of the Penman-Monteith model used for coniferous species predicts transpiration as a function of vapor pressure deficit and stomatal conductance, and not available energy (Whitehead and Jarvis 1981). The models generated in our study, although empirical, converge with the simplified Penman-Monteith model used for coniferous species, in that vapor pressure deficit was the more powerful predictor and available energy, as estimated by PAR, did not help predict stem flow. Our results are also similar with other sap flow studies on *P. taeda* plantations that show that canopy transpiration is more correlated to vapor pressure deficit than available energy (Ewers and Oren 2000).

We found a relatively short time lag, 0-30 min, between basal stem flow and vapor pressure deficit in 32-year old *Pinus taeda* trees. Time lags between canopy transpiration and stem flow measured at 1.5 m above the ground are related to tree size and wood anatomy. Reported time lags for coniferous species with tracheid xylem anatomy are longer compared to

those of angiosperm species with diffuse- and ring-porous xylem anatomy. Also, longer time lags have been reported for older (and thus generally larger and taller) trees compared to younger (and thus generally smaller and shorter) trees. For example, in angiosperms the time lag between basal stem flow of 70-year old aspen trees and forest vapor flux measured by eddy covariance was 1 h (Hogg et al. 1997), while the basal stem flow of 30-year old *Fagus sylvatica* trees had a maximum correlation with canopy transpiration assessed with eddy covariance at a lag of 0-30 min (Granier et al. 2000). In a tropical, seasonally moist forest in Panama, Goldstein et al. (1998) found time lags ranging from 1-5 h between maximum flow in the branch and at the base of the stem in *Anacardium excelsium, Ficus insipida, Luehea seemannii, Spondias mombin, and Cecropia longipes*, with smaller, shorter trees having shorter time lags (0-1 h) than larger, taller trees (4-5 h). In gymnosperms, young trees have been reported to have relatively short time lags between basal stem flow and canopy transpiration when compared to older trees. Ewers and Oren (2000) found that basal stem sap flow in 12-year old *P. taeda* trees was most correlated with *D* at a lag of 0-30 min. Similarly, Phillips et al. (1997) found that basal stem sap flow in 12-year old loblolly pine trees lagged canopy transpiration by 30 min. Sevanto et al. (2002) found a 50 min time lag between xylem diameter changes between the base and crown of a 38-year old *Pinus sylvestris* tree. In 35-year old *Pinus sylvestris* trees, Köstner et al. (1996) and Granier et al. (1996) found that basal stem flow lagged canopy water vapor flux by 90 min. Trees in the age range of 50-100 years have been reported as having even longer time lags between stem sap flow and canopy transpiration. For example, in 75-90 year old *Pinus banksiana* trees, Saugier et al. (1997) found that basal stem flow lagged leaf transpiration by 1 to 1.5 hours. In 58-67 year old *Pinus pinaster* trees, Loustau et al. (1996) and Berbigier et al. (1996) found that stem flow measured at the base of the crown lagged canopy water vapor flux

by 1-1.5 hours. In 72-year old *Picea abies* trees, Schulze et al. (1985) found that needle transpiration started 3 hours earlier than basal stem sap flow. Our results conform to this general pattern.

The physiological significance of the time lag detected between canopy transpiration and basal stem flow is a function of stored water usage. For any given pressure gradient and hydraulic conductance from soil to leaf, a longer time lag should result with increasing use of stored water in the sapwood (capacitance, $C = dV/d\Psi$ or $d\theta/d\Psi$, Edwards and Jarvis 1982). Jarvis (1975) presented evidence showing that for stands comprised of older and larger trees, the amount of exchangeable water stored in sapwood contributing to transpiration should be much greater than for younger stands. To this end, Phillips et al. (2003) recently demonstrated that older and larger trees used more stored water than younger trees on a diurnal scale. They further show that as drought conditions develop in the growing season, the use of stored water (estimated as sap flow when PAR=0) increased in *Pinus ponderosa*. Our results obtained from *P. taeda* trees of equal age and approximately equal sapwood area and height, also show that reliance on stored water increases as soil moisture content declines.

Finally, we feel that the method of analyzing data that we present in this paper offers advantages over those commonly used because of the problems associated with time lags, and the spatial distribution of sap flow in the stem. When scaling within-day sap flow measured in the stem to canopy transpiration or conductance, a time lag must be incorporated and this is commonly done by regressing sap flow on canopy transpiration or calculating a correlation coefficient between the two series. Not only are these methods manual and thus cumbersome, but also the series violate the underlying assumptions of regression and correlation techniques because 1) the series contain autocorrelated residuals and 2) observations in time are not

independent, thus correlations can be spurious. Granier and Loustau (1994) discuss the importance of measuring and accounting for the time lag between sap flow and transpiration. Similarly, Oren et al. (1998) warn of the consequences of not carefully choosing a time lag that represents stem flow behind transpiration. Using time series analysis techniques such as those used in the present study, time lags are automatically and conclusively identified and thus the subjectivity in choosing a time lag is avoided (e.g. Martin et al. 2001). Rather than empirically modeling sap flow with ARIMA models, time series analysis can be used to automatically identify the time lag and this information can be used to manually phase shift the sap flow series for use in Penman-Monteith models. This method of analysis is suitable for addressing many emerging questions in tree water relations, especially those relating size and age of individuals to capacity of stored water used and if the amount used changes over seasons or the lifetime of the individual.

Acknowledgements

This study was supported by the University of Georgia Daniel B. Warnell School Of Forest Resources, the Robert W. Woodruff Foundation and the Joseph W. Jones Ecological Research Center. This publication was also developed under EPA STAR Fellowship Agreement No. 91617001-0 awarded by the U.S. Environmental Protection Agency. It has not been formally reviewed by EPA. The views expressed in this document are solely those of the authors and EPA does not endorse any products or commercial services mentioned in this publication. We thank Bob Cooper, Lisa Donovan, Christopher Fonnesbeck, Ron Hendrick, Mary Anne McGuire, Jon Miniat, and Jason Nedlo for their logistical help, help with field work, and overall support.

References

Becker, P. 1996. Sap flow in Bornean heath and dipterocarp forest trees during wet and dry periods. Tree Physiol. 16:295-299.

Berbigier, P., J.M. Bonnefond, D. Loustau, M.I. Ferreira, J.S. David and J.S. Pereira. 1996. Transpiration of a 64-year-old maritime pine stand in Portugal 2. Evapotranspiration and canopy conductance measured by an eddy covariance technique. Oecologia. 107:43-52.

Box, G.E.P. and G.M. Jenkins. 1976. Time series analysis: forecasting and control. Holden-Day, San Francisco. 575 p.

Brockwell, P.J. and R.A. Davis. 2002. Introduction to time series and forecasting. Springer-Verlag, New York. 434 p.

Burnham, K.P. and D.R. Anderson. 2002. Model selection and multimodel inference: A practical information-theoretic approach. Springer-Verlag, New York. 488 p.

Čermák, J. and N. Nadezhdina. 1998. Sapwood as the scaling parameter-defining according to xylem water content or radial pattern of sap flow? Ann. For Sci. 55:509-521.

Cinnirella, S., F. Magnani, A. Saracino and M. Borghetti. 2002. Response of a mature *Pinus laricio* plantation to a three-year restriction of water supply: structural and functional acclimation to drought. Tree Physiol. 22:21-30.

Clearwater, M.J., F.C. Meinzer, J.L. Andrade, G. Goldstein and N.M. Holbrook. 1999. Potential errors in measurement of nonuniform sap flow using heat dissipation probes. Tree Physiol. 19:681-687.

Constantz, J. and F. Murphy. 1990. Monitoring moisture storage in trees using time domain reflectometry. J. Hydrol. 119:31-42.

Edwards, W.R.N. and P.G. Jarvis. 1982. Relations between water content, potential and permeability in stems of conifers. Plant Cell Environ. 5:271-277.

Ewers, B.E. and R. Oren. 2000. Analyses of assumptions and errors in the calculation of stomatal conductance from sap flux measurements. Tree Physiol. 20:579-589.

Ford, C.R., M.A. McGuire, R.J. Mitchell and R.O. Teskey. 2004. Assessing variation in the radial profile of sap flux density in *Pinus* species and its effect on daily water use. Tree Physiol. 24:241-249.

Goldstein, G., J.L. Andrade, F.C. Meinzer, N.M. Holbrook, J. Cavelier, P. Jackson and A. Celis. 1998. Stem water storage and diurnal patterns of water use in tropical forest canopy trees. Plant Cell Environ. 21:397-406.

Granier, A. 1985. Une nouvelle méthode pour la mesure du flux de sève brute dans le tronc des arbres. Ann. Sci. For. 42:193-200.

Granier, A., P. Biron, B. Köstner, L.W. Gay and G. Najjar. 1996. Comparisons of xylem sap flow and water vapour flux at the stand level and derivation of canopy conductance for Scots pine. Theoretical and Applied Climatology. 53:115-122.

Granier, A., P. Biron and D. Lemoine. 2000. Water balance, transpiration and canopy conductance in two beech stands. Agric. For. Meteorol. 100:291-308.

Granier, A. and D. Loustau. 1994. Measuring and modelling the transpiration of a maritime pine canopy from sap-flow data. Agric. For. Meteorol. 71:61-81.

Hatton, T.J., E.A. Catchpole and R.A. Vertessy. 1990. Integration of sapflow velocity to estimate plant water-use. Tree Physiol. 6:201-209.

Hogg, E.H., T.A. Black, G. den Hartog, H.H. Neumann, R. Zimmermann, P.A. Hurdle, P.D. Blanken, Z. Nesic, P.C. Yang, R.M. Staebler, K.C. McDonald and R. Oren. 1997. A

comparison of sap flow and eddy fluxes of water vapor from a boreal deciduous forest. J. Geophys. Res., Atmospheres. 102 D24:28929-28937.

Holbrook, N.M. 1992. Frequency and time-domain dielectric measurements of stem water content in the arborescent palm, *Sabal palmetto*. J. Exp. Bot. 43:111-119.

Irvine, J. and J. Grace. 1997. Non-destructive measurements of stem water content by time domain reflectometry using short probes. J. Exp. Bot. 48:813-818.

Jarvis, P.G. 1975. Water transfer in plants. *In* Heat and mass transfer in the biosphere Eds. D.A. deVries and N.H. Afgan. John Wiley & Sons, Washington DC, pp. 369-394.

Köstner, B., P. Biron, R. Siegwolf and A. Granier. 1996. Estimates of water vapor flux and canopy conductance of Scots pine at the tree level utilizing different xylem sap flow methods. Theor. Appl. Climatol. 53:105-113.

Lassoie, J.P., D.R.M. Scott and L.J. Fritschen. 1977. Transpiration studies in Douglas -fir (*Pseudotsuga menziesii*) using the heat pulse technique. For. Sci. 23:377-390.

Lo Gullo, M.A. and S. Salleo. 1992. Water storage in the wood and xylem cavitation in 1-year-old twigs of *Populus deltoides* Bart. Plant Cell Environ. 15:431-438.

Loustau, D., P. Berbigier, P. Roumagnac, C. Arruda-Pacheco, J.S. David, M.I. Ferreira, J.S. Pereira and R. Tavares. 1996. Transpiration of a 64-year-old maritime pine stand in Portugal 1. Seasonal course of water flux through maritime pine. Oecologia. 107:33-42.

Mark, W.R. and D.L. Crews. 1973. Heat-pulse velocity and bordered pit condition in living Engelmann spruce and Lodgepole pine trees (*Picea engelmannii, Pinus contorta*). For. Sci. 19:291-296.

Martin, T.A., K.J. Brown, J. Kučera, F.C. Meinzer, D.G. Sprugel and T.M. Hinckley. 2001. Control of transpiration in a 220-year-old *Abies amabilis* forest. For. Ecol. Manage. 152:211-224.

Medhurst, J.L., M. Battaglia and C. Beadle. 2002. Measured and predicted changes in tree and stand water use following high-intensity thinning of an 8-year-old *Eucalyptus nitens* plantation. Tree Physiol. 22:775-784.

Nadezhdina, N. and J. Čermák. 2000. Responses of sap flow rate along tree stem and coarse root radii to changes of water supply. *In* The supporting roots of trees and woody plants: form, function and physiology Ed. A. Stokes. Kluwer Academic Publishers, Netherlands, pp. 227-238.

Nadezhdina, N., J. Čermák and R. Ceulemans. 2002. Radial patterns of sap flow in woody stems of dominant and understory species: scaling errors associated with positioning of sensors. Tree Physiol. 22:907-918.

Oren, R., N. Phillips, G. Katul, B.E. Ewers and D.E. Pataki. 1998. Scaling xylem sap flux and soil water balance and calculating variance: a method for partitioning water flux in forests. Ann. For Sci. 55:191-216.

Phillips, N., A. Nagchaudhuri, R. Oren and G. Katul. 1997. Time constant for water transport in loblolly pine trees estimated for time series of evaporative demand and stem sapflow. Trees-Struct. Funct. 11:412-419.

Phillips, N.G., M.G. Ryan, B.J. Bond, N.G. McDowell, T.M. Hinckley and J. Čermák. 2003. Reliance on stored water increases with tree size in three species in the Pacific Northwest. Tree Physiol. 23:237-245.

Rasmussen, P.W., D.M. Heisey, E.V. Nordheim and T.M. Frost. 2001. Time series intervention analysis: unreplicated large-scale experiments. *In* Design and analysis of ecological experiments Eds. S.M. Scheiner and J. Gurevich. Oxford University Press, New York, pp. 158-177.

SAS 1991. Modeling with explanatory variables. *In* SAS/ETS Software: Applications Guide 1, Version 6. Time Series Modeling and Forecasting, Financial Reporting, and Loan Analysis. SAS Institute, Inc., Cary, NC, pp. 149-188.

Saugier, B., A. Granier, J.Y. Pontailler, E. Dufrêne and D.D. Baldocchi. 1997. Transpiration of a boreal pine forest measured by branch bag, sap flow and micrometeorological methods. Tree Physiol. 17:511-519.

Schulze, E.-D., J. Čermák, R. Matyssek, M. Penka, R. Zimmermann, F. Vasicek, W. Gries and J. Kučera. 1985. Canopy transpiration and water fluxes in the xylem of the trunk of *Larix* and *Picea* trees- a comparison of xylem flow, porometer and cuvette measurements. Oecologia. 66:475-483.

Sevanto, S., T. Vesala, M. Peramaki and E. Nikinmaa. 2002. Time lags for xylem and stem diameter variations in a Scots pine tree. Plant Cell Environ. 25:1071-1077.

Soil Survey Division, Natural Resources Conservation Service, United States Department of Agriculture. Official Soil Series Descriptions [Online WWW]. Available URL: " http://ortho.ftw.nrcs.usda.gov/osd/" [Accessed 13 Nov 2003].

Sparks, J.P., G.S. Campbell and R.A. Black. 2001. Water content, hydraulic conductivity, and ice formation in winter stems of *Pinus contorta*: a TDR case study. Oecologia. 127:468-475.

Spicer, R. and B.L. Gartner. 2001. The effects of cambial age and position within the stem on specific conductivity in Douglas-fir (*Pseudotsuga menziesii*) sapwood. Trees Structure and Function. 15:222-229.

Swanson, R.H. 1967. Seasonal course of transpiration of lodgepole pine and Engelmann spruce. *In* International Symposium on Forest Hydrology Eds. W.E. Sopper and H.W. Lull, Pennsylvania State University, pp. 419-434.

Teskey, R.O. and D.W. Sheriff. 1996. Water use by *Pinus radiata* trees in a plantation. Tree Physiol. 16:273-279.

Whitehead, D. and P.G. Jarvis. 1981. Coniferous forests and plantations. *In* Water deficits and plant growth Ed. T.T. Kozolwski. Academic Press, Inc., New York, pp. 49-152.

Wilson, K.B., P.J. Hanson, P.J. Mulholland, D.D. Baldocchi and S.D. Wullschleger. 2001. A comparison of methods for determining forest evapotranspiration and its components: sap- flow, soil water budget, eddy covariance and catchment water balance. Agric. For. Meteorol. 106:153-168.

Wullschleger, S.D., P.J. Hanson and D.E. Todd. 1996. Measuring stem water content in four deciduous hardwoods with a time-domain reflectometer. Tree Physiol. 16:809-815.

Wullschleger, S.D. and A.W. King. 2000. Radial variation in sap velocity as a function of stem diameter and sapwood thickness in yellow-poplar trees. Tree Physiol. 20:511-518.

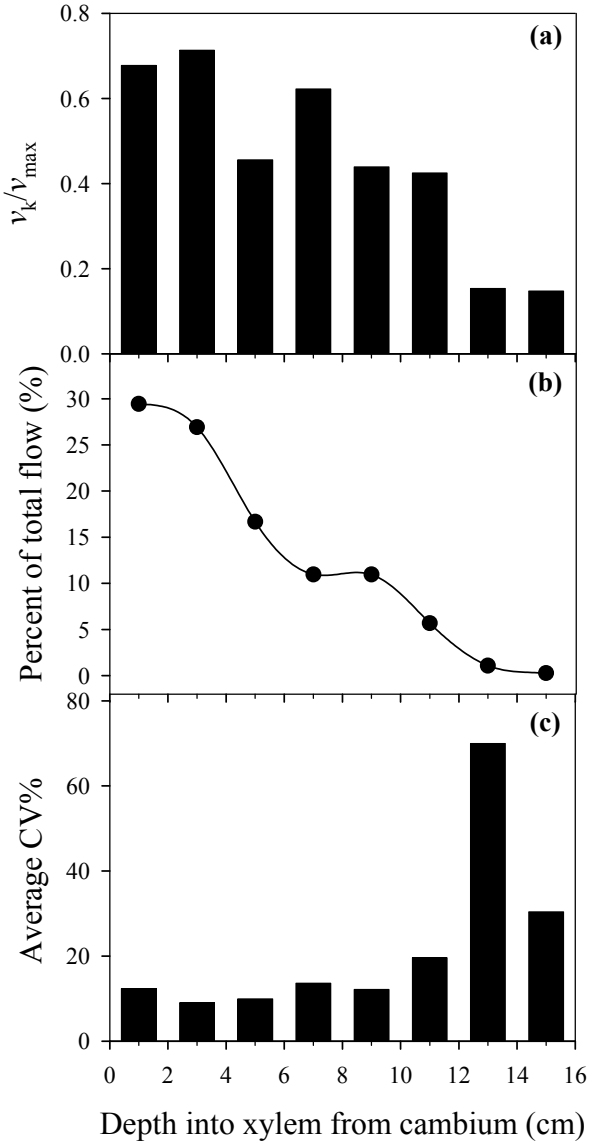

Figure 4.1 Average relative sap flux density (a), percent flow (b), and coefficient of variation (CV) (c) for different radial positions in the six *P. taeda* trees measured. Points and bars represent the average relative sap flux density, percent flow and CV for all measurement days, during times 0800-2000 h, and are the average for the six trees monitored.

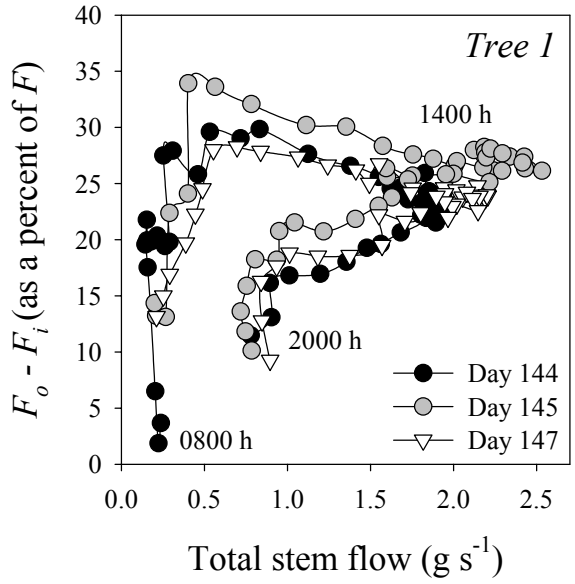

Figure 4.2 Typical diurnal relationship of outer flow (F_o, flow in the outer 4 cm of xylem), minus inner flow (F_i, all remaining xylem flow) with time and total stem flow (F). Trace lines represent time, starting at 0800 h and ending at 2000 h. Graph shows data for tree 1 on three measurement days.

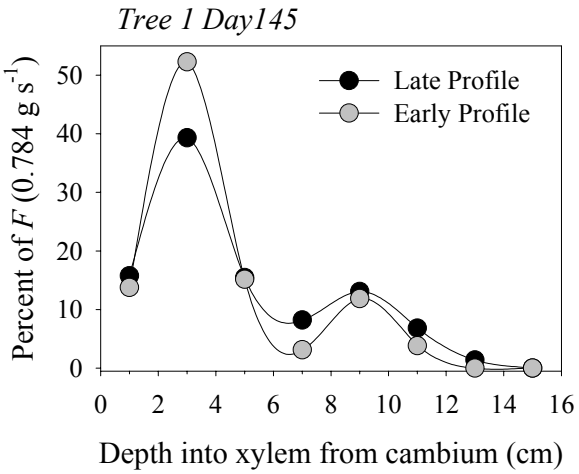

Figure 4.3 Percent of total flow (*F*) as a function of depth into the xylem at a flow of 0.784 g s^{-1} in the stem of tree 1 on day 145. Graph shows that for a given flow rate, a steeper radial profile exists early in the day while a more even profile exists later in the day.

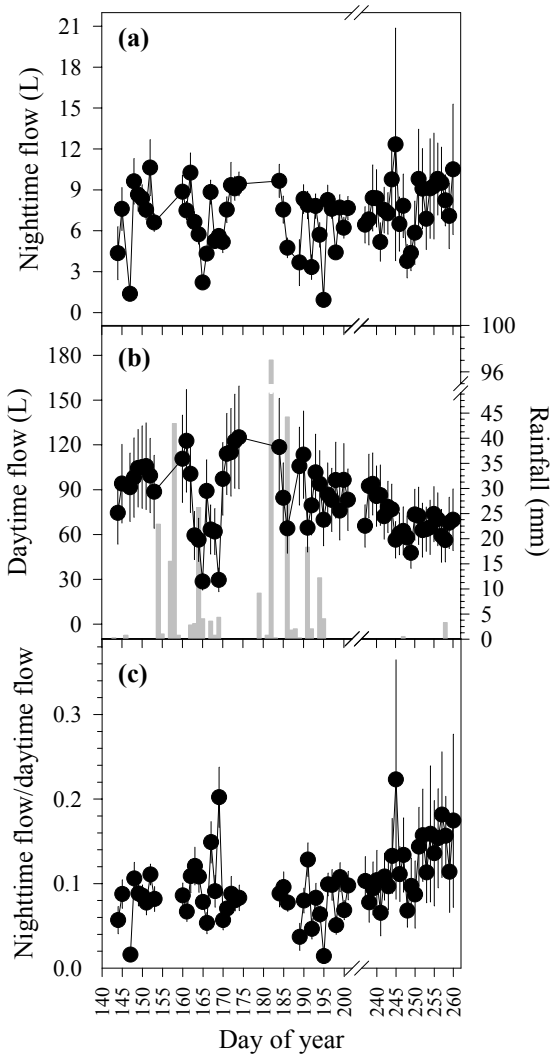

Figure 4.4 Average total nighttime flow determined when PAR=0, 2015-515 h EST (a), average total daytime flow determined when PAR>0, 530-2000 h EST (b), and the ratio of nighttime to daytime flow (c). Points represent the average value for all six trees measured and bars are 1 standard error. Vertical grey bars represent daily rainfall totals (b).

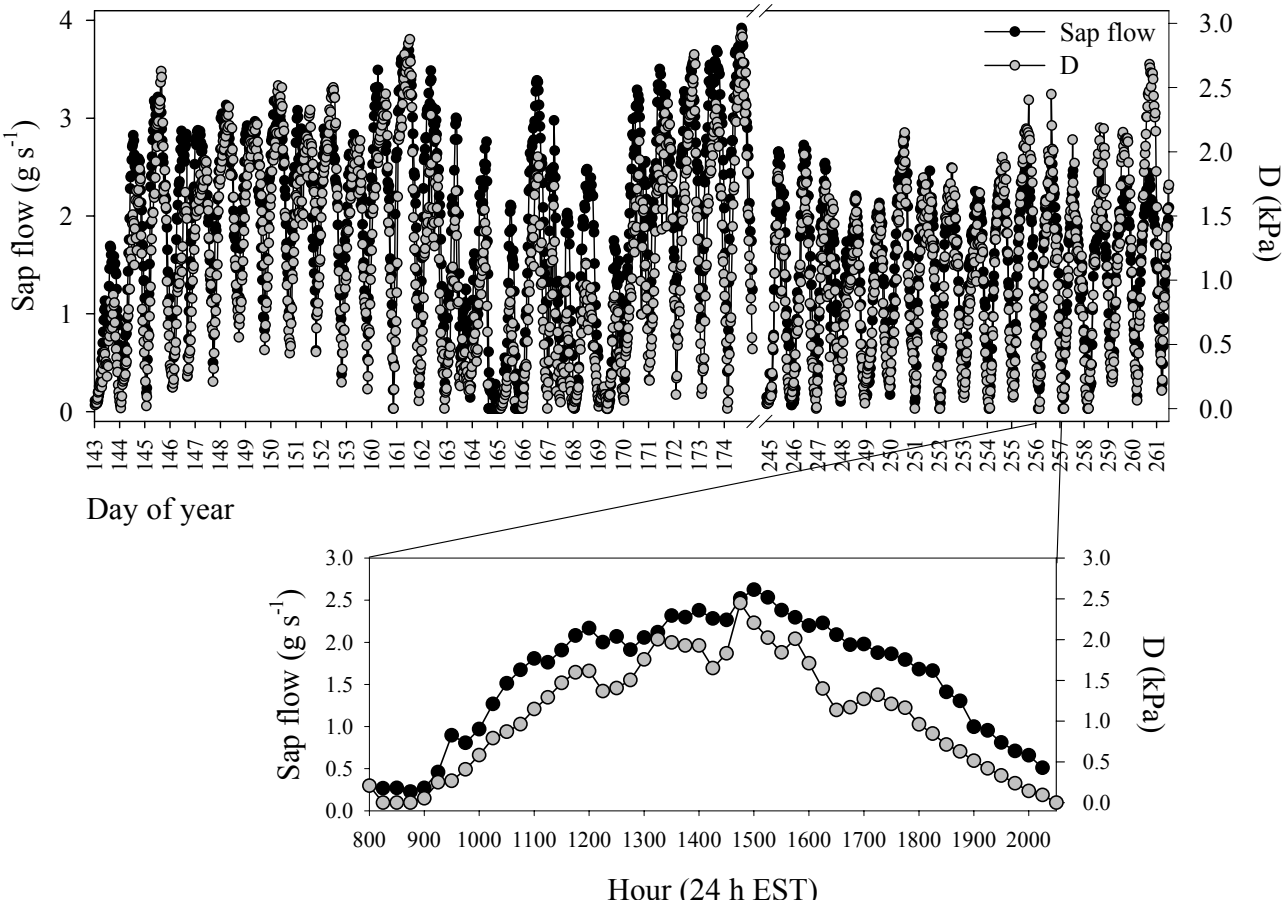

Figure 4.5 Average total stem flow from all six trees and vapor pressure deficit (*D*) during times 0800-2000 h over portion of monitoring period. During days 143-174, average fractional soil moisture content was 0.34; while during days 245-261, average fractional soil moisture content was 0.23. Outset of day 256 shows within-day variability, relationship between stem flow and *D*, and time lag of stem flow behind *D*.

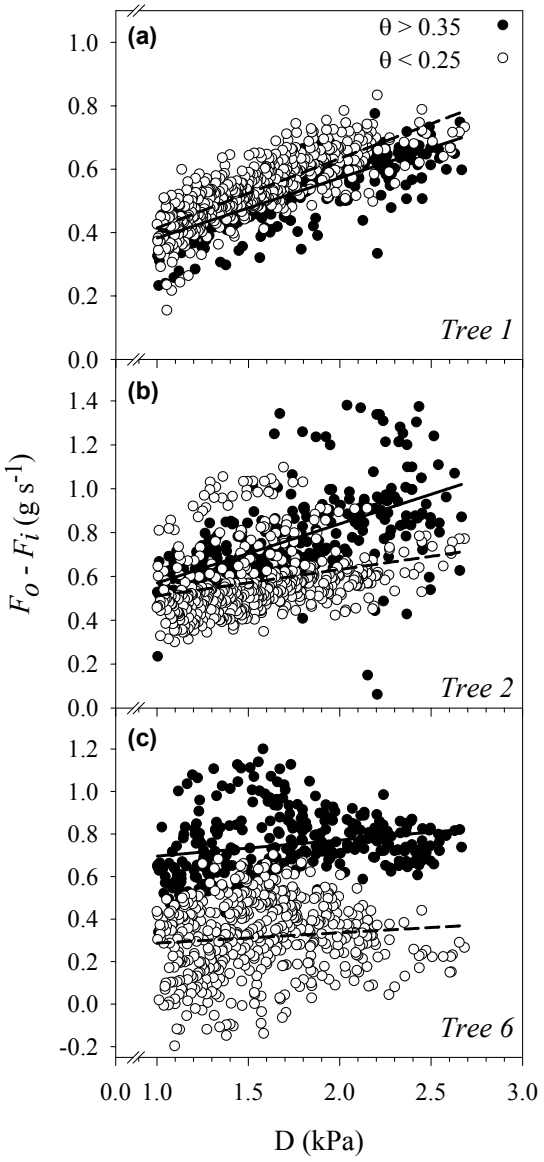

Figure 4.6 Range of seasonal relationships for outer flow (F_o, flow in the outer 4 cm of xylem), minus inner flow (F_i, all remaining xylem flow) with vapor pressure deficit (D, kPa) and high and low fractional soil moisture (θ > 0.35 solid line, filled symbols and θ < 0.25 dashed line, open symbols, respectively). Shape of radial profile in trees 2 and 6 (panels b and c) change with changing soil moisture; however, the shape of the radial profile in tree 1 (panel a) does not change seasonally.

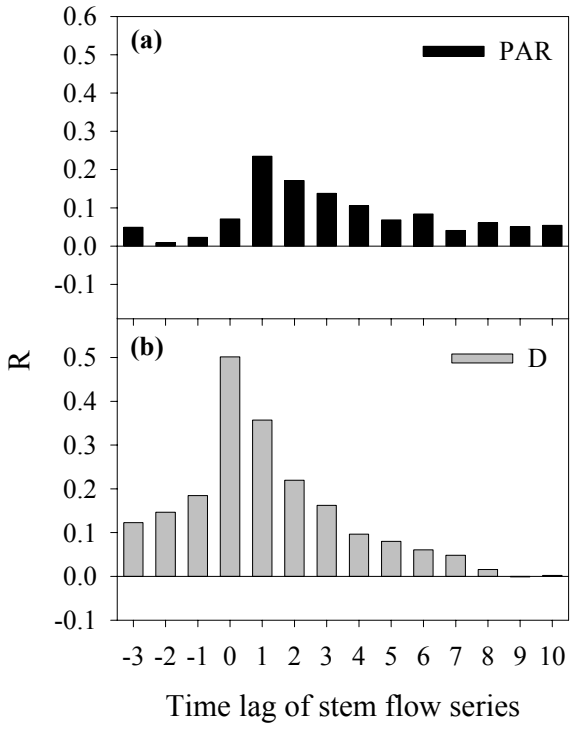

Figure 4.7 Average correlation coefficients (*R*) between average total stem flow in all trees and PAR (a) and *D* (b). Plots show a strong correlation between *D* and stem flow. PAR is ahead of stem flow in time by 15-30 minutes (no correlation with lag 0 but correlation with + lags), while stem flow is responsive to current (0-15 min, lag 0) and previous values of *D* (+ lags).

Table 4.1 Predictive equations for average F_t in six trees as functions of independent variables: PAR (P_t), D (D_t), and fractional moisture in the upper 30 cm of soil (S_t).

F_t ARIMA structure	*Equation*	*AIC*[§]	*w_i*[†]	*S^2_i*[‡]	*S^2_f*[‡]	*% Variance Explained*
(2,1,2)	$F_t = 0.506\left(\frac{1-0.355b^1}{1-0.405b^1}\right)D_t + \left(\frac{(1-0.480b^1)(1-0.416b^2)}{(1-0.610b^1)(1-0.428b^2)}\right)a_t$	-1637.3	0.76	0.96	0.03	97.2

[§]Akaike information criterion.
[†]Akaike weight of model selected relative to all models fitted for that tree.
[‡]Initial (S^2_i) and final (S^2_f) variance in F_t series. Final variance is the unexplained variance in F_t series.

CHAPTER 5

MODELING CANOPY TRANSPIRATION USING TIME SERIES ANALYSIS: A CASE STUDY ILLUSTRATING THE EFFECT OF SOIL MOISTURE DEFICIT ON *PINUS TAEDA* [1]

[1] Ford, C. R., C. E. Goranson, R. J. Mitchell, R. E. Will, and R. O. Teskey. Submitted to *Agricultural and Forest Meteorology*, 07/23/2004.

Abstract

Bulk sap flow measurements are widely used to assess and model the hydrological process of canopy transpiration (E_c); however, common analysis techniques of these data do not identify and/or incorporate time lag effects, multiple variables affecting canopy transpiration at different temporal scales or thresholds, and interactions of environmental variables. Here we describe how autoregressive-integrated-moving average (ARIMA) time series models can be used with bulk sap flow and climate data to estimate E_c. We illustrate parameterizeing and forecasting the ARIMA model using bulk sap flow data collected in a plantation of *Pinus taeda* trees during a period of relatively high soil moisture (wet period) and use this model to predict E_c during a seasonal drought (dry period). The time series model that best fit the data during the wet period was an ARIMA model of order (3, 1, 1). The environmental variable that explained the most partial variance was vapor pressure deficit (D). Photosynthetically active radiation (PAR) was significant, but only explained a small amount of partial variance. When the wet period model was used to forecast daily E_c during the dry period, a systematic overestimate occurred compared to measured values. The difference between actual and forecasted E_c for the 25-day dry period was 12.29 mm, or an overestimate of 29%. In general, the model did not perform well when soil moisture dropped below 0.25 fractional soil moisture content (θ). We added a step intervention term to the model to represent this threshold effect of θ on E_c. The intervention term was significant and explained a higher amount of partial variance in the dry period than did PAR. The ARIMA model explained more than 97% of the total variance in the data and performed well during the wet and dry periods, as well as during an independent validation period that was intermediate in soil moisture and similar in climatic conditions. We discuss the assumptions and

limitations of common analysis techniques of bulk sap flow data and suggest that these approaches be carefully considered when using sap flow measurements to estimate either E_c or canopy conductance, g_c.

Key words: Autocorrelation, autocorrelation function, canopy, transpiration, sap flow

Introduction

Forest transpiration on a land area basis is generally considered a conservative hydrological process, with many factors such as differing suites of species and structures (understory—overstory) decreasing the variability in annual transpiration observed among forests with similar climate and soil regimes (Phillips and Oren, 2001; Roberts, 1983). Even though variability in transpiration among these forests can be low, modeling the physiological process of canopy transpiration is useful for management (Landsberg, 2003), particularly when estimates of actual transpiration are compared to potential transpiration. Robust and versatile predictive models that estimate canopy transpiration are becoming particularly useful for addressing the issues concerning the hydrologic cycle on local and regional scales (Jackson et al., 2001). Moreover, these models are increasingly used to assess water use and plant responses under different climate change scenarios (Martinez-Vilalta et al., 2002).

The hydrological process of canopy transpiration is driven by evaporative demand and available energy, but it is often limited by water availability (Jarvis, 1976; Schulze et al., 1994). Quantifying the impact of soil moisture availability on canopy transpiration is difficult, because for most forests, transpiration is only limited by soil moisture during periods of high soil water deficit. Furthermore, soil moisture deficits generally affect transpiration at different temporal scales than evaporative demand and available energy are measured. Canopy transpiration is often estimated with the Penman-Monteith equation, which uses the variables of evaporative

demand and available energy, intrinsic properties of water, leaf area, stomatal conductance, and wind speed (Whitehead and Jarvis, 1981). Canopy conductance (the product of leaf area and stomatal conductance) takes soil moisture into account because under low soil moisture stomata close. The number of parameters required in the Penman-Monteith model can make it cumbersome to use, and less parsimonious than other empirical models that predict bulk sap flow (i.e. a proxy for canopy transpiration) as a function of evaporative demand and available energy. This latter method of predicting canopy transpiration has been plagued with difficulties, including: fitting the function using observations in time that are not independent; trying to account for the time lag between bulk sap flow and canopy flux via manual synchronization; and using the Penman-Monteith equation to derive a canopy conductance function from bulk sap flow which is then used to develop an empirical model between canopy conductance and environmental variables. Using bulk sap flow over leaf-level measurements is advantageous because bulk sap flow inherently integrates the entire canopy. A method that would allow identification and incorporation of (1) time lag effects, (2) multiple driving variables affecting canopy transpiration at different temporal scales or thresholds, and (3) interactions of environmental variables would improve the utility of bulk sap flow measurements for estimating canopy transpiration.

Our overall goal in this paper is to describe how autoregressive-integrated-moving average (ARIMA) time series models can be used with bulk sap flow and climate data to estimate canopy transpiration, and illustrate the use of ARIMA modeling on *Pinus taeda* canopy transpiration as it is affected by evaporative demand, available energy, and declining soil moisture. Specifically, we will (1) model the effect of declining soil moisture on canopy

transpiration, (2) estimate potential transpiration under no soil moisture stress, and (3) quantify the effect of seasonal soil moisture depletion on canopy transpiration.

Materials and methods

Site description and environmental measurements

This experiment was conducted at the University of Georgia's Whitehall Forest in northeast Georgia USA (N33°57' W83°19'). Our study site within the forest was a 32-year-old loblolly pine (*Pinus taeda* L.) plantation, with approximately 3 x 3 m tree spacing. The soil type at the site is classified as a Pacolet Series, Fine, kaolinitic, thermic Typic Kanhapludults (Soil Survey Division, Natural Resources Conservation Service, 2003), and is an eroded clay soil approximately 0.9 m deep with a poorly developed A horizon and low nutrient availability. The site index, or expected height for 25-year old dominant trees, is 16.6 m, which indicates low to moderate height growth potential for this region. Within the site, we measured and recorded sap flux density (v, g H_2O m^{-2} sapwood s^{-1}) on six trees. The diameters of the trees ranged 29.1 to 38.6 cm and averaged 33.3 cm, sapwood area averaged 754.9 cm^2, and sapwood radius averaged 15.5 cm. We also measured soil water content in the 0-30 cm depth using time domain reflectometry (CS616; Campbell Scientific, Inc., Logan, UT, USA) every 5 min and recorded 15 min averages with a datalogger (CR23X; Campbell Scientific, Inc., Logan, UT, USA).

A weather station was located in an adjacent open field less than 20 m away, which measured the following parameters every 5 min and logged 15 min averages (CR10X, Campbell Scientific, Inc., Logan, UT, USA): ambient air temperature and relative humidity (CS500; Campbell Scientific, Inc., Logan, UT, USA); PAR (LI190SB; Campbell Scientific, Inc., Logan, UT, USA); and rainfall (TE525; Campbell Scientific, Inc., Logan, UT, USA). Ambient vapor

pressure (e, kPa) and saturation vapor pressure (e_{sat}, kPa) were used to compute vapor pressure deficit ($D = e_{sat} - e$).

Sap flux density measurements

We used 16-cm-long Granier-style thermal dissipation probes that spanned the sapwood in the sample trees to measure v. Probe construction, performance, and assumptions are described in detail by Ford et al. (2004a; 2004b). The probes were coated with high-conducting silicone grease (Heat sink grease; Chemtronics, Kennesaw, GA, USA) and placed in each sample tree approximately 1.5 m above the ground on the north side of the tree. A 30 cm section of stem above and below the probes was wrapped in reflective insulation (Reflectix; Reflectix Inc., Markleville, IN, USA) to shield the probes from solar radiation, thermal gradients, and rainfall. Each tree (n=6) was monitored during April 13- September 18 (days of year 103-261), 2003. We analyzed data from days 143-153, 160-174, 184-186, 189-201, and 237-261. Several days of sap flow data collected on days of year 113-123, 130, 132-133, 137-139, and 142 were not initially analyzed and reserved for a later analysis validating model predictions against independent data. Data could not be analyzed for the other days because of equipment failure caused by severe thunderstorms.

All lead wires were soldered to copper, double shielded cable wires (Model 9927; Belden Inc., Richmond, IN, USA). Thermocouple wires were differentially connected to a data logger (CR23X; Campbell Scientific, Logan, UT, USA) measured every 5 min and compiled into 15 min averages. The temperature difference (ΔT) between the probes was converted to v using the equation of (Granier, 1985). Heated probe resistance wires were connected to a power board regulating current such that the probe dissipated 0.1W/cm.

All sample trees were cored at the end of the measurement period just above the areas where the probes were installed. The length of the sapwood radius was measured with a ruler on each core. For all trees, the radius to the center of the tree was found to be sapwood (i.e. no heartwood). We converted each 15 min average v to tree sap flow (F, g H_2O s^{-1}) by weighting each sap flux density (v_k) measurement by the sapwood area each TC junction was assumed to measure (Hatton et al., 1990). All models (described below) were parameterized on this 15 min data. To assess daily total sap flow we integrated the 15 min F values to 24 h. All data analyses were based on the mean F time series from the six trees measured. All tree water use data are presented on a ground area basis in mm (e.g. canopy transpiration, E_c), which was calculated using the measured crown area of all trees monitored for sap flux in 2003.

Modeling transpiration from sap flow

We used a time series approach to identify and model the relationship between the environmental variables and sap flow. This approach is appropriate because of the serial dependence inherent in sap flow data collected in time (e.g. sap flow observations at time t are highly correlated and dependent upon observations at time t-1). Because of this autocorrelation, observations over time for a single individual are not independent; therefore, correlations with observations of environmental data at various times violate the underlying assumptions of the correlation analysis. Serial dependence can be a characteristic of sap flux data collected at the time scale of minutes (representing hydraulic resistance, capacitance, and high frequency changes in climate), as well as at daily and seasonal scales (representing low frequency changes in climate, and leaf and root growth dynamics). In this study, we model sub-daily scale time lags and autocorrelation. To account for serial dependence, we used the general set of time series models termed autoregressive integrated moving average (ARIMA) models (for general reference see

Box and Jenkins (1976), Rasmussen et al. (2001), and Brockwell and Davis (2002)). Briefly, ARIMA models can have an autoregressive term (AR) of order p, a differencing (integrating) term (I) of order d, and a moving average term (MA) of order q. Notation for specific models takes the following form: (p, d, q). Determination of the order of each term in the model is made by examining the raw data and plots of the autocorrelation function of the data. For example, if a series has significant autocorrelation coefficients between x_t and x_{t-1} and x_{t-2}, that would indicate that a second order AR (p=2) term in the model would be appropriate. As in other regression methods, the AR and MA parameters, p and q, have coefficients, ϕ and θ, respectively. ARIMA models fit to time series data use AR and MA terms to describe the serial dependence, and use other time series data from independent variables to describe the linear and nonlinear dependence on outside factors through the use of transfer functions. The residual series remaining should have characteristics of random error (e.g. uncorrelated random variables with a mean of 0 and variance of σ^2). An underlying assumption of ARIMA models is that the series being modeled is stationary, i.e. the series exhibits the same mean level and variance in time. Differencing the series by a period of d can yield a series that satisfies this assumption, (e.g. $x_t - x_{t-1}$ for d=1). In practice, stationarity allows statistical inference and estimation in time without genuine replication (Rasmussen et al., 2001).

We assumed that the environmental variables of PAR, D, and soil moisture determined canopy transpiration. We also assumed that the time series of basal sap flow (F_t) shifted forward in time relative to canopy transpiration (due to a time lag associated with the product of resistance and capacitance, (Phillips et al., 1997; Phillips et al., 2004) could estimate the time series of canopy transpiration (E_t):

$$E_t = f^n(F_t) \qquad \text{(Equation 5.1)}$$

where f^n is a forward shift operator, which shifts the F_t series forward n observations in time. A forward shift operator is similar to a backward shift operator (b^n), in that a backward shift operator shifts a series backward n observations in time. We used both forward and backward shift operators in our analysis at different stages of developing candidate models. For example, although our assumption was that the dependent variable of basal sap flow (F_t) would need shifting forward in time to estimate canopy transpiration, in practice we shifted the series of independent variables— PAR (P_t), D (D_t), and fractional moisture in the upper 30 cm of soil (S_t)— backward in time to estimate basal sap flow. For this analysis we only used times of sap flow during 0800-2000 h EST from the average F_t series. We used PROC ARIMA in SAS software (v8.02 SAS Institute Inc., Cary, NC, USA) for this analysis; however, many software packages include time series analysis procedures. A differencing period of 1 (e.g. d=1) resulted in all series being stationary. We used plots of cross correlation coefficients between the independent and dependent variables to identify direct and inverse relationships at various lags or time shifts. For example, we computed correlation coefficients between PAR at time t and sap flow at time t, t+1, t+2..., t+10. If variation in the independent variable causes variation in the dependent variable, variation in the independent series should always precede variation in the dependent series (i.e. significant correlations between sap flow and D at time t, and at positive time lags (or shifts) of sap flow). We then fit ARIMA models to the dependent variable using independent variables as predictor variables. We used maximum likelihood to estimate the model parameters. ARIMA models are versatile and can incorporate many series of independent variables, including independent variables that may only be important or intervene after a known time, t_{int} (SAS, 1991). For a general series differenced by a period of 1 (Y_t) that can be predicted by one independent variable (Z_t) for all times, and that can be predicted by another independent

variable that is only important after a known intervention time (X_t), the (1, 1, 1) ARIMA model has the general form:

$$Y_t = \mu + \omega_0\left(\frac{1-\omega_1 b^1}{1-\delta_1 b^1}\right)Z_t + \omega_2 X_t + \left(\frac{\left(1-\theta_1 b^1\right)}{\left(1-\phi_1 b^1\right)}\right)a_t \qquad \text{(Equation 5.2)}$$

where μ is a constant; b^1 is the backward shift operator (shifting the independent series backward 1 period in time relative to the dependent series); ϕ_1 is the coefficient for the first order autoregressive parameter; θ_1 is the coefficient for the first order moving average parameter; a_t is noise; ω_0, ω_1 and δ_1 are coefficients for the polynomial parameters in the numerator (direct effects) and denominator (decay effects) for the transfer function relating the first independent variable series to the dependent variable series; and ω_2 is the coefficient for the intervention series X_t. The intervention series is binomial in nature, similar to an indicator variable, where values of the series are 0 before t_{int} and 1 for all other times:

$$X_t = \begin{cases} 1, t \geq t_{int} \\ 0, t < t_{int} \end{cases} \qquad \text{(Equation 5.3)}$$

We developed many models for the average F_t series with a 15 min time step. We first developed a model using F_t data that were collected during days of year 143-202, when soil moisture was relatively high and rain events recharged soil moisture, (henceforth wet period, n=2009 observations). We then developed a model using F_t data that were collected during days of year 143-261, which included a late season drying period when soil moisture declined and rain events did not recharge soil moisture, (henceforth dry period, n=3200 observations). After model development, we used autocorrelation plots of the residuals to verify that the residual series had characteristics of random error, or white noise (i.e. all non-zero time lags have a correlation coefficient of zero). For model selection, we computed Akaike's information

criterion (AIC) for each model, which is a statistic used to evaluate the goodness of fit and parsimony of a candidate model, with smaller AIC values indicating a better fitting and more parsimonious model than larger values (Johnson and Omland, 2004). We used the differences in the AIC values among candidate models (Δ_i=AIC$_i$-AIC$_{min}$) to compute a relative weight (w_i) for each model relative to all models fit:

$$w_i = \frac{e^{-0.5\Delta_i}}{\sum_{r=1}^{R} e^{-.5\Delta_r}} \qquad \text{(Equation 5.4)}$$

with the sum of all w_i equal to 1. The final model selected was the model with the highest w_i (Burnham and Anderson, 2002; Johnson and Omland, 2004).

We reserved 18 days of environmental and sap flow data to use in evaluating the performance of the model. These data were reserved *a priori* because conditions were intermediate between the wet and dry periods used to parameterize the models. Independent variables were used with the model to forecast estimates for the 18 days (n=1176 observations). Observed values and forecasted values were scaled to daily values and plotted and assessed for bias.

Results

Environmental conditions

During days of year 143-201 (henceforth wet period), rainfall ranged from days with no precipitation to a day with more than 97 mm of rain, with a 59-day total of 320.8 mm (Figure 5.1). Average yearly rainfall for this site is approximately 1100 mm, which is approximately

evenly distributed throughout the year (Figure 5.2). The average 59-day total rainfall for the wet period during the 13 years preceding the study was 217.6 mm (Figure 5.2).

As a consequence of the numerous rainfall events during this period, fractional soil moisture on these shallow soils was relatively high during the study with a maximum of 0.37 with an average of 0.34 (Figure 5.1). Soil water content (θ) at saturation for an idealized clay texture soil is 0.45, while field capacity (i.e., water potential (Ψ_{FC}) = -.01MPa) is approximately 0.38 θ, and permanent wilting point (Ψ_{WP} = -1.5MPa) is approximately 0.19 θ (David Radcliff unpublished data). Average daily PAR and *D* during 0800-2000 h for the wet period ranged 410-982 μmol m^{-2} s^{-1} and 0.18-1.73 kPa, respectively (Figure 5.1).

During days of year 237-261 (henceforth dry period), rainfall events were scarce, with 3.8 mm of total rainfall during the 25 day period (Figure 5.1). The average 25-day total rainfall for the dry period during the 13 years preceding the study was 75.3 mm (Figure 5.2).

As a consequence of scarce rainfall events, fractional soil moisture during this period of the study fell to a minimum of 0.21 and averaged 0.24. PAR and *D* during 0800-2000 h for the dry period were similar to those recorded for the wet period; however, there was less variance in these parameters due to infrequent rain cloud cover.

During days of year 113-142 (henceforth validation period), rainfall and soil moisture were intermediate between the wet and dry period conditions. Total rainfall during the validation period was 187.9 mm and fractional soil water content averaged 0.35. The average total rainfall for the validation period during the 13 years preceding the study was 79.4 mm (Figure 5.2).

Modeling E_c under high soil moisture

Daily canopy transpiration (E_c, based on the average of six trees measured) during the wet period ranged 0.70 mm to 3.07 mm, and averaged 2.18 mm (Figure 5.3). Sap flow (F), our estimate of E_c, was positively related to D and PAR (Figure 5.4). The relationship of F with D was much stronger than the relationship with PAR (Figures 5.4a & 5.4b). Cross-correlation coefficients calculated between F and D series showed the strongest correlation at a lag of 0, with a weaker correlation at a lag of +1. This indicated that changes in F lagged changes in D by 0-15 min, but were also strongly related to and lagged D by 15-30 min. This relationship was noted in the model by using backshift operators on the D series at these two times, along with a polynomial term in the denominator to describe the nonlinear time dependent decay (Table 5.1). Cross-correlation coefficients calculated between F and PAR series showed a weaker relationship compared to that with D, with changes in PAR lagging changes in F by +1 (Figure 5.4). A relationship between F and PAR at other time lags was not apparent. This indicated that changes in F lagged changes in PAR by 15-30 min, but were not strongly related to other values of PAR. This relationship was noted in the model by relating values of F_t to values of P_{t+1} (Table 5.1). No correlation was found between diurnal moisture in the top 30 cm of soil and diurnal F. There was little or no diurnal variation in soil moisture; therefore, it was not correlated with F on this time scale.

The time series model that best fit F during the wet period was a (3, 1, 1) model and had a w_i of 1.00 (Table 5.1). All regression terms in the model were significant at the α=0.05 level. The best overall regression factor, i.e. the factor that explained the most partial variance, was D at 0.44252. PAR, although significant, explained a small amount of variance and had an overall

regression factor of 0.00007 (Table 5.1). The wet period model explained more than 97% of the total variance in the F_t series during the wet period.

Measured and forecasted E_c under soil moisture deficit

As soil moisture declined, E_c also declined, and during the dry period ranged from 0.11 mm day^{-1} to 2.33 mm day^{-1} and averaged 1.69 mm day^{-1} (Figure 5.3). When the wet period model was used to forecast daily E_c during the dry period, a systematic overestimate occurred compared to measured values (Figs. 3 & 5a). Although the model predicted actual daily E_c during high soil moisture well, it did not perform well when soil moisture dropped below 0.25 (Figure 5.5a). For example, on day of year 260 actual daily E_c was 1.76 mm while forecasted E_c was 2.89 mm, an overestimate of 1.12 mm. The difference between actual E_c and forecasted E_c using this model for the 25-day dry period was 12.29 mm, or an overestimate of 29%.

Soil moisture deficit modeled as an intervention

The correlation coefficients between *F* and *D* and PAR stayed relatively constant between the wet period and the dry period (Figure 5.4). The time lag between *F* and *D* and PAR also did not change between periods (*cf.* Granier et al., 2000). However, as fractional soil moisture fell below 0.25, forecasted E_c diverged from observed E_c (Figs. 3 & 5a).

The time series model that best fit the wet and dry period *F* data was again a (3, 1, 1) model taking the same form as the wet period model and having a w_i of 1.00 (Table 5.1). The best fitting model introduced soil moisture as a linear step intervention. When soil moisture fell below 0.28, a linear regression term was added to the model. All regression terms in the model were significant at the α=0.05 level. The best overall regression factor was vapor pressure deficit at 0.38073. PAR, although significant, explained a small amount of variance and

had an overall regression factor of 0.00006. The soil moisture intervention term was significant with an overall regression term of –0.00054 (Table 5.1). Interestingly, the soil moisture intervention term explained a higher amount of partial variance in the dry period than did PAR. The wet and dry period model with the intervention term explained more than 97% of the total variance in the F_t series during the wet and dry period. The intervention model performed well for both wet and dry period data (Figs. 5b & 6).

Validation

During the validation period, actual daily E_c ranged 0.12 mm to 2.87 mm, and averaged 1.20 mm. These values approximately spanned the range of daily E_c on which the intervention model was parameterized. Using the intervention model parameterized on the wet and dry period data, estimated daily E_c during the validation period ranged 0.19 mm to 2.99 mm, and averaged 1.31 mm. The intervention model appeared to have no systematic bias when actual daily E_c from the validation period was evaluated against estimated daily E_c (Figure 5.5b).

Discussion

Canopy transpiration (E_c) for this 32-year old *P. taeda* plantation was comparable to other coniferous forests under conditions of high soil moisture availability, averaging 2.18 mm day^{-1} with a maximum of 3.07 mm day^{-1}. In general, maximum E_c values for coniferous forests range from 2.4 to 5.5 mm day^{-1} (Whitehead and Jarvis, 1981; Kelliher et al., 1993; Schulze at al., 1994; Cienciala et al., 1997; Cienciala et al., 1999; Phillips and Oren, 2001; Lagergren and Lindroth, 2002), with intensively managed plantations having maximum E_c values as high as 6.8 mm day^{-1} (Teskey and Sheriff, 1996). When soil moisture declined, we found that E_c in the dry period dropped to an average of 1.69 mm day^{-1} with minimum values of 0.44 mm day^{-1}. Other studies

report declining E_c as soil moisture declines (Granier and Loustau, 1994; Teskey and Sheriff, 1996; Cienciala et al., 1997; Phillips et al., 1997; Ewers et al., 1999; Lagergren and Lindroth, 2002). However, D and PAR alone are more commonly used to describe E_c (Tuzet et al., 2003). Usually only under very low soil moisture availability does E_c show a strong relationship with soil moisture (Rutter, 1968; Granier and Loustau, 1994; Bauerle et al., 2002). In the present study, we found that diurnal E_c could be accurately predicted by D under high soil moisture. During the dry period when soil moisture limited transpiration, our model parameterized under high soil moisture did not perform well (Figs. 3 and 5a). After a step intervention of soil moisture limitation was added to the model, our model could accurately predict transpiration under non-limiting and limiting soil moisture regimes (Figs. 5b and 6).

Compared to this study that uses multivariate time series analysis to estimate autocorrelation, previous studies that use sap flux data to predict E_c have generally taken a least-squares regression approach, whether the goal of the predictive equation is to back-cast (e.g. how well the predictive equation describes the data that were used to fit it) or forecast (e.g. how well the predictive equation describes independent data). For example, Granier et al. (1996) used sap flow collected on one site and developed a predictive equation of transpiration as a function of D. They then estimated E_c on a second site using the predictive equation, and compared those estimates with actual measured E_c at the site. They found that the relationship could predict E_c well in the second site with an R^2 of 0.95. Wullschleger et al. (2001) developed a regression equation relating E_c of southeastern deciduous trees to radiation and D which explained 85% of the variation in the data, and used this to forecast E_c for the next year. Similarly, Oren and Pataki (2001) use least-squares regression to develop two predictive equations relating E_c in *Quercus alba* and *Acer rubrum* to D and PAR. They found that the relationships only explained

59% and 22% of the variation in their data, respectively. Phillips and Oren (2001) used least-squares regression to develop a predictive equation relating E_c to D in a southeastern mixed pine/deciduous forest. They found that the relationship only explained 70% of the variation in their data, and that this predictive relationship improved under conditions of high soil moisture. Ewers et al. (1999) use least-squares regression to develop a predictive equation relating E_c of *P. taeda* to D. They found that the relationship only explained 82% of the variation in their data. The literature is replete with studies that relate, and thus back- or fore-cast, E_c as functions of environmental variables using least-squares regression.

A second approach to empirically modeling E_c from sap flux estimates involves solving the Penman-Monteith formula for canopy conductance (g_c) given sap flow estimates of canopy transpiration (E_c). Once a series of g_c is calculated in this way, relationships between maximal g_c values and environmental variables are developed. These relationships are then combined into a multiplicative constraint function for maximal g_c values (Jarvis, 1976; Reed et al., 1976; Schulze et al., 1994), which adjusts the maximal rate of conductance ($g_{c\,max}$) downward using a series of fitted general relationships between environmental variables and conductance:

$$g_c = g_{c\,max} \cdot f(PAR) \cdot f(T) \cdot f(D) \cdot f(\Psi) \qquad \text{(Equation 5.5)}$$

where T is temperature and Ψ is water potential (however, this last variable is often replaced with soil water content). Forecasts of E_c can then be made, given the predictive relationship for g_c and climate variables. For example, Granier and Loustau (1994), Martin et al. (1997), Bernier et al. (2002) and Gash et al. (1989) all approach modeling the observed variation in E_c in this way; yet, this method of predicting E_c is labor and data intensive. The approach we illustrate in this study can also be used on a time series of g_c, so that the mechanisms regulating transpiration can be explored (as was the emphasis of the above cited studies). Two analyses would need to be made.

Initially, using the time series of sap flow, the time lag would need to be identified, and the sap flow series would have to be subsequently shifted in time. Next, the series of g_c would have to be computed. Finally, *in lieu* of using a multiplicative constraint function, the ARIMA approach could be used.

Both empirical methods of predicting E_c described above use least-squares regression to fit the relationships between concurrent values of E_c or g_c and environmental variables. This fitting method violates the assumption of independence because values of E_c or g_c are related in time, and some studies using this approach even report that residuals are related to time or day of year (see Bernier et al. (2002) Figure 5.3e). Furthermore, by using data that are not independent, statistics such as R^2, P, t, and F values are artificially inflated and can not be used as indicators of goodness of fit of these models. Models based on this approach often report relatively high R^2 values between actual and estimated canopy transpiration, in the range of 0.60-0.95. Although these R^2 values are relatively high, and moreover artificially inflated, we have not found any model based on these empirical approaches that explains as much as 97% of the variation between modeled (either back- or forecasted) and measured canopy transpiration, as our model based on time series intervention analysis above does. Although process models of E_c and g_c are becoming more refined and thus predictive (Buckley et al., 2003; Tuzet et al., 2003), empirical and hybrid models are still widely used (Landsberg 2003). Given that the empirical modeling methods described above violate assumptions, have no true replication (Hurlbert, 1984), and have artificially inflated R^2 values, these modeling approaches should be carefully considered when using sap flux measurements to estimate either E_c or g_c.

Conclusions

Multivariate time series methods allow identification of relationships between variables over time that are sometimes not readily apparent, but nonetheless important in describing, and thus predicting, complex systems or processes. More importantly, pulse stresses or perturbations to these systems or processes can be incorporated to these models. Studies have used these methods to model a variety of systems, processes and behavior, including the effect of drought stress on long-term oak (*Quercus*) growth (Pederson, 1998); volcanic tephra deposition on growth decline in Pacific silver fir (*Abies amabalis*) (Segura et al., 1995); tree thinning on growth increases of Norway spruce (*Picea abies*) (Mäkinen, 1997); animal population decreases in response to environmental stresses (Lewellen and Vessey, 1998; Chan et al., 2003); and typhoon disturbances on stream flow (Kuo and Sun, 1993). In general, these data analysis methods are commonly used in hydrology, dendrochronology, and demography, but rarely used in plant physiological ecology. In this study, however, we used time series of environmental variables to model canopy transpiration by incorporating soil moisture depletion as a step intervention. The analytical approach we describe in this paper would also be appropriate for other plant physiological ecology data. For example, studies evaluating the impact of rainfall events or vegetation removal on soil respiration, or studies evaluating the impact of increasing temperature, O_3, CO_2 on plant gas exchange or net ecosystem exchange (i.e. eddy covariance). The data analysis technique we describe above allows quantification of the disturbance *in situ* while achieving replication in time. As advances in sensor technology and data capture allow longer and high frequency monitoring of physiological processes, data analysis techniques such as those described in this paper that allow identification of relationships and incorporation of

known or hypothesized significant changes over time are a useful and appropriate way to examine these data.

Acknowledgements

This study was supported by the University of Georgia Daniel B. Warnell School of Forest Resources, the Robert W. Woodruff Foundation and the Joseph W. Jones Ecological Research Center. This publication was also developed under EPA STAR Fellowship Agreement No. 91617001-0 awarded by the U.S. Environmental Protection Agency. It has not been formally reviewed by EPA. The views expressed in this document are solely those of the authors and EPA does not endorse any products or commercial services mentioned in this publication. We thank Tim Martin and Nathan Phillips for helpful reviews of this paper. We thank Bob Cooper, Lisa Donovan, Christopher Fonnesbeck, Ron Hendrick, Mary Anne McGuire, Jon Miniat, and Jason Nedlo for their logistical help, help with field work, and overall support.

References

Bauerle, W.L., Post, C.J., McLeod, M.F., Dudley, J.B. and Toler, J.E., 2002. Measurement and modeling of the transpiration of a temperate red maple container nursery. Agricultural and Forest Meteorology, 114(1-2): 45-57.

Bernier, P.Y., Breda, N., Granier, A., Raulier, F. and Mathieu, F., 2002. Validation of a canopy gas exchange model and derivation of a soil water modifier for transpiration for sugar maple (*Acer saccharum* Marsh.) using sap flow density measurements. Forest Ecology and Management, 163(1-3): 185-196.

Box, G.E.P. and Jenkins, G.M., 1976. Time series analysis: forecasting and control. Holden-Day, San Francisco, 575 pp.

Brockwell, P.J. and Davis, R.A., 2002. Introduction to time series and forecasting. Springer-Verlag, New York, 434 pp.

Buckley, T.N., Mott, K.A. and Farquhar, G.D., 2003. A hydromechanical and biochemical model of stomatal conductance. Plant Cell and Environment, 26(10): 1767-1785.

Burnham, K.P. and Anderson, D.R., 2002. Model selection and multimodel inference: A practical information-theoretic approach. Springer-Verlag, New York, 488 pp.

Chan, K.S., Stenseth, N.C., Lekve, K. and Gjpsaeter, J., 2003. Modeling pulse disturbance impact on cod population dynamics: The 1988 algal bloom of Skagerrak, Norway. Ecological Monographs, 73(1): 151-171.

Cienciala, E., Kučera, J. and Lindroth, A., 1999. Long-term measurements of stand water uptake in Swedish boreal forest. Agricultural and Forest Meteorology, 98-99: 547-554.

Cienciala, E. et al., 1997. Canopy transpiration from a boreal forest in Sweden during a dry year. Agricultural and Forest Meteorology, 86: 157-167.

Ewers, B.E., Oren, R., Albaugh, T.J. and Dougherty, P.M., 1999. Carry-over effects of water and nutrient supply on water use of Pinus taeda. Ecological Applications, 9(2): 513-525.

Ford, C.R., Goranson, C.E., Mitchell, R.J., Will, R.E. and Teskey, R.O., 2004a. Diurnal and seasonal variability in the radial distribution of sap flow: predicting total stem flow in *Pinus taeda* trees. Tree Physiology, 24(9): 951-960.

Ford, C.R., McGuire, M.A., Mitchell, R.J. and Teskey, R.O., 2004b. Assessing variation in the radial profile of sap flux density in *Pinus* species and its effect on daily water use. Tree Physiology, 24(3): 241–249.

Gash, J.H.C., Shuttleworth, W.J. and Lloyd, C.R., 1989. Micrometeorological measurements in Les Landes forest during HAPEX-MOBILHY. Agricultural and Forest Meteorology, 46: 131-147.

Georgia State Climate Office, Athens GA Station [Online WWW]. Available URL: "http://climate.engr.uga.edu/athens/index.html" [Accessed 01 Feb 2004].

Granier, A., 1985. Une nouvelle méthode pour la mesure du flux de sève brute dans le tronc des arbres. Annales des Sciences Forestieres, 42(2): 193-200.

Granier, A. and Loustau, D., 1994. Measuring and modelling the transpiration of a maritime pine canopy from sap-flow data. Agricultural and Forest Meteorology, 71: 61-81.

Granier, A., Biron, P., Kostner, B., Gay, L.W. and Najjar, G., 1996. Comparisons of xylem sap flow and water vapour flux at the stand level and derivation of canopy conductance for Scots pine. Theoretical and Applied Climatology, 53(1-3): 115-122.

Granier, A., Loustau, D. and Breda, N., 2000. A generic model of forest canopy conductance dependent on climate, soil water availability and leaf area index. Annals of Forest Science, 57(8): 755-765.

Hatton, T.J., Catchpole, E.A. and Vertessy, R.A., 1990. Integration of sapflow velocity to estimate plant water-use. Tree Physiology, 6(2): 201-209.

Hurlbert, S.H., 1984. Pseudoreplication and the design of ecological field experiments. Ecological Monographs, 52(2): 187-211.

Jackson, R.B. et al., 2001. Water in a changing world. Ecological Applications, 11(4): 1027-1045.

Jarvis, P.G., 1976. The interpretation of the variations in leaf water potential and stomatal conductance found in canopies in the field. Philosophical Transactions of the Royal Society of London, B, 273: 593-610.

Johnson, J.B. and Omland, K.S., 2004. Model selection in ecology and evolution. Trends in Ecology and Evolution, 19(2): 101-108.

Kelliher, F.M., Leuning, R. and Schulze, E.-D., 1993. Evaporation and canopy characteristics of coniferous forests and grasslands. Oecologia, 95: 153-163.

Kuo, J.-T. and Sun, Y.-H., 1993. An intervention model for average 10 day streamflow forecast and synthesis. Journal of Hydrology, 151(1): 35-56.

Lagergren, F. and Lindroth, A., 2002. Transpiration response to soil moisture in pine and spruce trees in Sweden. Agricultural and Forest Meteorology, 112(2): 67-85.

Landsberg, J.J., 2003. Physiology in forest models: history and the future. Forest Biometry, Modelling and Information Sciences, 1: 49-63.

Lewellen, R.H. and Vessey, S.H., 1998. The effect of density dependence and weather on population size of a polyvoltine species. Ecological Monographs, 68(4): 571-594.

Mäkinen, H., 1997. Reducing the effects of disturbance on tree-ring data using intervention detection. Scandinavian Journal of Forest Research, 12: 351-355.

Martin, T.A. et al., 1997. Crown conductance and tree and stand transpiration in a second-growth *Abies amabilis* forest. Canadian Journal of Forest Research, 27(6): 797-808.

Martinez-Vilalta, J., Pinol, J. and Beven, K., 2002. A hydraulic model to predict drought-induced mortality in woody plants: an application to climate change in the Mediterranean. Ecological Modelling, 155(2-3): 127-147.

Oren, R. and Pataki, D.E., 2001. Transpiration in response to variation in microclimate and soil moisture in southeastern deciduous forests. Oecologia, 127: 549-559.

Pederson, B.S., 1998. The role of stress in the mortality of midwestern oaks as indicated by growth prior to death. Ecology, 79(1): 79-93.

Phillips, N., Nagchaudhuri, A., Oren, R. and Katul, G., 1997. Time constant for water transport in loblolly pine trees estimated for time series of evaporative demand and stem sapflow. Trees- Structure and Function, 11: 412-419.

Phillips, N. and Oren, R., 2001. Intra- and inter-annual variation in transpiration of a pine forest. Ecological Applications, 11(2): 385–396.

Phillips, N., Oren, R., Licata, J. and Linder, S., 2004. Time series diagnosis of tree hydraulic characteristics. Tree Physiology, 24(8): 879-890.

Rasmussen, P.W., Heisey, D.M., Nordheim, E.V. and Frost, T.M., 2001. Time series intervention analysis: unreplicated large-scale experiments. In: S.M. Scheiner and J. Gurevich (Editors), Design and Analysis of Ecological Experiments. Oxford University Press, New York, pp. 158-177.

Reed, K.L., Hamerly, E.R., Dinger, B.E. and Jarvis, P.G., 1976. Analytical model for field measurements of photosynthesis. Journal of Applied Ecology, 13(3): 925-942.

Roberts, J., 1983. Forest transpiration: A conservative hydrological process? Journal of Hydrology, 66: 133-141.

Rutter, A.J., 1968. Water consumption by forests. In: T.T. Kozolwski (Editor), Water Deficits and Plant Growth. Academic Press, Inc., New York, pp. 23-84.

SAS, 1991. Modeling with explanatory variables, SAS/ETS Software: Applications Guide 1, Version 6. Time Series Modeling and Forecasting, Financial Reporting, and Loan Analysis. SAS Institute, Inc., Cary, NC, pp. 149-188.

Schulze, E.-D., Kelliher, F.M., Korner, C., Lloyd, J. and Leuning, R., 1994. Relationship among maximum stomatal conductance, ecosystem surface conductance, carbon assimilation rate, and plant nitrogen nutrition: A global ecology scaling exercise. Annual Review of Ecology and Systematics, 25: 629-660.

Segura, G., Hinckley, T.M. and Brubaker, L.B., 1995. Variations in radial growth of declining old-growth stands of *Abies amabilis* after tephra deposition from Mount St. Helens. Canadian Journal of Forest Research, 25: 1484-1492.

Soil Survey Division, Natural Resources Conservation Service, United States Department of Agriculture. Official Soil Series Descriptions [Online WWW]. Available URL: " http://ortho.ftw.nrcs.usda.gov/osd/" [Accessed 13 Nov 2003].

Teskey, R.O. and Sheriff, D.W., 1996. Water use by *Pinus radiata* trees in a plantation. Tree Physiology, 16: 273-279.

Tuzet, A., Perrier, A. and Leuning, R., 2003. A coupled model of stomatal conductance, photosynthesis and transpiration. Plant Cell and Environment, 26: 1097-1116.

Whitehead, D. and Jarvis, P.G., 1981. Coniferous forests and plantations. In: T.T. Kozolwski (Editor), Water Deficits and Plant Growth. Academic Press, Inc., New York, pp. 49-152.

Wullschleger, S.D., Hanson, P.J. and Todd, D.E., 2001. Transpiration from a multi-species deciduous forest as estimated by xylem sap flow techniques. Forest Ecology and Management, 143: 205-213.

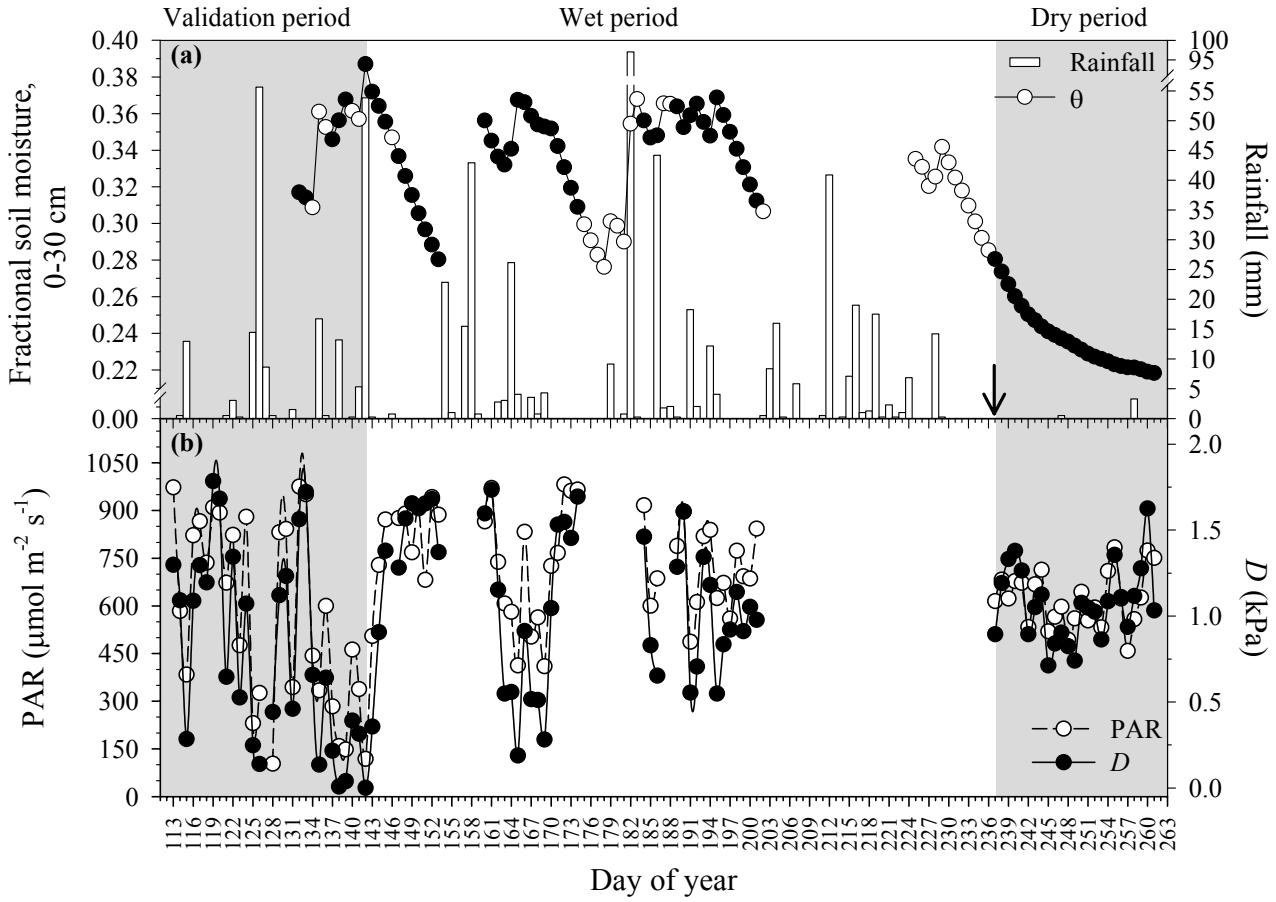

Figure 5.1 Total rainfall (24 h) and average daily (0800-2000 h) fractional soil moisture in the 0-30 cm depth (θ) during the study period (a). Filled soil moisture symbols indicate days when concurrent sap flow measurements were recorded, while open symbols indicate days when sap flow measurements were not recorded. Arrow indicates timing of hypothesized intervention due to soil moisture depletion (day of year 237). Average daily PAR and D (0800-2000 h) during the study period (b).

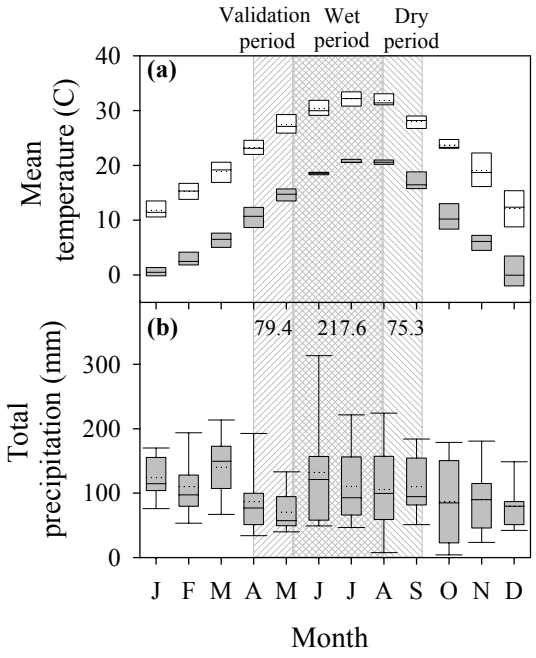

Figure 5.2 Four-year average monthly maximum and minimum temperature (years 2000-2003) (a), and 13-year total rainfall (years 1990-2002) (b). Solid lines in box plots indicate median, dashed line indicates mean, top and bottom of box indicates 75th and 25th percentiles (range for panel a), and whiskers indicate 95th and 5th percentile, hatched areas represent timing of sap flux and environmental measurements for 2003. Numbers in hatched areas in panel (b) are the 13-year average total rainfall recorded for the days in the measurement period. Data obtained from Georgia State Climate Office (2004).

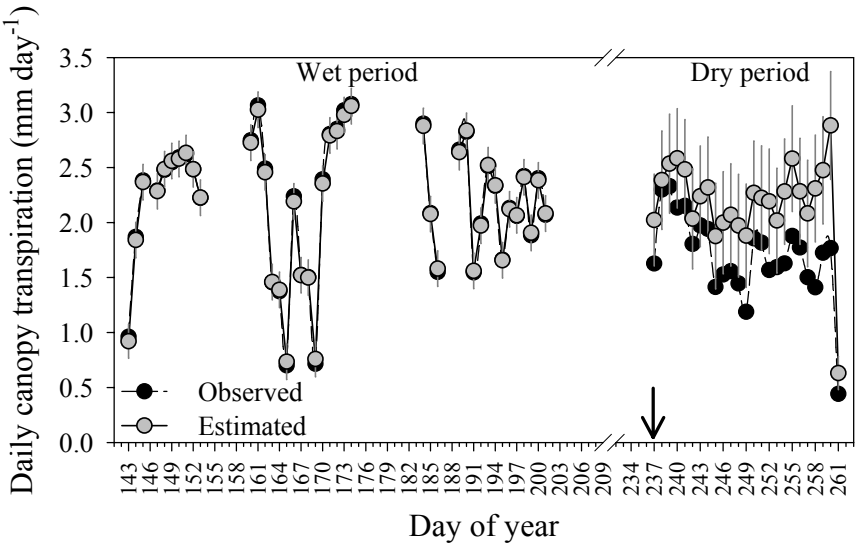

Figure 5.3 Time series of observed daily canopy transpiration (black symbols) and of estimated daily canopy transpiration (grey symbols). Estimated values were computed using a time series model fit to the data during the wet period only (e.g. days of year 143-203, before hypothesized intervention) and forecasted into the dry period. Vertical bars on estimated values are one standard deviation. Arrow indicates timing of hypothesized intervention due to soil moisture stress (day of year 237).

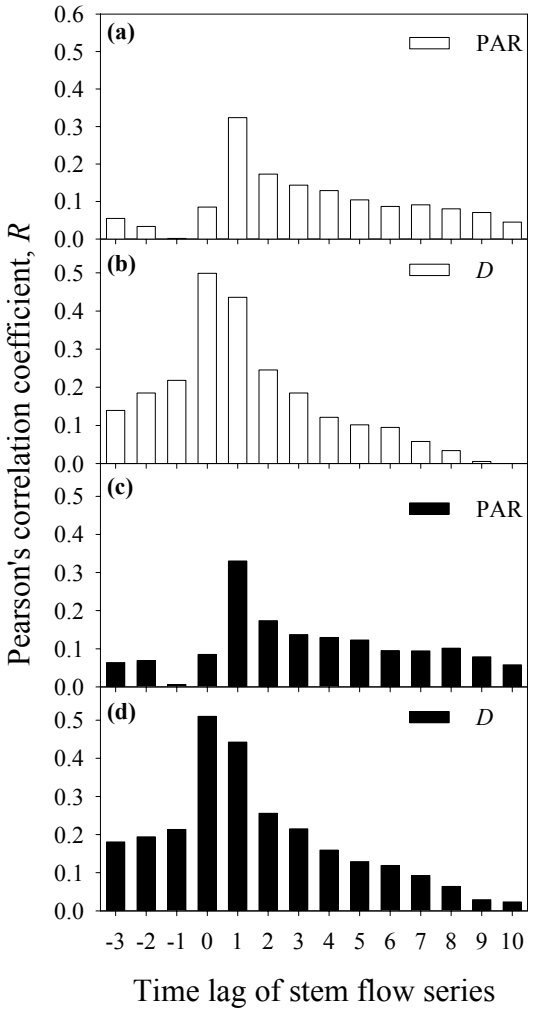

Figure 5.4 Pearson's correlation coefficients (*R*) between average total sap flow (average of all trees) and PAR (a, c) and *D* (b, d). Panels (a) and (b) were computed using the data during the wet period before the hypothesized intervention (e.g. days of year 143-203). Panels (c) and (d) were computed using all the data from the wet and dry periods (e.g. days of year 143-261). Plots show a strong correlation between *D* and sap flow. PAR is ahead of sap flow in time by 15-30 minutes (no correlation with lag 0 but correlation with + lags), while sap flow is responsive to current (0-15 min, lag 0) and previous values of *D* (+ lags).

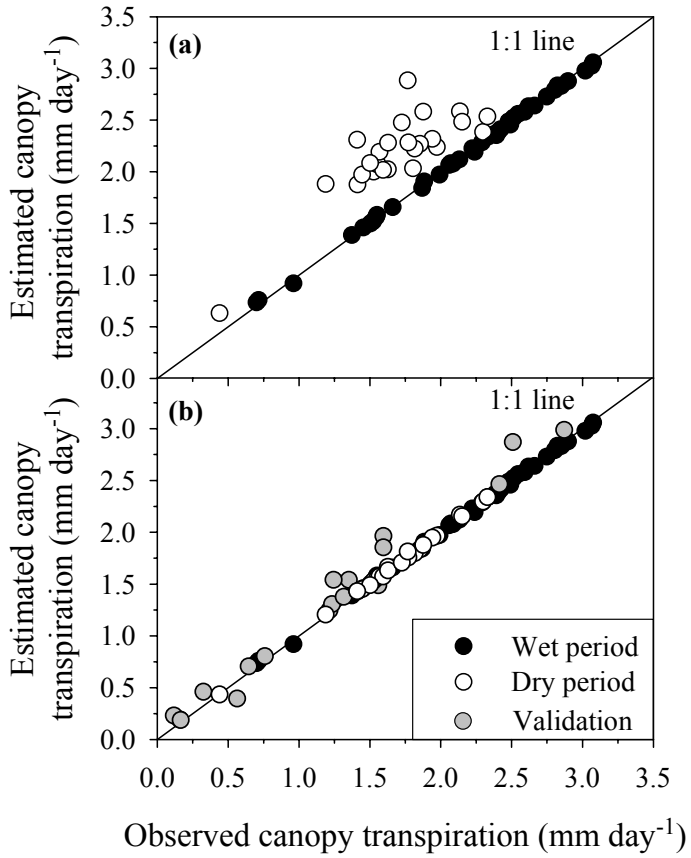

Figure 5.5 Performance of model predicting daily canopy transpiration. Estimated values were computed (a) using a time series model fit to the data during the wet period only (e.g. days of year 143-203, before hypothesized intervention) and forecasted into the dry period, and (b) using an intervention time series model fit to all data collected (e.g. days of year 143-261). Open symbols indicate days after the hypothesized intervention due to soil moisture stress (day of year 237); closed symbols indicate days before the intervention (days of year 143-203). Grey symbols indicate the independent data used for model validation.

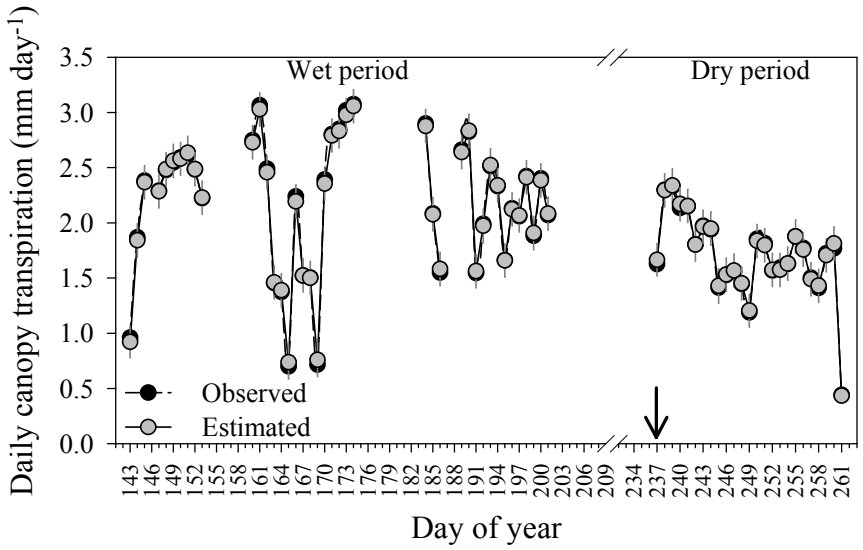

Figure 5.6 Time series of observed daily canopy transpiration (black symbols) and of estimated daily canopy transpiration (grey symbols). Estimated values were computed using a time series model fit to all data collected in wet and dry periods (e.g. days of year 143-261). Vertical bars on estimated values are one standard deviation. Arrow indicates timing of hypothesized intervention due to soil moisture stress (day of year 237).

Table 5.1 Predictive equations for average F_t in six trees as functions of independent variables: PAR (P_t), D (D_t), and fractional moisture in the upper 30 cm of soil (S_t).

Description	Equation	AIC[a] (w_i[b])	S^2_i[c] (S^2_f[c])	Variance Explained (%)
Wet period model	$F_t = 0.44252\left(\frac{(1-0.63697.b^1)(1-0.22271b^2)}{(1-1.47645b^1)(1+0.53921b^2)}\right)D_t + (0.00007)P_{t+1} + \left(\frac{(1-0.99608b^1)}{(1-1.10665b^1)(1-0.09784b^2)(1-0.11356b^3)}\right)a_t$	-1976.5 (1.00)	0.99 (0.02)	97.8
Wet & dry period model	$F_t = 0.38073\left(\frac{(1-0.68826.b^1)(1-0.18437b^2)}{(1-1.49791b^1)(1+0.55373b^2)}\right)D_t + (0.00006)P_{t+1} - (0.00054)S_t + \left(\frac{(1-0.99683b^1)}{(1-1.06821b^1)(1-0.06119b^2)(1-0.10993b^3)}\right)a_t$	-3620.5 (1.00)	0.91 (0.02)	97.9

[a]Akaike information criterion.
[b]Akaike weight of model selected relative to all models fitted for that tree.
[c]Initial (S^2_i) and final (S^2_f) variance in F_t series. Final variance is the unexplained variance in F_t series.

CHAPTER 6

CONCLUSIONS

Conclusion

Variable distributions of water as a transpiration source can have consequences not only on the estimates of plant and ecosystem transpiration, but also on the production potential and stability of transpiration rates for different plants within an ecosystem. In the preceding chapters we evaluated the spatial distribution of water flow in the stems of mature *Pinus spp.* and calculated the errors that can result in estimates of whole-tree water use if this variability is not incorporated. For individual trees, we found that the radial distributions of water flow in the stems of trees were Gaussian shaped, with a larger proportion of stem transpiration flux occurring in the outer xylem compared to the inner xylem. Consistent with this type of radial profile, other studies have shown that in mature trees as the heartwood is approached, hydraulic conductivity of the sapwood declines (Spicer and Gartner 2001). This may be a function of age-related changes, such as higher resistance due to bordered pit membrane encrustation (Mark and Crews 1973), tracheid damage caused by repeated and un-repaired cavitation events (Sperry et al. 1991), or general changes in connectivity between inner xylem elements and foliage (v. Dye et al. 1991; Jiménez et al. 2000). More interestingly, we found that the steepness of radial distributions in sap flow was greater earlier in the day, and became less steep later in the day. As a result, time-dependent changes in the shape of the radial profile were sometimes correlated with daily changes in evaporative demand. As the radial profile became less steep, the inner xylem contributed relatively more to total tree sap flow than it did earlier in the day. This could be occurring due to a variety of reasons, such as: stem water storage depletion; tracheid cavitation; water withdrawal from ray cells; changes in the distribution of incident radiation across the canopy; or if the driving gradient to move water in the inner sapwood, with its probable higher hydraulic resistance compared to that of the outer xylem, is only met later in the

day. Although the distribution was variable, it was predictable, allowing the development of a general mathematical function to describe it. Parameters in the function were biologically meaningful, including the parameter β that describes the rate of radial change in water flow with radial depth. Most importantly, we found that whole-tree water use could be grossly overestimated in trees with deep sapwood if the complexity of the radial distribution of water flow in the stem was not accounted for.

In another study, we not only again observed this pattern of diurnal variation in the radial profile, but we also observed a seasonal pattern of decreasing steepness of the radial distribution, with the radial profile becoming less steep as the soil moisture content (θ) declined. Throughout the season, daytime sap flow decreased as θ decreased; yet, nighttime sap flow (an estimate of stored water use) remained relatively constant. In other words, reliance on stored water in the stem increased as soil moisture content declined. This has also recently been found for *Pinus ponderosa* experiencing seasonal water deficits (Phillips et al. 2003). Whether the reliance on stored water increasing with drought is common to all trees or to those only with deep functional sapwood, or perhaps even nonfunctional heartwood via ray conduction, is not known and remains an intriguing question.

In this same forest at the stand level, we also quantified the impact that the declining soil moisture had on canopy transpiration with a modeling exercise. We estimated that had the trees not experienced declining soil moisture, transpiration would have been 12.29 mm higher over the 25-day period. The modeling specific approach was uniquely applied to forest transpiration data here, and we show that this approach allows for multiple driving variables to influence transpiration on different time scales, and in linear and nonlinear ways.

Finally, at the ecosystem level, we investigated the processes by which the dominant plant life forms in a savanna, trees and grasses, partition and use water, and how these feedback onto carbon gain. We hypothesized that the different water sources used by trees and grasses were linked to their productivity, and that the proportion of groundwater used varied across a natural hydrologic gradient. We predicted that trees would have access to deep water sources and have less variability in transpiration rates over time; while grasses would rely more on shallow soil water sources and have more variability in transpiration rates over time. Across the natural hydrologic gradient, we found that trees were using groundwater almost exclusively, while grasses used a higher proportion of soil water. This finding is consistent with reported rooting distributions of trees and grasses across diverse biomes (Jackson et al. 1996). Our results are also consistent with descriptions of longleaf pine rooting systems (Heyward 1933), and conform to the emerging general pattern that trees and grasses in savanna systems have different functional rooting zones (Smith et al. 1997; Weltzin and McPherson 1997; Dodd et al. 1998; Ludwig 2001; Hungate et al. 2002; Moreira et al. 2003) . We also found that the variability in transpiration rates was affected by the source water utilized. Because trees were able to rely on groundwater for transpiration, presumably a more stable water source than shallow soil water, the variability in rates of transpiration was always lower for pines compared to grasses. Within the grass plant functional type, we found that percentage of groundwater utilized varied across the hydrologic regime. Grasses in the xeric site used a higher percentage of groundwater than grasses in the mesic site. Moreover, we found that this variation could be linked to annual aboveground net primary productivity. Because the xeric sites have lower soil moisture content in the upper 15 cm of the soil, we may have expected productivity of grasses to be constrained. However, grasses were significantly more productive in the xeric sites compared to mesic.

When distributions of water within plants and ecosystems are not accounted for, patterns in tree and ecosystem water use, and even productivity may be perplexing. This is true at the scale of the ecosystem, in which access to different water resources can feedback to increases in productivity and decreases in transpiration rate variability, as well as at the scale of the tree stem, where the spatial distribution of water flux may contribute to the reliance on stored water in the stem as soil water becomes less available.

References

Dodd, M.B., J.M. Lauenroth and J.M. Welker 1998. Differential water resource use by herbaceous and woody plant life-forms in a shortgrass steppe community. Oecologia. 117:504-512.

Dye, P.J., B.W. Olbrich and A.G. Poulter 1991. The influence of growth rings in *Pinus patula* on heat pulse velocity and sap flow measurement. J. Exp. Bot. 42:867-870.

Heyward, F. 1933. The root system of longleaf pine on the deep sands of western Florida. Ecology. 14:136-148.

Hungate, B.A., M. Reichstein, P. Dijkstra, D. Johnson, G. Hymus, J.D. Tenhunen, C.R. Hinkle and B.G. Drake 2002. Evapotranspiration and soil water content in a scrub-oak woodland under carbon dioxide enrichment. Global Change Biology. 8:289-298.

Jackson, R.B., J. Canadell, J.R. Ehleringer, H.A. Mooney, O.E. Sala and E.D. Schulze 1996. A global analysis of root distributions for terrestrial biomes. Oecologia. 108:389-411.

Jiménez, M.S., N. Nadezhdina, J. Cermák and D. Morales 2000. Radial variation in sap flow in five laurel forest tree species in Tenerife, Canary Islands. Tree Physiol. 20:1149-1156.

Ludwig, F. 2001. Tree-grass interactions on an east African savanna: The effects of competition, facilitation and hydraulic lift. Wageningen University, p. 139.

Mark, W.R. and D.L. Crews 1973. Heat-pulse velocity and bordered pit condition in living Engelmann spruce and Lodgepole pine trees (*Picea engelmannii, Pinus contorta*). For. Sci. 19:291-296.

Moreira, M.Z., F.G. Scholz, S.J. Bucci, L.S. Sternberg, G. Goldstein, F.C. Meinzer and A.C. Franco 2003. Hydraulic lift in a neotropical savanna. Functional Ecology. 17:573-581.

Phillips, N.G., M.G. Ryan, B.J. Bond, N.G. McDowell, T.M. Hinckley and J. Cermak 2003. Reliance on stored water increases with tree size in three species in the Pacific Northwest. Tree Physiol. 23:237-245.

Smith, D.M., P. Jarvis and J.C.W. Odongo 1997. Sources of water used by trees and millet in Sahelian windbreak systems. J. Hydrol. 198:140-153.

Sperry, J.S., A.H. Perry and J.E.M. Sullivan 1991. Pit Membrane Degradation and Air-Embolism Formation in Aging Xylem Vessels of Populus-Tremuloides Michx. J. Exp. Bot. 42:1399-1406.

Spicer, R. and B.L. Gartner 2001. The effects of cambial age and position within the stem on specific conductivity in Douglas-fir (*Pseudotsuga menziesii*) sapwood. Trees Structure and Function. 15:222-229.

Weltzin, J.F. and G.R. McPherson 1997. Spatial and temporal soil moisture resource partitioning by trees and grasses in a temperate savanna, Arizona, USA. Oecologia. 112:156-164.